5-2014

Weir-Baffled Culvert Hydrodynamics Evaluation for Fish Passage Using Particle Image Velocimetry and Computational Fluid Dynamic Techniques

Mohanad A. Khodier
Utah State University

WEIR-BAFFLED CULVERT HYDRODYNAMICS EVALUATION FOR FISH PASSAGE

USING PARTICLE IMAGE VELOCIMETRY AND COMPUTATIONAL

FLUID DYNAMIC TECHNIQUES

by

Mohanad A. Khodier

A dissertation submitted in partial fulfillment
Of the requirements for the degree

of

DOCTOR Of PHILOSOPHY

in

Civil and Environmental Engineering

Approved:

Dr. Blake P. Tullis	Prof. Mac McKee
Major Professor	Committee Member
Dr. Michael C. Johnson	Dr. Barton Smith
Committee Member	Committee Member
Dr. Gilberto Urroz	Dr. Mark R. McLellan
Committee Member	Vice President for Research
	and Dean of the School of
	Graduate Studies

UTAH STATE UNIVERSITY
Logan, Utah

2014

ABSTRACT

Weir-Baffled Culvert Hydrodynamics Evaluation for Fish Passage Using Particle Image

Velocimetry and Computational Fluid Dynamic Techniques

by

Mohanad A. Khodier, Doctor of Philosophy

Utah State University, 2014

Major Professor: Dr. Blake P. Tullis
Department: Civil and Environmental Engineering

Due to a recent increase in environmental awareness regarding fish passage through hydraulic constructions including culverts, an evaluation for the passage of wild brown trout through a weir-baffled prototype-scale culvert was performed under a variety of culvert slopes and discharge conditions. The influence of the sample fish population and the length of the individual fish on passage rates were investigated; the data showed that the brown trout fish passage sample size evaluated in this study (25 per test) was sufficiently large to minimize sample size dependency. Fish behavior while traversing the culvert was observed and reported, including resting/staging zone locations.

Turbulent flow through weir baffled-culvert was also simulated numerically using three-dimensional numerical model employing the (k-ϵ) model, Renormalized Group k-ϵ model (RNG), and Large Eddy Simulation (LES) model. Experimental data measured with the Particle Image Velocimetry (PIV) were used to assess the accuracy and the

applicability of these turbulence models in predicting the turbulent flow characteristics of the flow through a weir-baffled culvert at different spatial locations inside the culvert for variety of culvert slopes and flow rates. The influence of flow rates and culvert slopes on the forward velocities and reverse velocities was evaluated. It was noted that the influence of the flow rates on the flow velocities depends on the culvert slopes. Turbulent kinetic energy and flow direction effects on flow characteristic were also evaluated. Validation of Manning's equation and Manning's roughness coefficient for the tested culvert were reported.

(128 pages)

PUBLIC ABSTRACT

Weir-Baffled Culvert Hydrodynamics Evaluation for Fish Passage Using Particle Image

Velocimetry and Computational Fluid Dynamic Techniques

by

Mohanad A. Khodier, Doctor of Philosophy

Utah State University, 2014

Major Professor: Dr. Blake P. Tullis
Department: Civil and Environmental Engineering

Due to a recent increase in environmental awareness regarding fish passage through hydraulic structures, including culverts, an evaluation of passage of wild brown trout through a weir-baffled, prototype-scale culvert, was conducted under a variety of culvert slopes and discharge conditions. The influence of the fish sample population and the lengths of the individual fish on passage rates were investigated. The data showed that the fish sample size of 25 per test was sufficiently large to minimize sample size dependency. Fish behavior, including resting/staging zone locations, while traversing the culvert was observed and reported. Two preferable resting zones for the fish were noted while swimming upstream in baffled culvert.

The influence of flow rates and culvert slopes on the forward velocities and reverse velocities were evaluated. An inverse relationship was observed between fish passage success and flow rate and/or culvert slope. No fish successfully passed through

the baffled culvert at the maximum discharge (85 L/s) for culvert slope of 5 and 6%. New culvert designs should provide appropriate hydraulic conditions to improve the fish upstream movements.

ACKNOWLEDGMENTS

CONTENTS

LIST OF TABLES

LIST OF FIGURES

NOMENCLATURE

A	=	culvert cross-sectional flow area;
α_k	=	empirical coefficient;
α_ε	=	empirical coefficient;
B_n	=	the nth baffle from the culvert entrance;
B_S	=	Baffle spacing;
β	=	constant;
C	=	coefficient;
$C_{1\varepsilon}$	=	empirical coefficient;
$C_{2\varepsilon}$	=	empirical coefficient;
C_μ	=	empirical coefficient;
D	=	culvert inside diameter;
D_h	=	hydraulic diameter;
Δx	=	particles displacement;
Δt	=	the time separation between the two laser pulses;
δ	=	Kronecker delta;
E	=	exponent;
ε	=	turbulent dissipation rate per unit mass;
$\overline{f_i}$	=	gravity force;
g	=	gravitational acceleration;
g_x	=	gravitational acceleration in the x-direction;

g_z	=	gravitational acceleration in the z-direction;
η	=	a function of k, ε, and S_t;
η_o	=	a constant;
h	=	baffle height;
H_O	=	inlet water depth;
$\overline{H_w}$	=	average water depth;
θ	=	culvert inclination angle;
i	=	1, 2, 3;
I	=	turbulent intensity;
k	=	turbulent kinetic energy per unit mass;
L	=	length scale;
μ	=	fluid dynamic viscosity;
μ_t	=	eddy viscosity;
n	=	Manning's roughness coefficient;
n_1	=	Manning's roughness coefficient using method-1;
n_2	=	Manning's roughness coefficient using method-2;
v	=	kinematic viscosity of the fluid;
v_{eff}	=	combination of the fluid and turbulent kinematic viscosity;
v_t	=	turbulent kinematic viscosity;
P	=	wetted perimeter;
$\bar{p}$	=	mean pressure;
Q	=	culvert flow rate;

$Q*$ =   dimensionless discharge;

ρ =   density;

R   =   RNG model source term;

R_{B_fs} =   bursting speed to the region average flow velocity ratio;

R_{C_fs} =   cruising speed to the region average flow velocity ratio;

Re =   Reynolds number ($\frac{\rho \bar{u} D_h}{\mu}$);

R_h =   hydraulic radius;

R_{S_fs} =   sustained speed to the region average flow velocity ratio;

σ_k =   empirical coefficient;

σ_ϵ =   empirical coefficient;

S =   culvert slope;

S_t =   mean rate of strain tensor;

τ =   stress;

u =   velocity in the x-direction;

u' =   the average fluctuating velocity in the x-direction;

$\bar{u}$ =   average velocity in the x-direction;

$\bar{u}_i$ =   average velocity in the i-direction;

v =   velocity in the y-direction;

v' =   the average fluctuating velocity in the y-direction;

$\vec{v}$ =   fluid local velocity vector;

w =   velocity in the z-direction;

w' =   the average fluctuating velocity in the z-direction;

x = x-direction;

x_b = distance from a baffle in the x-direction divided by the baffle spacing;

x_i = i-direction;

x_o = distance from the inlet to a baffle in the x-direction;

y = y-direction;

y^* = non-dimensional y (y/D);

z = z-direction;

z^* = non-dimensional z (z/D)

CHAPTER 1

INTRODUCTION

Background

Culverts are used to pass a water flows safely from one side of a road to the other without overtopping the roadway. Beside their effective purpose of providing safety for the traveling public, culverts may prevent or limit the upstream movement and migration of many aquatic species including fish. Migration is very important for aquatic species to continue their life cycle. The environmental concerns about fish passage through culverts started in the 1960's and 1970's and the new culvert designs should provide appropriate hydraulic conditions to improve the fish upstream movements (where appropriate). Upstream movements are essential for spawning during the spawning season, searching for appropriate water temperature, or food (Baker and Votapka 1990). Culverts can produce a negative impact on fish passage by creating excessively high flow velocities, inadequate flow depths, excessive turbulence, and debris accumulation within the culvert especially at the inlet. Debris accumulation is due to inadequate maintenance.

Excessive flow velocities and inadequate flow depths are very important factors that influence the fish passage through culverts (Maine DOT 2007). Flow velocities through culverts tend to be higher than the stream velocity because the culverts dimensions are narrower than the stream cross section. In order to pass upstream, fish must overcome the hydraulic conditions associated with the flow. Fish have three types of swimming speeds: cruising speed, sustained speed, and darting (bursting) speed (Bell 1986). Cruising speed can be maintained indefinitely and sustained speed can be

maintained only for a few minutes. Whereas darting (bursting) speed can be maintained for only 5 to 10 seconds. Fig. 1-1 shows the relative swimming speed for different types of fish species. Apparently, fish with higher swimming speeds are considered strong swimmers. Fish have two types of muscle systems: white muscles that are used for short vigorous swimming and red muscles that used for long sustained swimming (Bell 1986). According to Behlke et al. (1991), red muscle can recover with a short time after use but the using of white muscle requires a rest period in order to be used again. Powers and Orsborn (1985) found that fish are able to swim for a short distance in shallow water without being fully submerged.
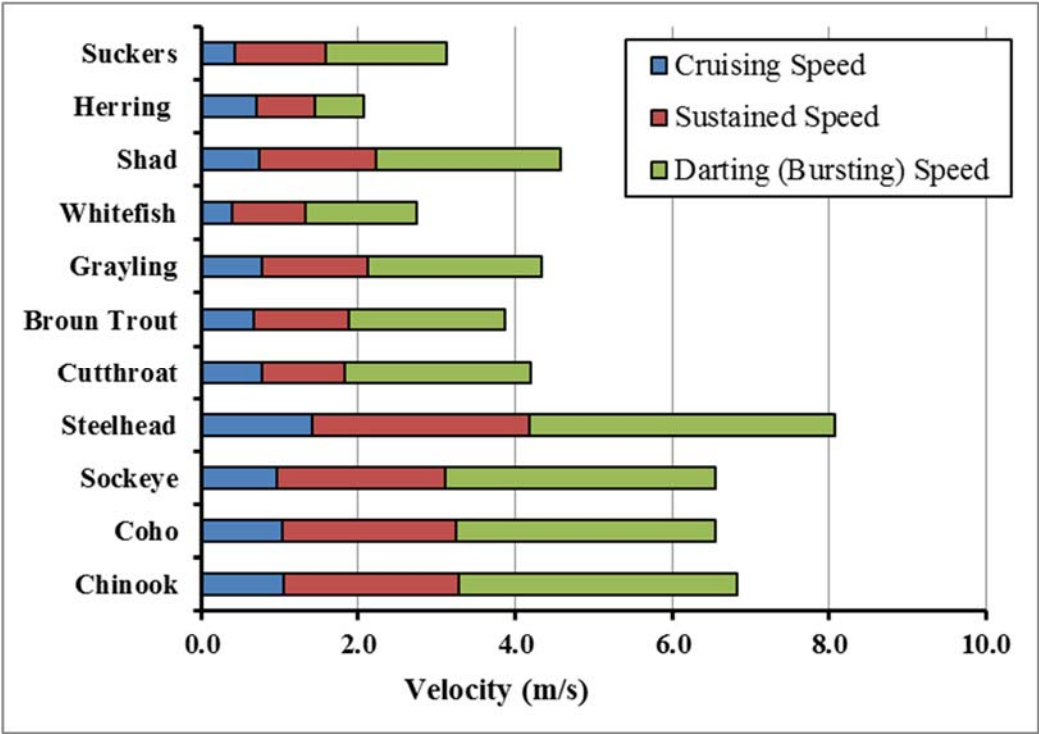
Fig.1-1. Swimming speeds for adult-sized fish. Adapted from Bell, 1986

However, full submergence is recommended for better swimming performance. According to Tillinger and Stein (1996), larger fish are considered stronger swimmers than smaller fish of the same species. Larger fish have larger muscles that increases the swimming ability. Behlke et al. (1991) developed a relationship relating fish swimming strength to fish total length. Watts (1974) concluded that the swimming speed of juvenile fish is proportional to the fork length of the fish tail and total fish length, whereas Belford and Gould (1989) reported that there is no relation between the fish size and successful culvert passage. They found that small fish were able to take advantage of low velocities found near culvert walls. The length of the culvert has significant influence of fish success passage especially if there is a lack of resting areas while passing upstream.

Another factor that influences the fish passage is the flow turbulence. Morrison et al. (2009) evaluated the interaction between juvenile salmon culvert passage and turbulence but found no significant correlation. The effect of turbulent eddy diameter and vorticity on the swimming speed and stability of creek chub (*Semotilus atromaculatus*) was investigated by Tritico and Cotel (2010). They concluded that fish's habitat selection, migration, and ability to maintain posture in a flow were affected by the presence of turbulent eddies in the flow. Liao et al. (2003) concluded that fish could reduce the amount of energy expending using the presence of distributed flow eddies as a swim aid.

Baffle Designs

Due to recent increase in the environmental concerns regarding fish passage though culverts, where applicable, a culvert should be designed to provide passage for

various fish species in the water conveyed by the culvert. One possible solution to improve the fish passage through culverts is by installing baffles inside the culvert. Baffles are short, thin vertical walls (i.e., weirs) that are built inside a culvert with regular spacing and a specific height. There are many different types of baffles, but the most common types are offset baffles, slotted-weir baffles, weir baffles, and spoiler baffles (see Fig. 1-2). Baffles increase the flow depth and decrease the flow velocities by creating pools with slower velocities where fish can rest (Rajaratnam and Katopodis 1990). Rajaratnam and Katopodis (1990) studied the flow characteristic through a culvert of 0.301 m in diameter and 6.3 m in length with different weir baffles height and spacing. The height of the baffles was $0.15D$ and $0.1D$ with baffles spacing equals to $0.6D$ and $1.2D$, where the D is the pipe diameter.
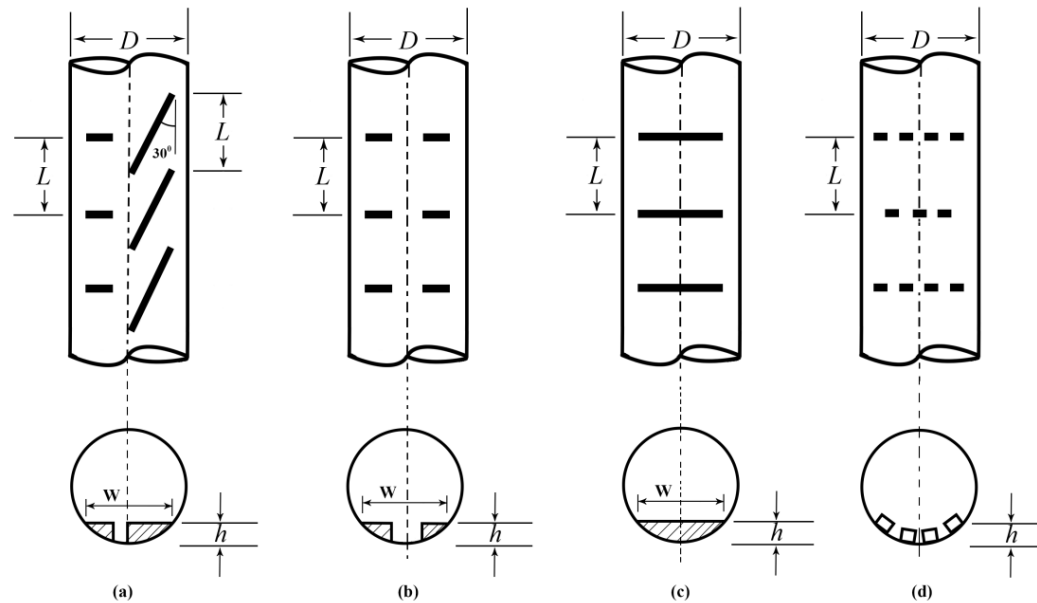
Fig.1-2. Examples of culvert baffle: (a) offset baffle; (b) slotted-weir baffle; (c) weir baffle; spoiler baffle

They developed a flow equation that correlated the dimensionless flow rate with relative flow depth. They concluded that different baffles designs have similar performance in reducing the flow velocity and may enhance the fish passage although no biological tests were conducted. Furthermore, Rajaratnam et al. (1989) conducted studies on the slotted weir baffles with different baffle designs. The pipe diameter (D) was 0.30 m with the baffle heights of 0.1D and 0.15D. Each baffle height was tested with three baffle spacing involving 0.6D, 1.2D, and 2.4D. The slot opening was 0.1D. They found that a baffle design of 0.15D height and 0.6D spacing acted as efficient as the baffle of 0.1D height and 1.2D spacing in producing a larger depth of flow in the culvert compared with plain culvert for the same flow rate.

Feurich et al. (2011) investigated numerically the flow characteristics in "spoiler-baffle" geometry inside a culvert of 1.3 m diameter. They concluded that using of spoiler baffles will reduce the water velocities and the baffles size is independent on the culvert size. Morrison et al. (2009) studied the influence of flow turbulence characteristics on fish passage through spiral-corrugated culvert of 1.83 m diameter fitted with baffles at a single culvert slope (S) of 1.14% and Q ranging from 43 to 198 L/s. No significant correlation was observed between flow turbulence and fish passage. Tritico and Cotel (2010) found that the presence of turbulent eddies in the flow affects the fish's habitat selection, migration, and ability to maintain posture in a flow. Smith et al. (2005) investigated the influence of the flow velocities and turbulence on the focal position (the place where there are a large number of fish) of juvenile rainbow trout *Oncorhynchus mykiss* through a flume of 7.3 m long × 0.61 m deep × 0.91 m wide. They observed

juvenile rainbow trout selected focal positions with low turbulence and high velocities over high turbulence and low velocities. No fish passage tests were conducted through culvert. Olsen and Tullis (2013) evaluated wild brown trout fish passage through smooth-walled baffled and non-baffled culverts of 0.6 m diameter. They concluded that the average flow velocity has an inverse relationship with the fish passage performance and suggested that fish passage success rates can be improved by installing baffles.

Research Objectives

The main objectives of this study were to

- Evaluate the fish passage of brown trout through weir baffled- culvert at different flow rate and culvert slopes.

- Report the relationship between fish passage, culvert slope, and flow rate.

- Investigate in the influence of the sample fish population and the length of the individual fish on passage rates.

- Study the fish behavior while passing upstream through the culvert and detect the preferable zones.

- Simulate the flow through the weir baffled-culvert numerically with different turbulence models in three dimensions.

- Collect PIV measurements to provide more details about the hydraulic characteristics of the flow and use the PIV measurements to validate the numerical simulations for the same culvert flow conditions, using different turbulence modeling methods.

- Use the velocity distributions and turbulent kinetic energy to explain the fish behavior and the success of the fish passage percentage at each flow conditions.

CHAPTER 2

EXPERIMENTAL SETUP AND NUMERICAL SIMULATIONS

Test Facilities

All experiments were conducted at the Utah Water Research Laboratory (UWRL) located at Utah State University. The test facilities including a head tank, a weir baffled-culvert with adjustable slope, a tail water tank, a supply piping, a tail water box, and a fish holding tank (see Fig. 2-1).

Baffled-Culvert

The culvert was made from high-density polyethylene (HDPE) pipe of 0.610 m in diameter with a wall thickness of 19.1-mm. Rectangular slots (0.014 m wide × 0.408 m long) were cut laterally into the bottom of the culvert with 0.518 m interval. Rectangular baffles were inserted into these rectangular windows and sealed on the outside of the pipe using an HDPE welder. The rectangular baffles had a height of 0.15*D,* where *D* is the inner diameter of the culvert. Other small rectangular observation windows (0.10 m wide × 0.30 m long) cut into the crown of the culvert on 1.5-m centers provided viewing and instrumentation access along the culvert (Fig. 2-2).
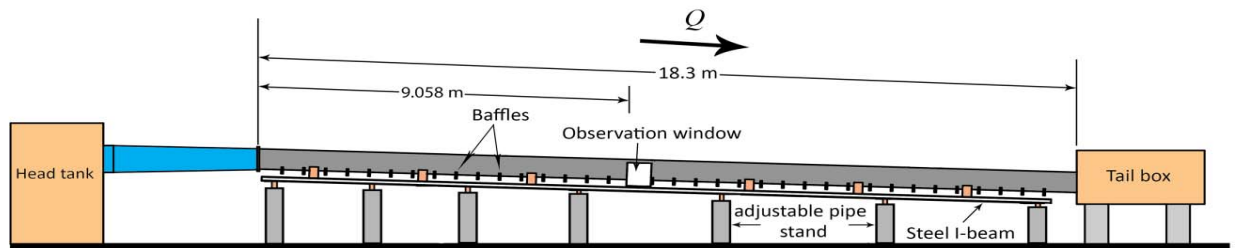
Fig. 2-1. Schematic of culvert fish passage test facility

Also, the rectangular observation windows were used to collect the fish that were unable to pass through the culvert. To maintain uniform culvert slopes, the culvert was continuously supported by a steel I-beam assembly. The pipe and I-beam assembly were supported by adjustable pipe stand, which were used to adjust the culvert slope. The upstream end of the culvert was connected to the head tank via a flexible coupler. The downstream end of the culvert was connected to the tail water box. A water-tight observation/instrumentation window was installed in the side wall near the mid span of the culvert between two baffles. A 355-mm width by 406-mm tall flexible sheet of clear Lexan was used to replace a curved section of culvert wall that was removed (Fig. 2-3).

Fig. 2-2. Small rectangular observation windows

In order to eliminate the optical distortion for the video imaging through the curved window, a clear acrylic box with dimensions 584 mm × 685 mm × 635 mm (1.27 mm wall thickness) was attached and sealed to the pipe exterior around the view window and filled with water. This window was used to observe and record the fish behavior while passing upstream with a high resolution video camera and used to collect the Particle Image Velocimetry (PIV) measurements.

Fig. 2-3. Water-tight observation window

Head Tank

The head tank was connected to the upstream end of the culvert via a flexible coupler, which served as the pivot point for culvert slope changes; a water supply connection entered the tank near the bottom (Fig. 2-4). A mesh plate was attached to the inlet of the tank to prevent the fish from swimming upstream beyond the head tank. The tank was used to convey water to the culvert and provide a large pool with lower velocities for the fish that succeed in passing so that the fish were prevented from swimming downstream.

Fig. 2-4. Head tank and the flexible coupler

Tail Box

A wooden box (2.1 m wide × 4.2 m long × 1.2 m height) was attached to the downstream end of the culvert (Fig. 2-5). The tail water box outlet was screened to prevent fish from escaping (Fig.2-6). The tail water box height was adjusted according to the culvert slope via stands with varying heights.

Fig. 2-5. Tail box

Fig. 2-6. Tail water box outlet

Supply Piping

The UWRL supplied with water from Fist Dam located on the Logan River, Utah. The water was conveyed to the supply tank via a pipe of 0.30 m in diameter (Fig. 2-7); flow rates were measured using calibrated venturi flow meters (±0.25%).

Fish Holding Tank

Wild brown trout (*Salmo trutta*) were collected from the Logan River (located adjacent to the laboratory facility) using either electroshocking or hook and line techniques. All fish were measured (length), tagged, and numbered for identification. A 350-gallon tank was used to hold the fish when not being tested (Fig. 2-8). The tank was continuously supplied with raw river water in an effort to maintain as natural of an environment (water temperature, organic content, etc.) as possible while in captivity. A netting was also placed over the tank to prevent fish from jumping out.

Fig. 2-7. Supply piping for the culvert (0.3 m pipe)

Fig. 2-8. Fish holding tank

Fish Testing Methodology

An evaluation of wild brown trout passage through weir-baffled culvert was conducted under variety of steep culvert slopes ($3.0\% \leq S \leq 6$ %) and discharge conditions (28.3 to 85 L/s). For each experiment of specific flow rate and culvert slope, the fish were inserted into the tail water box near the culvert exit. Typically 25 fish were used on each experiment except when conducting the fish sample size experiments. Flow rates used were measured using calibrated Venturi flow meters (±0.25%). The water depth was measured using piezometer tubes (Fig.2-9). A high-resolution video camera was used to record fish behavior while swimming upstream past the observation window.
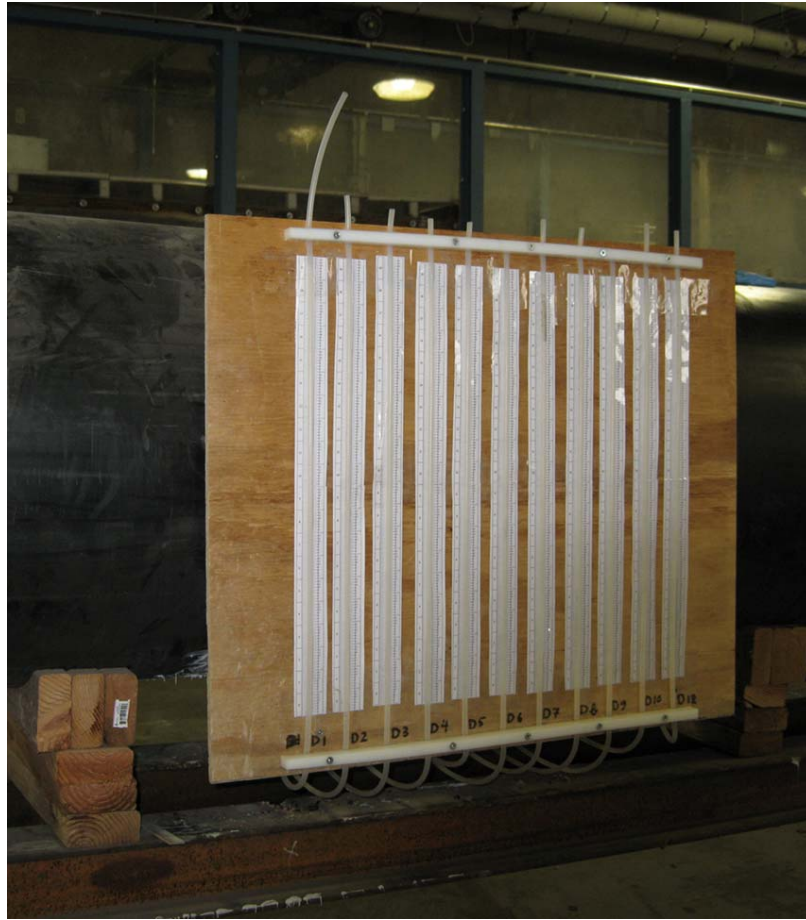
Fig. 2-9. Piezometer tubes

The head tank was observed every five minutes during the experiment to record any fish passage success. The fish that succeed were netted out of the head tank, tag number noted, the time needed to swim the culvert recorded, and returned to the holding tank. Typically test durations were 1.5 hours but occasionally were extended to 2 hours when fish were found near the upstream end of the culvert but hadn't yet exited into the head tank. The fish percentage passing was evaluated for each discharge-slope combination and the fish that were unable to swim upstream were netted out of the culvert and returned back into the fish holding tank.

Particle Image Velocimetry (PIV)

Particle Image Velocimetry (PIV) is a technique which measures the instantaneous velocities of a fluid throughout a region illuminated by a light sheet. Basically the PIV consists of light source (laser), light optics, seed particles (tracers), camera, and computer (Fig. 2-10). Very small neutrally buoyant particles (tracers) are illuminated twice within a small time separation (Δt) by a light sheet produced by passing the laser light beam through an optical arrangement of cylindrical lenses. The positions of the particles at first and the second laser pulses are recorded as a single image exposed twice or as a pair of two single exposure images by Charge-Coupled Device (CCD) camera that is typically positioned perpendicular to the plane of the light sheet. The particle displacements are measured locally and scaled by the image magnification. By knowing the particle displacement (Δx) and the time separation between the two laser pulses (Δt), the two-dimensional fluid local velocity vector can be calculated per the following equation

$$\vec{v} = \frac{\Delta x}{\Delta t} \tag{2-1}$$

This technique does not need the placement of any probe in the flow field which could affect the flow characteristics of the medium. Furthermore, PIV can provide more information for the entire flow at the same time whereas the probe measurements can only measure the velocity at a single point in the flow. The seed particles, ideally, are assumed to be small and neutrally buoyant with respect to the fluid medium and would not response to the buoyancy forces so that they would represent the local velocities of the fluid correctly.
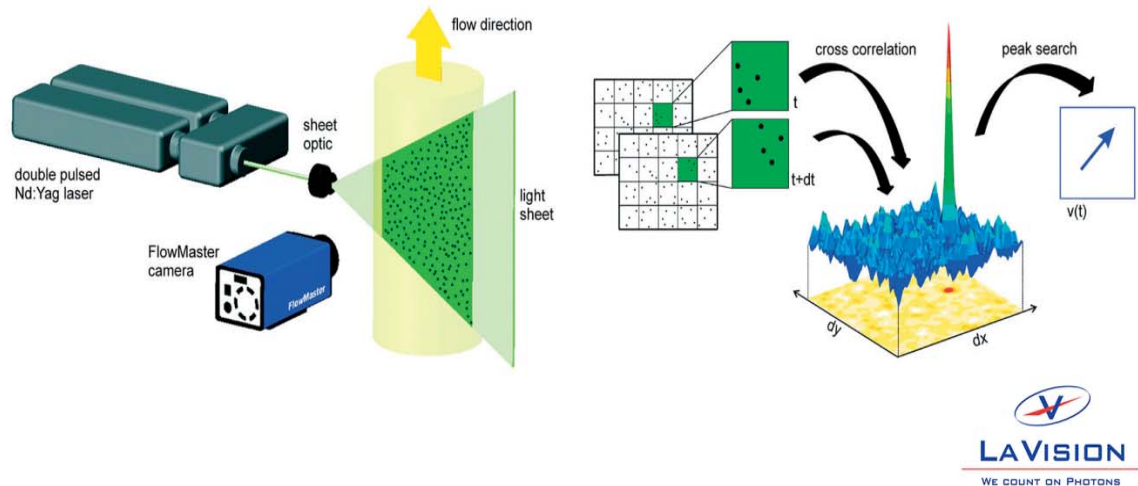
Fig. 2-10. 2D Particle Image Velocimetry System (LaVision, 2012)

The digital images acquired by the CCD camera are divided into small areas called the interrogation windows (IW). A correlation between the interrogation windows of the first and the second image are evaluated statistically resulting in one local displacement vector for each interrogation window. The size of the interrogation window is one of the most important factors that should be selected such that the particles move in the same direction and the same distance homogeneously within the interrogation window. Typically, a minimum of ten particles within the interrogation windows are required for good results. There are two techniques to record the scattered light of both illuminations: single frame-double exposure or double frame-double exposure. In the case of single frame-double exposure, the particle images are evaluated by auto-correlation, whereas cross-correlation is used to evaluate the particle images in the double frame-double exposure.

Auto-Correlation

Auto-correlation is used to evaluate the particle images when the scattered light of both illuminations are recorded in one image (Fig. 2-11). As shown in Fig. 2-11, the evaluation of the particle images are characterized by two identical correlation peaks around a highest central peak. The central peak represents zero displacement of the particles and the very small peaks represent noise. Each of the two identical correlation peaks is a possible flow displacement but different directions. The disadvantage of this technique is that in order to detect the right sign of the displacement, previous information about the observed flow is needed. Furthermore, for small particle displacement, the two identical peaks become very close to the central peak which makes them difficult to be detected. In addition to that, the displacement correlation peak might disappear if the noise increases.
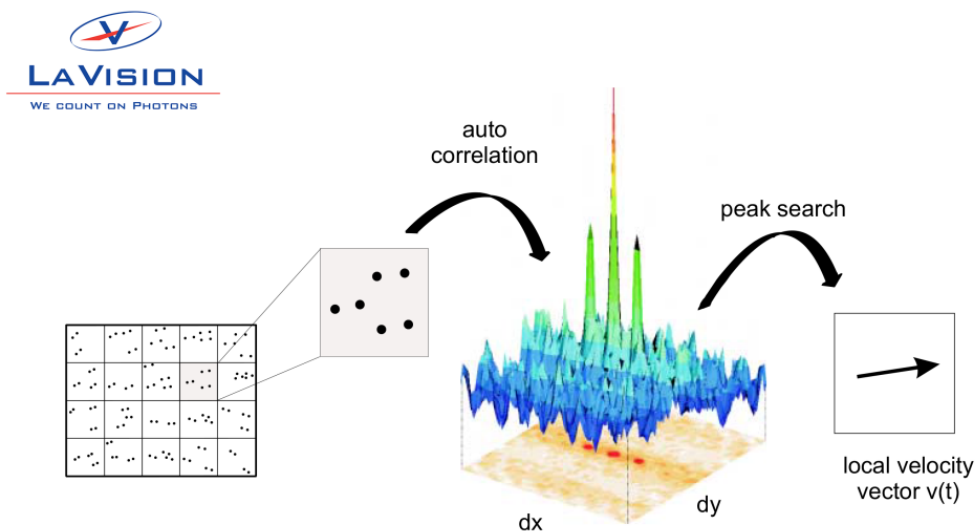
Fig. 2-11. Evaluation of PIV recording with auto-correlation (LaVision 2012)

Cross-Correlation

Auto-correlation is used to evaluate the particle images when the scattered light of both illuminations are recorded in two different images (Fig. 2-12). The cross-correlation function is characterized by one highest correlation peak surrounded with noise. Comparing to the auto-correlation the cross-correlation peaks are significantly higher. The theoretical maximum amplitude of the displacement-correlation peak for the cross-correlation is one. The advantages of the cross-correlation are: fast data transfer, no directional ambiguity, and small displacement can be detected. In this study, the cross-correlation was used to evaluate the particle images.

Image Preprocessing

The image preprocessing is used to manipulate the particle images before the vector calculation is performed. This will provide an improvement for the quality of the results.
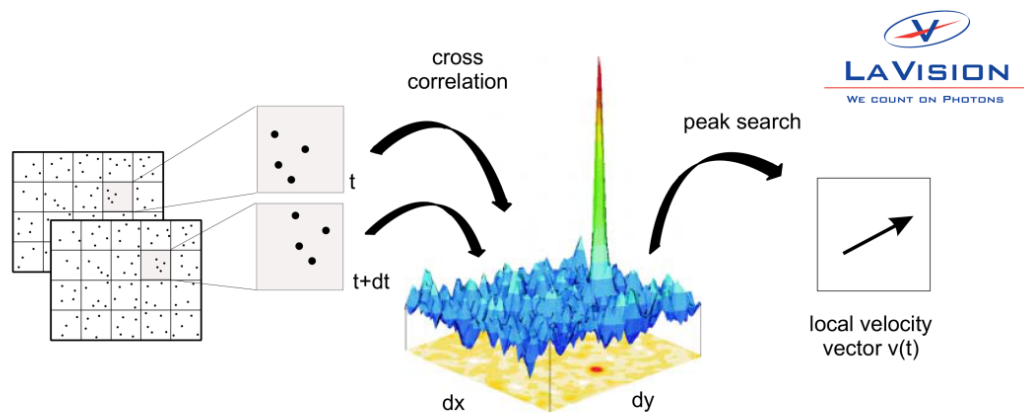
Fig. 2-12. Evaluation of PIV recording with auto-correlation (LaVision 2012)

Vector Calculation

In DaVis (the PIV software), there are two options to calculate the vector: vector calculation-double frames and vector calculation-time series of single frame. The former was used in this study. The selection of these options depends on the way the particle images have been acquired. The vector calculation-double frames is used when the particle images have been recorded with double frame-double exposure. Whereas the vector calculation-time series of single frame is used when the particle images have been recorded with single frame-double exposure.

Vector Postprocessing

In this process, the false vectors are filtered out from the vector calculation field. One criteria used to eliminate the false vectors is to remove the vectors whose velocity components are out of specified range. This requires prior information about the maximum and the minimum velocities in the flow. Another criteria is to use the peak ratio (Q_{PIV}) defined as

$$Q_{PIV} = \frac{P1 - min}{P2 - min} \qquad (2\text{-}2)$$

where min is the lowest value of the correlation plane and *P1* and *P2* are the peak heights of the first and second highest correlation peak respectively (Fig.2-13). The higher the correlation value is the more confidence about this vector. The median filter is other criteria that calculate a median vector from a group of neighboring vectors. The calculated vector is compared with the neighboring vectors and rejected if its value is outside the allowed range of the average vector. This is very important setting in the PIV to remove the bad vectors but sometime it will remove the good one too.
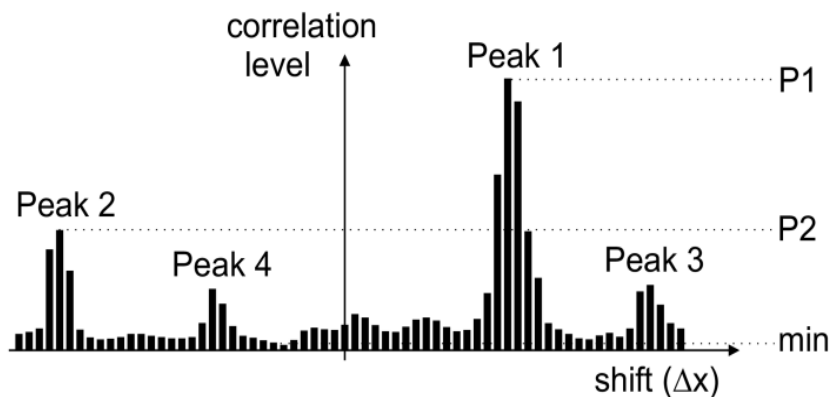
Fig. 2-13. Definition of peak ratio (LaVision 2012)

Numerical Simulation

FLOW-3D®, a computational fluid dynamics (CFD) model developed by Flow Science, is used to numerically solve the Reynolds-Averaged Navier-Stokes (RANS) equations for the flow through a baffled culvert. In Flow-3D®, the conservation of mass, momentum, and energy equations in a fluid are solved using a finite volume or finite difference method in an Eulerian rectangular or cylindrical grid domain. The fully three-dimensional transient Navier-Stokes equations are formulated using the Fractional Area/Volume Obstacle Representation (FAVOR) and the Volume of Fraction (VOF) methods. The FAVOR is used to model the complex geometric regions and the VOF tracks the interface shape in the two-phase flow. Flow-3D® can solve the model equations by explicit or implicit scheme with using first-order or second-order accuracy.

The continuity equations in the Cartesian coordinates for incompressible flow two-phase flow in Flow-3D® is given per the following equation (Flow Science 2006)

$$\frac{\partial}{\partial x}(uA_x) + \frac{\partial}{\partial y}(vA_y) + \frac{\partial}{\partial z}(wA_z) = 0 \qquad (2\text{-}2)$$

where A_x, A_y, and A_y are the fractional area open flow in the x, y, and z directions, respectively. ρ is the fluid density. The momentum equations for the fluid velocity (u, v, w) in the three coordinate directions (x, y, z) are given as (Flow Science 2006)

$$\frac{\partial u}{\partial t} + \frac{1}{V_F}\left(uA_x\frac{\partial u}{\partial x} + vA_y\frac{\partial u}{\partial y} + wA_z\frac{\partial u}{\partial z}\right) = -\frac{1}{\rho}\frac{\partial p}{\partial x} + G_x + f_x + b_x$$

$$\frac{\partial v}{\partial t} + \frac{1}{V_F}\left(uA_x\frac{\partial v}{\partial x} + vA_y\frac{\partial v}{\partial y} + wA_z\frac{\partial v}{\partial z}\right) = -\frac{1}{\rho}\frac{\partial p}{\partial y} + G_y + f_y + b_y \qquad (2\text{-}3)$$

$$\frac{\partial w}{\partial t} + \frac{1}{V_F}\left(uA_x\frac{\partial w}{\partial x} + vA_y\frac{\partial w}{\partial y} + wA_z\frac{\partial w}{\partial z}\right) = -\frac{1}{\rho}\frac{\partial p}{\partial z} + G_z + f_z + b_z$$

where V_F is the fractional volume open to flow. G_x, G_y, and G_z are the body accelerations in the x, y, and z directions, respectively. (f_x, f_y, f_z) are the viscous accelerations in (x, y, z) directions and (b_x, b_y, b_z) are flow losses in porous media in (x, y, z) directions. In Flow-3D®, there are five turbulence models for viscous flow; Prandtl mixing length model, one-equation, two-equation k-ϵ model, Renormalized Group k-ϵ model (RNG), and Large Eddy Simulation (LES) model. In the current study, two-equation k-ϵ, Renormalized Group k-ϵ model (RNG), and Large Eddy Simulation (LES) model were adopted to simulate the flow through baffled-culvert. Experimental data measured with the Particle Image Velocimetry (PIV) were used to assess the accuracy and the applicability of these turbulence models in predicting the turbulent flow characteristics of the flow through a weir-baffled culvert for various culvert slopes and flow rates.

Computational Details

A weir-baffled culvert of 18.3 m long, 0.57 m in diameter was simulated numerically with three turbulence models including two-equation k-ϵ model, Renormalized Group k-ϵ model (RNG), and Large Eddy Simulation (LES) model. The baffle spacing was 0.518 m and the baffle height was 0.086 m with a 0.014 m in thickness (consistent with the baffled culvert tested in the laboratory). The culvert was simulated in three-dimensions for a variety of culvert slopes (0.5% to 6%) at flow rates of Q=28.3 L/s, Q=56.5 L/s, and Q=85 L/s.

A no slip boundary condition was used for the wall boundary and the inlet boundary condition was set to volumetric flow with a specified water depth obtained experimentally via a piezometer tube. The exit boundary was set to outflow boundary condition and the symmetry boundary condition placed at the centerline of the culvert to minimize the computational grids and consumed time. The upper boundary was chosen to be a pressure boundary condition and placed at a distance far away from the water depth. The second-order scheme accuracy and explicit were adopted. The fluid in the culvert was specified as water with a density of 1000 kg/m^3 and a viscosity of 0.001 kg/m.s. The acceleration components are chosen based on the culvert slope. A non-uniform grid of 964×50×40 cells in the x, y, and z directions respectively was adopted (Fig. 2-14). The mesh was refined near the culvert wall and over the baffles to provide more details about the boundary layers. No-slip condition was used for the culvert wall. Table 2-1 summarizes the tested weir baffled-culvert over the range of slopes and flow rates for fish passage, PIV measurements, and turbulence models.
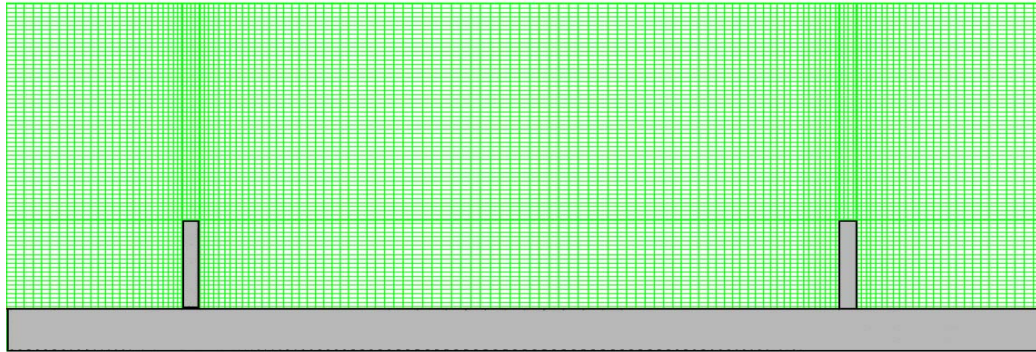
Fig. 2-14. Mesh geometry

Table 2-1. Summary of fish passage test conditions

S (%)	Q (L/s)	Fish Passage	$k\text{-}\epsilon$ model	RNG model	(LES) model	PIV
0.5	28.3	No	No	Yes	Yes	Yes
	56.6	No	No	Yes	No	Yes
	85.0	No	No	Yes	No	Yes
1.5	28.3	No	No	Yes	No	Yes
	56.6	No	No	Yes	No	Yes
	85.0	No	No	Yes	No	Yes
2.5	28.3	No	No	Yes	No	Yes
	56.6	No	No	Yes	No	Yes
	85.0	No	No	Yes	No	Yes
3.0	28.3	Yes	No	Yes	No	Yes
	56.6	Yes	No	Yes	No	Yes
	85.0	Yes	No	Yes	No	Yes
3.5	28.3	Yes	Yes	Yes	No	Yes
	56.6	Yes	Yes	Yes	No	Yes
	85.0	Yes	Yes	Yes	Yes	Yes
4.0	28.3	Yes	No	Yes	No	Yes
	56.6	Yes	No	Yes	No	Yes
	85.0	Yes	No	Yes	No	Yes
5.0	28.3	Yes	No	Yes	No	No
	56.6	Yes	No	Yes	No	No
	85.0	Yes	No	Yes	No	No
6.0	28.3	Yes	Yes	Yes	No	Yes
	56.6	Yes	Yes	Yes	No	Yes
	85.0	Yes	Yes	Yes	Yes	Yes

CHAPTER 3

FISH PASSAGE BEHAVIOR FOR SEVERE HYDRAULIC CONDITIONS IN BAFFLED CULVERTS[1]

Abstract

Laboratory tests were conducted with brown trout to evaluate their ability to pass through a small, baffled prototype-scale culvert under a variety of culvert slopes and discharge conditions. The culvert was 18.3 m long and 0.60 m in diameter with $0.15D$ baff25le height and $0.9D$ spacing, where D is the culvert inside diameter. An inverse relationship was observed between fish passage success and flow rate and/or culvert slope. The influence of the sample fish population and the length of the individual fish on passage rates were investigated; the data showed that the brown trout fish passage sample size evaluated in this study (25 per test) was sufficiently large to minimize sample size dependency. The elapsed time required for fish to traverse the culvert decreased with increasing hydraulic difficulty primarily owing to diminishing resting zones. The behavior of fish traversing the culvert was observed and reported, including resting/staging zone locations.

Introduction

Culverts are used to convey water from one side of a road to the other. One concern with culvert use is their potential to negatively impact the ability of fish to pass through them (Bell 1986; Clay 1995). Upstream culvert fish passage can be inhibited by a

---

[1] Khodier, M.A., and Tullis, B.P. (2014). "Fish Passage Behavior for Severe Hydraulic Conditions in Baffled Culverts." *J. Hydraul. Eng.*, ASCE, 140(3), 322-327.
Used with permission from ASCE (see Appendix B)

variety of parameters, including culvert flow velocities, culvert length, insufficient water depth, hydraulic roughness, and increased turbulence (Pearson et al. 2006). One technique for improving the likelihood of fish passage is to install baffles along the culvert invert. Baffles are weir elements built inside the culverts at regular spacing and specific height. The baffles decrease the flow velocity and increase flow depth, both of which help improve fish passage. At smaller discharges, a chutes-and-pools flow pattern develops in culverts, providing fish places to rest (Rajaratnam et al. 1988). At larger discharges, two flow regions are established: skimming and recirculating eddy flow. A skimming flow region forms above the baffles, which conveys flow through the culvert. Between the baffles, a recirculating flow eddy forms, creating a reverse velocity direction along the invert of the culvert (velocity is in the upstream culvert direction); fish seek resting zones in the eddy region but must pass through the higher velocity skimming flow region to progress upstream.

Many studies have investigated the influence of baffle design on flow characteristics in culverts. Rajaratnam et al. (1989) tested offset baffle and slotted-weir baffle designs in circular pipe. They developed relationships correlating discharge (Q), flow depth (y), culvert slope (S), and gravity acceleration (g) for baffle heights (h) equal to 0.1D and 0.15D and baffle spacing equal to 0.3, 0.6, 1.2, and 2.4D (where D is the culvert diameter). They concluded that all baffle designs tested produced similar results. Rajaratnam et al. (1991) and Feurich et al. (2011) tested a spoiler-baffle geometry using physical and computational modeling approaches, respectively, but despite producing flow characteristics more conducive to fish passage, its use in practice would likely be

limited owing to a relatively high cost. Neither referenced study actually evaluated fish passage. In the present study, brown trout were tested in a baffled culvert, and the influences of culvert slope and discharge on fish passage were observed.

Morrison et al. (2009) investigated the interaction between flow turbulence characteristics and culvert fish passage. An experimental investigation was conducted on a spiral-corrugated culvert fitted with baffles at a single culvert slope (S) of 1.14% and Q ranging from 43 to 198 L/s. The culvert inside diameter was 1.83 m and had a length of 12.2 m. They evaluated the interaction between juvenile salmon culvert passage and turbulence but found no significant correlation. Tritico and Cotel (2010) studied the effect of turbulent eddy diameter and vorticity on the swimming speed and stability of creek chub (Semotilus atromaculatus). They concluded that the presence of turbulent eddies in the flow affects the fish's habitat selection, migration, and ability to maintain posture in a flow. Tritico and Cotel limited their study to a short test section of culvert; consequently, no fish passage data were reported.

Liao et al. (2003) suggested that fish could use the presence of distributed flow eddies as a swim aid, thereby reducing the amount of energy the fish expended while in motion. Pearson et al. (2005) performed field testing on juvenile coho salmon (Oncorhynchus kisutch) passage through corrugated nonbaffled culverts. In their study, they evaluated a range of discharges through culverts with slopes of 1.14 and 4.33%. They correlated the relationship between passage success and mean culvert flow velocity. Smith et al. (2005) observed that juvenile salomids preferred to swim in areas of high velocity and low turbulence and avoided areas of low velocity and high turbulence. Olsen

and Tullis (2013) conducted a laboratory study of wild brown trout fish passage through prototype-scale (0.6-m diameter) smooth-walled baffled and nonbaffled culverts under a variety of culvert slopes ($0\% \leq S \leq 3.5\%$) and discharges (28.3-85 L/s). They concluded that fish passage success rates in a smooth-walled culvert can be improved by installing baffles, and the average culvert flow velocity can be used as an indicator to predict fish passage success rates. To help with the hydraulic design and analysis of baffled culverts, Olsen and Tullis (2013) also evaluated the variation in hydraulic roughness (Manning's n) between 0.6-m diameter smooth-walled and baffled high-density polyethylene (HDPE) culverts.

Another factor that may influence fish passage is the physical characteristics of the individual fish, such as fish length and weight. Many studies have evaluated the influence of fish length on swimming strength (Tillinger and Stein 1996). Behlke et al. (1991) found that larger fish were more likely to be successful in culvert passage than smaller fish; they developed a relationship relating fish swimming strength to fish total length. Watts (1974) concluded that the swimming speed of juvenile fish increases with increasing fork length of the fish tail and total fish length. Conversely, Belford and Gould (1989) reported little correlation between fish size and ability to pass through culverts. This study evaluated wild brown trout passage through a weir-baffled culvert under a variety of steep culvert slopes ($3.0\% \leq S \leq 6\%$) and discharge conditions. The influences of fish sample size and experiment duration on fish passage results were also investigated. The behavior of fish passing through the baffled culvert and the ways fish

utilized flow zones created by the baffled flow for resting were investigated and are described in this study.

Experimental Setup

Experiments were conducted at the Utah Water Research Laboratory (UWRL) at Utah State University. An 18.3-m long, D=610 mm (19.1-mm wall thickness) weir-baffled culvert (Fig. 3-1) [same baffled culvert tested by Olsen and Tullis (2013)] was used to evaluate fish passage behavior. The culvert was made from high-density polyethylene (HDPE). The baffles spacing was 0.9D and the baffle height was 0.15D. The upstream end of the baffled culvert was connected to a head tank by a short 1.5-m long smooth-walled pipe segment, and the downstream end discharged to a tail box (Fig. 3-2). To maintain uniform culvert slopes, the culvert was continuously supported by a steel I-beam assembly. To adjust the culvert slope, a set of adjustable pipe stands was used to support the steel I-beam. A flexible coupler at the upstream and downstream ends of the test culvert facilitated culvert slope changes. The elevation of the head tank was fixed; the elevation of the tail box was adjusted with each culvert slope tested.
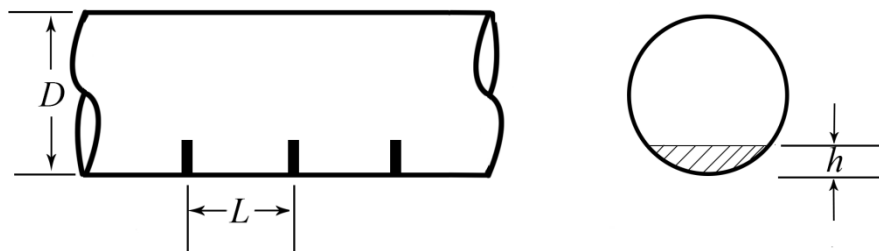
Fig. 3-1. Weir-baffled culvert geometry
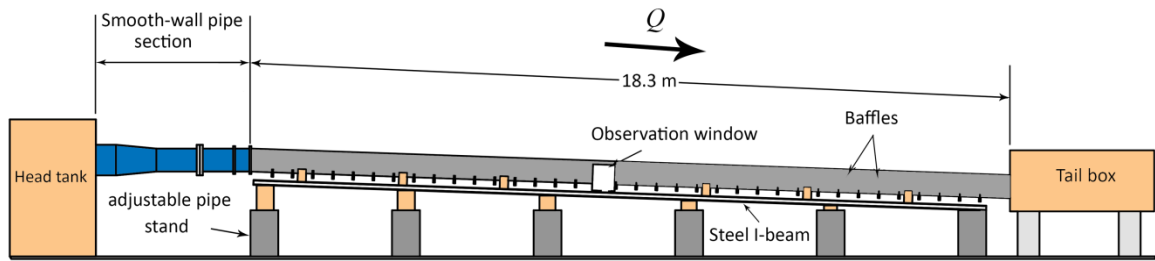
Fig. 3-2. Schematic of culvert fish passage test facility

Small rectangular observation windows cut into the crown of the culvert on 1.5-m centers provided viewing and instrumentation access. A water-tight observation/instrumentation window was installed in the side wall near the mid-span of the culvert between two baffles. A 355-mm-wide by 406-mm-tall flexible sheet of clear Lexan was used to replace the curved section of culvert wall that was removed. To eliminate the optical distortion for the video imaging through the curved window, a clear acrylic box with dimensions 584 × 685 × 635 mm (1.27 mm wall thickness) was attached and sealed to the pipe exterior around the view window (Fig. 3-3) and then filled with water.

A high-resolution video camera was used to record the behavior of fish swimming upstream past the observation window. The head tank was supplied with water through a 0.3-m-diameter pipe; flow rates were measured using calibrated Venturi flow meters (±0.25%). Average flow velocities at the baffle cross sections were evaluated by measuring the water surface elevations (measured using piezometer tubes), calculating the corresponding above-baffle flow area, and dividing that into the $Q(V = Q/A)$. All tests were conducted on wild brown trout (Salmo trutta) collected from the Logan River

(located adjacent to the laboratory facility) using either electroshocking or hook and line techniques. All fish were measured (length), tagged, and numbered for identification.

For each test, flow rate (Q), culvert slope (S), average flow velocity (V), timeline (the number of fish in the head tank as a function of time), and the tag number of each fish that passed the culvert were recorded; fish behavior and flow conditions were also documented using digital video. Test durations were typically1.5 h but were occasionally extended to 2 h when fish located near the upstream end of the culvert had not yet exited into the head tank.

Care of Fish

Fish were held in a 1325-L (350-gal.) tank when not being tested. A hose supplied continuous fresh water from the Logan River to maintain some level of consistency between the laboratory storage tank and the natural river environment in organic content, dissolved oxygen level, odor, and water temperature.
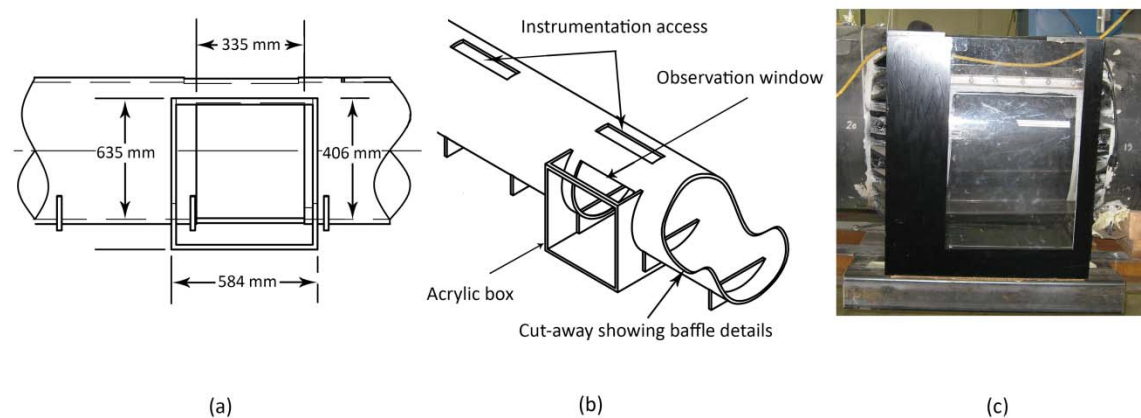
Fig. 3-3. Overviews of baffled culvert observation ports and windows for fish viewing (a) elevation; (b) perspective; (c) photographic

A nozzle attached to the end of the hose produced a high-velocity water jet at the water surface in the tank to supply oxygen to the fish. An overflow vertical drain pipe in the tank maintained the water elevation at a consistent level and prevented the tank from overflowing. One night crawler (worm) per fish was supplied to the tank daily. In addition to the continuous refreshing flow of river water, the water in the tank was changed every 5 days to avoid potential disease development and propagation in the tank. Biological fish waste and food remains were removed from the water every 2 days. A nonintrusive visual inspection of the fish in the tank was completed daily. The fish were allowed a minimum of 1-day of rest between culvert swim tests, although the rest periods were typically longer. Following the 6-week test program, the fish were returned to the Logan River.

Experimental Results and Discussion

Fish Passage Results

Olsen and Tullis (2013) evaluated brown trout passage through a baffled culvert with S ranging from 0 to 3.5% and Q equal to 28.3, 56.5, and 85 L/s. In this study, the same culvert test facility and discharges were evaluated for S ranging from 3 to 6%. The number of fish, percentage of fish passing, Q, and S for Olsen and Tullis (2013) and the current study are shown in Fig. 3-4. The 0.5 to 2.5%, slope data are from Olsen and Tullis (2013); the 3.0 to 6.0% slope fish passage data are from the current study. According to the Fig. 3-4 data, the percentage fish passage trend is inversely proportional, in general, to S and Q. For $S = 3.0$, 3.5, and 4.0%, the percentage of fish passage at the smallest discharge ($Q = 28.3$ L/s) was relatively consistent and successful (~75–84%); the

percentage fish passage at the middle discharge (Q = 56.5 L/s) was also relatively consistent (~60–63%). At the largest discharge (Q = 85 L/s), the fish passage dependency on slope was apparent; the percentage fish passage at Q = 85 L/s trended from 51% at S = 3.0%, to 43% at S = 3.5%, to 4% at S = 4.0%, and to 0% for S > 4.0%. The percentage fish passage significantly decreased (for all Q values) between S = 4.0 and S = 5.0%. The data in Fig. 3-4 show a few fish passing in the range of 1.3 < V < 1.5 with one exception test (S = 3.5% and Q = 85 L/s), but no fish passage occurred at V > 1.5 m=s (threshold velocity).
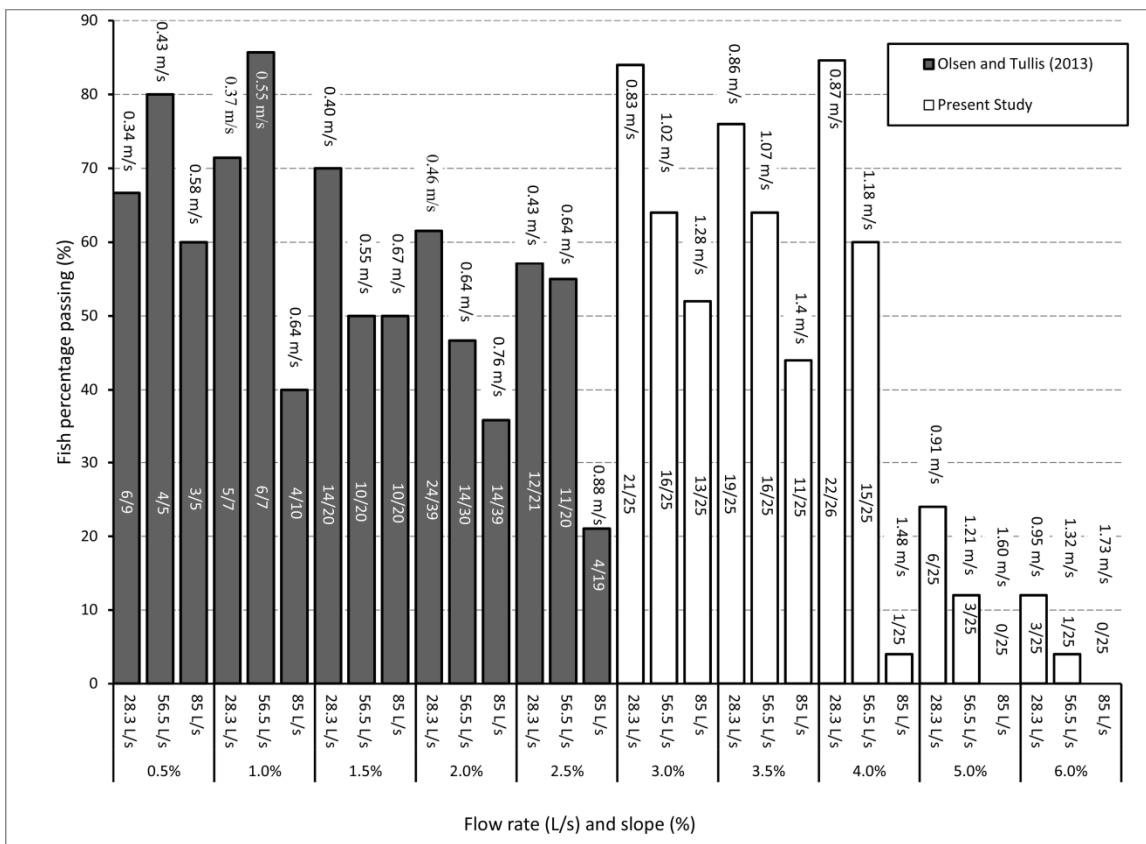
Fig. 3-4. Summary of baffled-culvert fish passage data as a function of S and Q

Repeatability and Fish Sample Size

For projects in which the data are heavily statistically based, it is important to develop some understanding of the influence of sample size on the results and result repeatability. Issues of minimum sample size and data repeatability become even more significant when biological components (e.g., fish behavior) are included. The influence of sample size (relative to brown trout and these culvert flow conditions) was evaluated by comparing $S = 3.0$ and $S = 3.5\%$ fish passage results from the present study and the Olsen and Tullis (2013) study as shown in Fig. 3-5 (different fish populations were used in each study). For the current study test data represented in Fig. 3-5, approximately 25 fish per test were used; 10–12 fish per test were used in the Olsen and Tullis (2013) trials.

In general, the inverse trend relationships between the percentage of fish passing and increasing Q and S are similar in both studies; however, as Fig. 3-5 shows, the correlation between tests is better for the three less challenging hydraulic conditions (28.3 L/s at 3.0%, 56.5 L/s at 3.0%, and 28.3 L/s at 3.5%) and poor (i.e., more scatter between studies) for the three more challenging hydraulic test conditions. The variability in the test results presented in Fig. 3-5 may be attributable, in part, to variation in swimming ability of individual fish (e.g., fish size), environmental changes (e.g., water temperature), and sample size. To further investigate the influence of sample size on the fish passage results, multiple tests were conducted in the current study for each hydraulic condition (S and Q) with varying fish sample sizes. Fig. 3-6 summarizes fish passage percentage with fish sample sizes, S and Q; fish sample sizes of 9, 17, and 25 fish were tested. The data in Fig. 3-6 show that for $S = 3.0$ and 4.0%, the deviation in fish percentage passing for each

sample size from the mean was less than approximately ±4.0% and approximately less than ±7.0% for S = 5.0 and 6.0%. No clear trends were apparent for the data in Fig. 3-6 relative to sample size, suggesting that the threshold for statistical independence is likely much higher than the 25-fish maximum sample size tested. The relative scatter in the data (< ±4.0 and < ±7.0%) also indicate that the sample sizes were sufficiently large to avoid gross errors. In general, subsequent current study test results presented in this paper are based on the 25-fish test sample size.
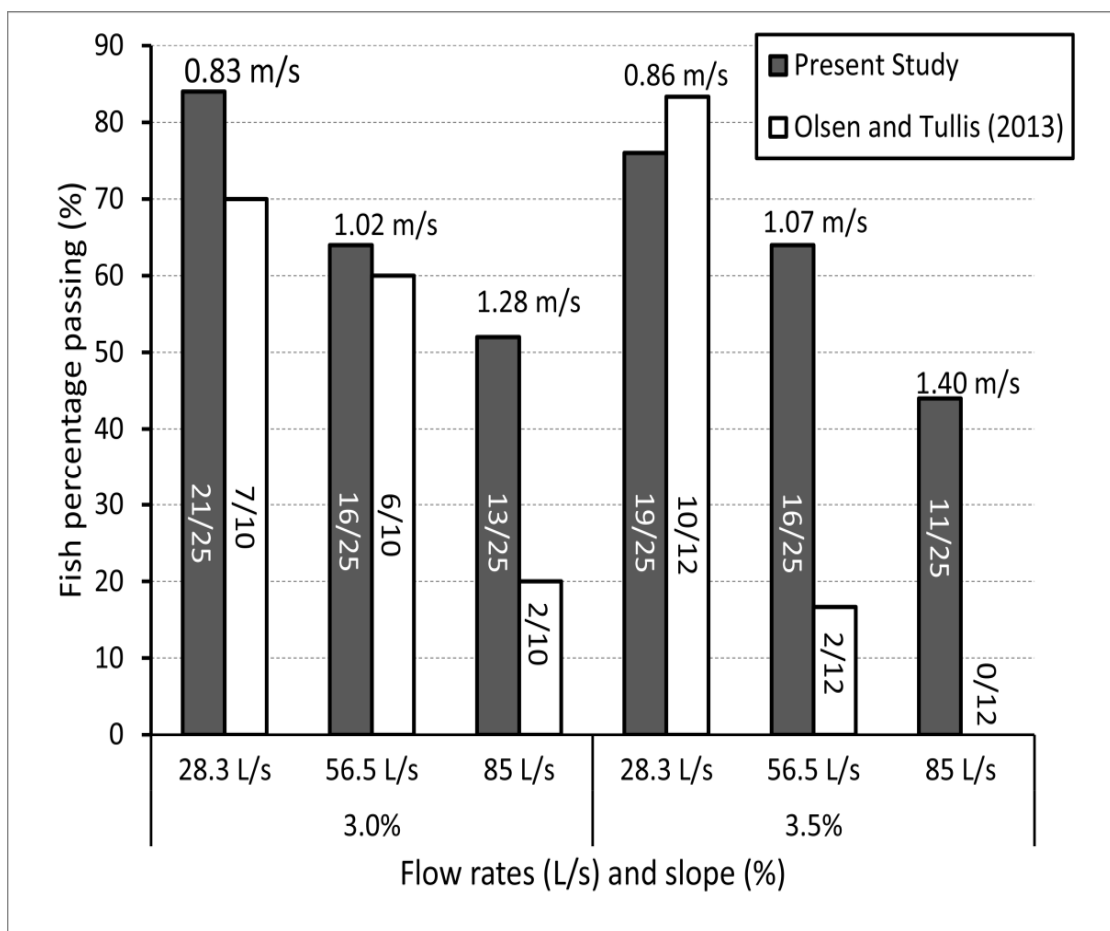
Fig. 3-5. Comparison of the present study baffled-culvert fish passage data and Olsen and Tullis (2013) for selected S and Q
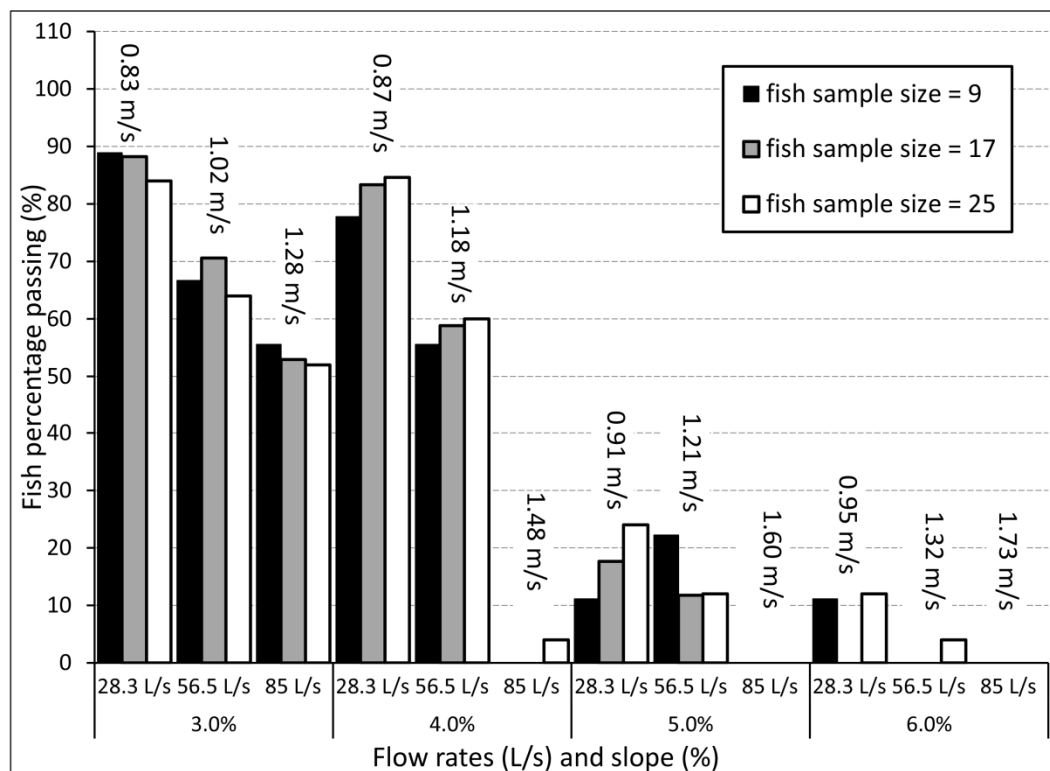
Fig. 3-6. Summary of baffled-culvert fish passage versus fish sample size

Fish Length and Fish Passage

The successful fish passage for each individual tested is reported in Fig. 3-7 as a function of fish length but independent of specific hydraulic test conditions. All reported fish were tested the same number of times: each fish had fifteen separate passage attempts. The data in Fig. 3-7 suggest that brown trout with lengths >279 mm are more likely to pass successfully through the baffled culvert than shorter brown trout. This supports the findings of Tillinger and Stein (1996), who determined that larger fish tend to be stronger swimmers owing to increased muscle mass development. The two fish with lengths of 268 and 272 mm appear to be outliers as they had the least number of successful
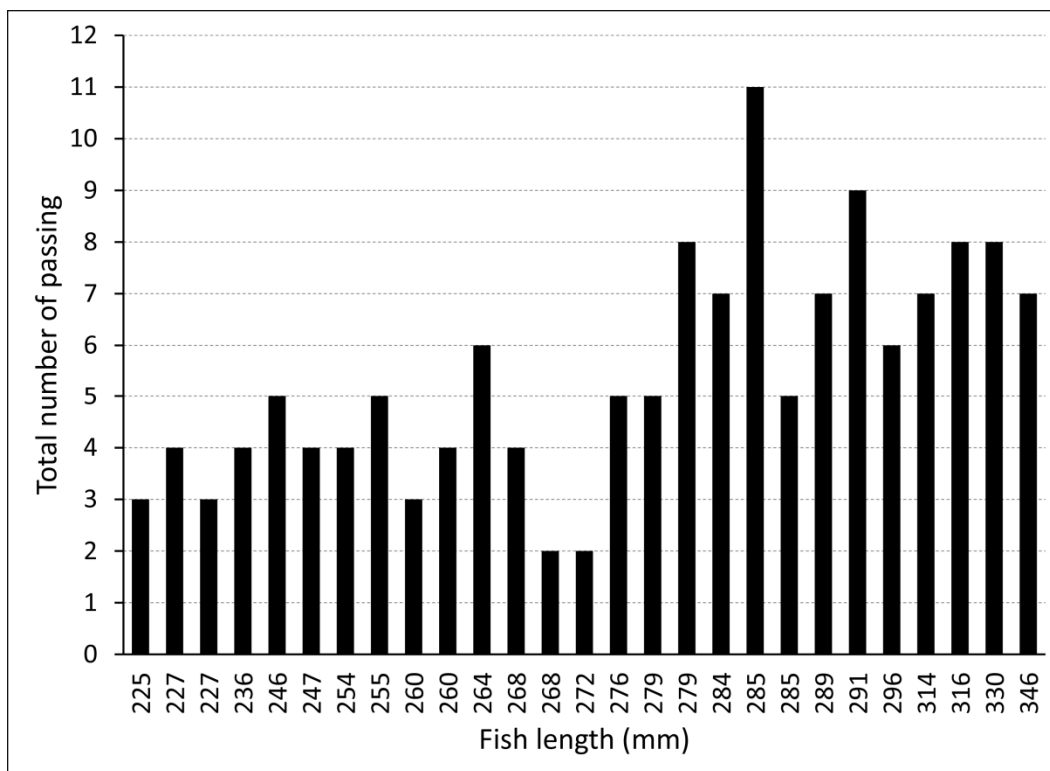
Fig. 3-7. Total number of successful culvert passages as a function of fish length (each column represents an individual fish, each fish participated in 15 trials)

 culvert passages despite the fact that their lengths fell in the average length range. This suggests that additional factors also influence a fish's ability to pass through baffled culverts.

Fish Passage Timeline

For each test, fish were introduced at the downstream end of the culvert. In 5-min increments, the locations of all the fish were noted, and in particular, the number of fish that had successfully traversed the baffled culvert and reached the head tank. Fig. 3-8 shows the number of fish in the head tank as a function of test time for $S = 3.0$ and $S = 5.0\%$ and different flow rates. The data in Fig. 3-8 indicate that the duration of the fish

passage tests were sufficiently long to be able to segregate the passing and nonpassing test fish. Observations revealed that the ability of the fish to find and utilize resting zones along the baffled culvert at easier hydraulic conditions (i.e., $S = 3\%$) increased the amount of time that fish would or could take to traverse through the culvert. As the hydraulic conditions became more severe (e.g., $S = 5\%$), the ability of the fish to maintain their position in resting zones along the culvert decreased. Consequently, the time required for successful fish passage typically decreased, as shown in Fig. 3-8. Many of the weaker swimmers were found at the downstream end of the pipe at the end of the test rather than distributed throughout.
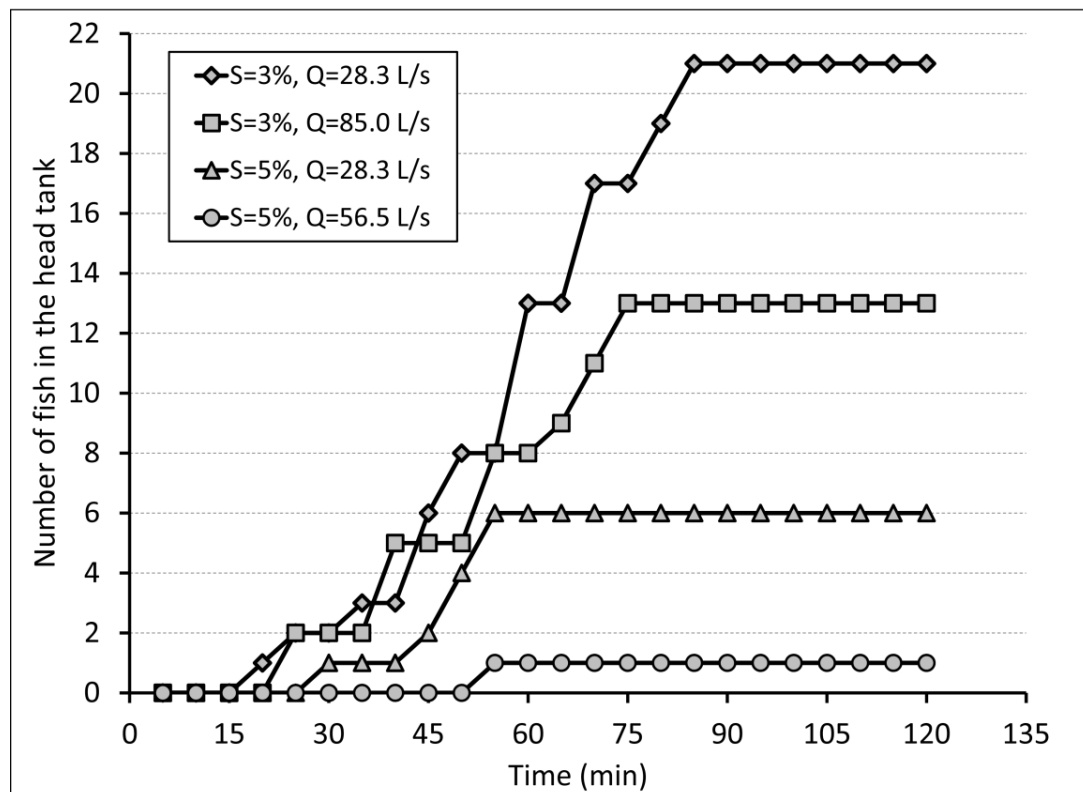
Fig. 3-8. Number of fish in the head tank (successful culvert passage) as a function of elapsed time

Fish Zones and Fish Behavior

The behavior of fish traveling past the observation window located at the midpipe location was monitored and recorded using a high-definition video camera. The fish were observed to prefer two zones in which they would typically hold up. Fig. 3-9 shows the locations of these zones (i.e., Zone 1and Zone 2) between two adjacent baffles. Zone 1 was located on the downstream side of the baffle, and Zone 2 was located along either sidewall in between baffles. When in Zone 1, the fish would typically align their bodies parallel to the baffle (perpendicular to the mean flow direction) as shown in Figs. 3-9(a) and 3-10(a). In Zone 2, fish could swim for a prolonged period of time; movement of fish between Zones 1 and 2 was also observed. Zone 1 was typically used more as a resting place; Zone 2 was typically used as more of a staging area before advancing farther upstream. Some fish bypassed the observation window without stopping in the resting zone.
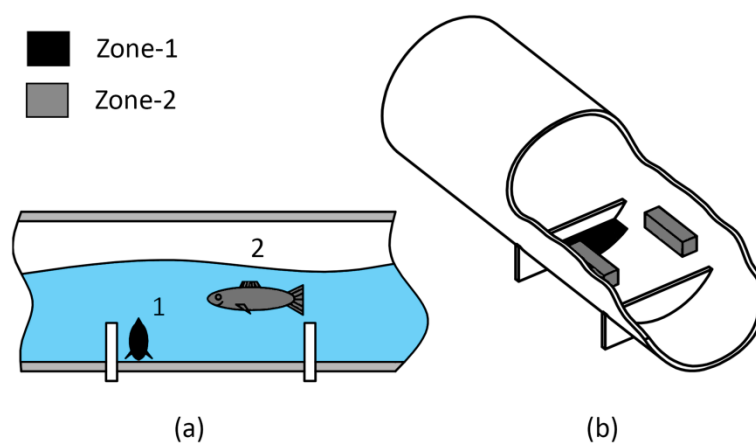
Fig. 3-9. Illustrations of fish resting/staging zones in the baffled culvert (a) elevation; (b) perspective
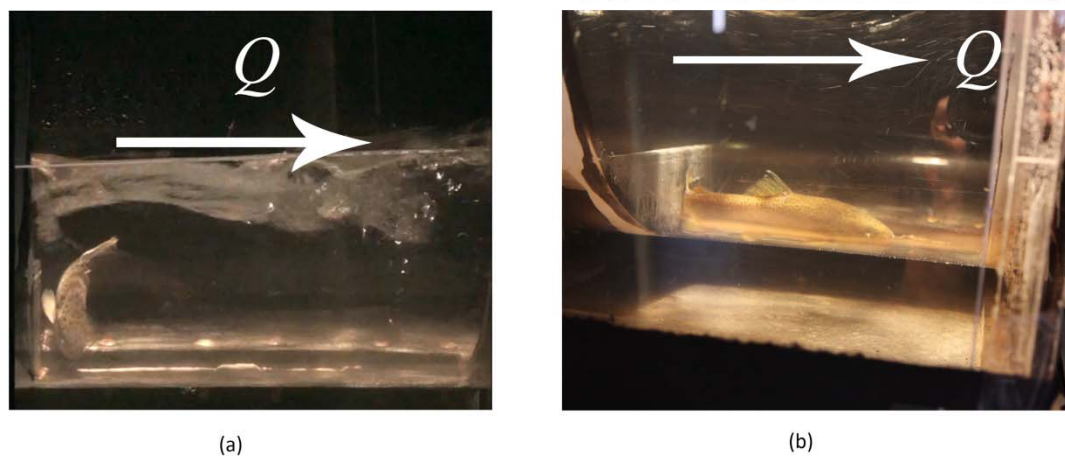
Fig. 3-10. Photographic examples of fish resting: (a) in Zone 1; (b) along the pipe invert facing the between-baffle recirculating eddy flow with its tail braced against a baffle

Fish behavior in Zone 1 and Zone 2 was observed visually along the entire culvert through the small rectangular observation windows cut into the crown of the culvert. In at least one case, one fish that appeared to be very fatigued planted itself in Zone 1, aligned itself with the culvert axis, and braced itself with its tail against the downstream side of the baffle for support [see Fig. 3-10(b)]. Its head was facing the mean-flow downstream direction, but locally, it faced the oncoming approach flow velocity created by the between-baffle flow eddy that formed near the culvert invert. The fish was able to hold its position but never advanced farther up the culvert.

Many of the fish spent a good deal of time resting near the transition between the baffled culvert and the smooth-walled pipe before passing into the upstream head tank. In some cases, fish were able to traverse the entire length of the baffled culvert but were not able to navigate the nonbaffled section until the flow rate was reduced at the end of the test. This indicates that baffle installation in culverts indeed helps the fish to pass and

increases the potential for successful fish passage; however, the smooth-walled pipe section may have also influenced the fish passage results obtained in this study.

Fish Passage Statistical Analysis

A statistical analysis was evaluated to investigate in the influence of fish sample size, flow rates, and culvert slope on the fish percentage passing data. The statistical software (R studio, version 2.15.2) was used to calculate the confidence interval which uses the analysis of variance method (AOV) with a confidence interval of 95%. Table 3-1 shows the results of the statistical analysis for the influence of the fish sample size on the fish percentage passing. As it shown in Table 3-1, the influence of the each fish sample size (9, 17, or 25) on the fish percentage passing is not different with a confidence interval greater than 95%. Pr represents the probability in Table 3-1. The influence of the fish sample size of 9 at culvert slope of 3% is different from the influence of the fish sample size of 17 at culvert slope of 6% on the fish passage results (for more details see Appendix: A, Table A.2).

Table 3-2 shows that the influence of the flow rates $Q = 28.3$ L/s on the fish passage results is different from the influence of the flow rates $Q = 85$ L/s. Table 3-3 shows that the influence of the culvert slope on the fish passage results. The red numbers indicate that there is a difference in the influence on the fish passage data. Note that the influence of culvert slope of ($S = 3\%$) and ($S = 4\%$) on fish passage results is not different and the same behavior for culvert slope of ($S = 5\%$) and ($S = 6\%$). Also, the influence of the culvert slope is more significant on the fish passage results than the influence of the flow rates. More explanation for this behavior will be discussed later.

Table 3-1. Statistical analysis for the fish sample size influence on the fish percentage passing

Fish Sample Size	VS.	Fish Sample Size	Diff.	Lower	Upper	Pr
9		17	-0.47583	-24.0833	23.1316	0.9986
9		25	0.965	-22.6424	24.5724	0.9942
17		25	1.40833	-22.1666	25.0483	0.9872

Table 3-2. Statistical analysis for the flow rates influence on the fish percentage passing

Q (L/s)		Q (L/s)	Diff.	Lower	Upper	Pr
28.3	VS.	56.5	-13.089170	-47.698020	21.519688	0.621634
28.3		85	-34.851670	-69.460520	-0.242812	0.048161
56.5		85	-21.762500	-56.371350	12.846354	0.280326

Table 3-3. Statistical analysis for the culvert slope influence on the fish percentage passing

S (%)		S (%)	Diff.	Lower	Upper	Pr
4.0		3.0	-22.0888	-52.2009	8.02318	0.207448
5.0		3.0	-58.2477	-88.3581	-28.1357	0.000099
6.0	VS.	3.0	-66.2066	-96.3187	-36.0945	0.0000164
5.0		4.0	-36.1588	-66.2709	-6.0468	0.0144643
6.0		4.0	-44.1177	-74.2298	-14.0057	0.0025005
6.0		5.0	-7.95888	-38.0709	22.2153	0.884454

Conclusion

Brown trout passage in a prototype-scale weir-baffled culvert (18.3 m long and 0.60 m in diameter, with 0.9D weir baffle spacing and 0.15D baffle height) under a

variety of steep-culvert slopes and discharge conditions was evaluated experimentally in a controlled laboratory environment. Tests were conducted at culvert discharges (Q) of 28.3, 56.5, and 85 L/s at slopes (S) of 3, 3.5, 4, 5, and 6%. Based on the results from this study, the following conclusions are made:

- Fish passage data indicated an inverse relationship between the fish passage percentages and both flow rate and culvert slope. No fish successfully passed through the baffled culvert at the maximum discharge ($Q = 85$ L/s) for $S = 5$ and 6%. Depending on anticipated prototype discharges, an alternative fish passage technique should be considered for $S \geq 5\%$.

- Tests comparing the influence of fish sample size effect on fish passage showed variation $< \pm 4.0\%$ for the less severe hydraulic test conditions (based on S and Q) and $< \pm 7.0\%$ for the more severe hydraulic test conditions. For the fish sample sizes tested (e.g., 9, 17, and 25), no clear trends were observed between fish passage results and sample size.

- In general, fish passage increased with fish length, particularly for brown trout longer than 279 mm. The poor test performance of the two midlength fish ($L =$ 269 and 272 mm), however, suggests that length is not the only factor that influences successful fish passage for the conditions tested in this study.

- For the cases in which fish successfully navigated the full length of the culvert, the culvert passage time generally decreased with increasing hydraulic difficulty as the fish were less likely/able to find effective resting locations. With less severe

hydraulic conditions, the successfully passing fish often spent more time in the culvert, attributable in part to the presence of useable resting zones.

- Two preferable resting zones where noted: Zone 1, which was located just downstream of the baffles, and Zone 2, which was located along the sidewalls. Fish would often use Zone 2 as a staging area before passing over the next baffle. Future studies related to fish passage through baffled culverts should include the evaluation of fish passage for additional fish species and variations in culvert diameter and baffle geometry. A field investigation should also be conducted to correlate fish passage behavior between field and laboratory conditions.

CHAPTER 4

EXPERIMENTAL PARTICLE IMAGE VELOCIMETRY (PIV) AND THREE-DIMENSIONAL NUMERICAL SIMULATION COMPARISON[2]

Abstract

Turbulent flow through weir baffled-culvert was simulated numerically using three-dimensional numerical model employing (k-ϵ) model, Renormalized Group k-ϵ model (RNG), and Large Eddy Simulation (LES) models. Experimental data measured with the Particle Image Velocimetry (PIV) were used to assess the accuracy and the applicability of these turbulence models in predicting the turbulent flow characteristics of the flow through a weir-baffled culvert for various culvert slopes and flow rates. The comparison of the velocity and turbulent kinetic energy between measured and simulated flow field found the Renormalized Group k-ϵ model (RNG) to be the most appropriate model for evaluating flow through this specific baffled culvert and discharge conditions. Renormalized Group k-ϵ model (RNG) more accurately represented the recirculation flow field on the downstream side of the baffles relative to the k-ϵ and LES models.

Introduction

Culverts are used to convey water from one side of a road to another. In some cases, culverts can become barriers to fish passage if flow velocities are too large and/or flow depths are too shallow. A number of studies have investigated the interaction between fish passage and culverts (e.g., Bell 1986; Clay1995; Olsen and Tullis 2013; see Chapter 3). In addition to the influence of the flow characteristics on the fish passage,

---

[2] Coauthored by Blake P. Tullis

physical characteristics of the fish also influence the fish passage success (e,g., Watts 1974; Belford and Gould 1989; Behlke et al.1991; Tillinger and Stein 1996; Chapter 3). One possible solution to improve the fish passage through culverts is to install baffles along the culvert invert at regular spacings. Rajaratnam et al. (1988), Rajaratnam et al. (1989), Rajaratnam and Katopodis (1990), and Rajaratnam et al. (1991) studied the flow characteristics of baffled culverts with different baffle designs. In their studies, a single point measurement of the velocity was collected using the pitot-static tube at the center line of the culvert, whereas Pearson et al. (2005), Pearson et al. (2006), and Morrison et al. (2009) collected the hydraulic data for the flow through baffle and non-baffled culverts using Acoustic Doppler Velocimetry (ADV) techniques. They studied the influence of flow turbulence characteristics on fish passage.

Liao et al. (2003) conducted Particle Image Velocimetry (PIV) experiments on a short test section of flume to study the effects of vortices on Rainbow trout swimming behavior. They concluded that fish use flow vortices as swimming aids to conserve energy. Also, Tritico and Cotel (2010) used PIV on a short test section (flume of 0.25 m long × 0.60 wide × 0.55 m height) to study the effect of turbulent eddy diameter and vorticity on fish swimming speed and stability. They observed that the turbulent eddies influence the fish's habitat selection, migration, and swimming stability. Smith et al. (2005) studied the effects of the velocity and turbulence on the juvenile rainbow trout focal positions using ADV. They concluded that fish preferred to swim in areas of high velocity and low turbulence and avoided areas of low velocity and high turbulence. Feurich et al. (2011) performed a three-dimensional numerical investigation to study the

effect of the spoiler baffles on the flow field. They discussed the reduction if flow velocities caused by the spoiler-baffled culverts relative to non-baffled culverts.

Formulating a better understanding of the flow hydrodynamics is essential to developing a better understanding of the relationship between fish passage and baffled culverts. Because an analytical solution is not available for characterizing baffled culvert flow hydrodynamics, numerical simulation can be used, provided that the numerical models can be validated using experimental data. As turbulence flow can't be solved directly, the accuracy with which turbulent flows can be simulated computationally may vary with the specific turbulent model utilized in the simulation.

The goal of this study was to compare numerical simulations of baffled culvert flow featuring different turbulence models with experimental velocity and turbulent kinetic energy data from a prototype-scale baffled culvert collected in the laboratory using a PIV system. The three turbulence models used in the numerical simulations were the k-ϵ model, Renormalized Group k-ϵ model (RNG), and the Large Eddy Simulation (LES) model. The numerical results including the velocity profiles and turbulent kinetic energy (TKE) profiles at different culvert location were compared with the experimental PIV data.

Experimental Setup

Flow conditions in a 18.3-m long, 570-mm inner diameter baffled culvert were quantified using a PIV system. Experiments were conducted at the Utah Water Research Laboratory (UWRL) at Utah State University. The test pipe was made of high-density polyethylene (HDPE). Rajaratnam et al. (1989) and Rajaratnam and Katopodis (1990)

tested a variety of baffle spacing to baffle height ratio between 2 and 12 to determine the ideal baffle configuration for weir and slotted-weir baffles. They found that the most successful baffle spacing to baffle height ratio being between 4 and 6, based on hydrodynamic constraints (no fish were tested). In the current study, the baffle spacing to baffle height ratio was 6. The wall thickness of the pipe was 19.1 mm, the uniform baffles spacing was $0.9D$ (514 mm) and the baffles height was $0.15D$ (85.75 mm), where D is the inner diameter of the pipe. The upstream end of the culvert was connected to a head tank and the downstream end discharged to a tail box that could be adjusted for elevation as shown in Fig. 4-1. A pipe coupling connection in the supply pipe, located between the head tank and the baffled culvert test section, allowed the slope of the pipe to be adjusted. The head tank was supplied with water via a 0.3-m diameter pipe; flow rates were measured using calibrated venturi flow meters (±0.25%).

Water surface elevations were measured using piezometer tubes. The culvert was supported underneath by a steel I-beam assembly to maintain uniform culvert slopes; the culvert slope could be changed using a set of adjustable pipe stand that supported the culvert. An observation window was created near the mid point of the pipe between two baffles. A flexible sheet of clear Lexan (355-mm width by 406-mm tall) was used to replace the removed wall section. The sidewall viewing window was 355.6 mm width and 406.4 mm tall. In order to eliminate the optical distortion of the image through the curved window, an acrylic box with dimensions 584.2 mm×685.8 mm×635 mm was attached to the pipe exterior around the view window (see Fig. 4-2). By allowing the PIV camera to image through a vertical plane oriented normal to the line of sight and filling

the acrylic box with water so that the same liquid was present on both sides of the curved view window, the PIV system was able to provide accurate, undistorted velocity vector data. The PIV system consisted of a CCD camera with 1376×1040 pixels resolution and a laser Nd:YAG (neodymium-doped yttrium- aluminum- garnet) with light sheet optics to illuminate the interrogation area.
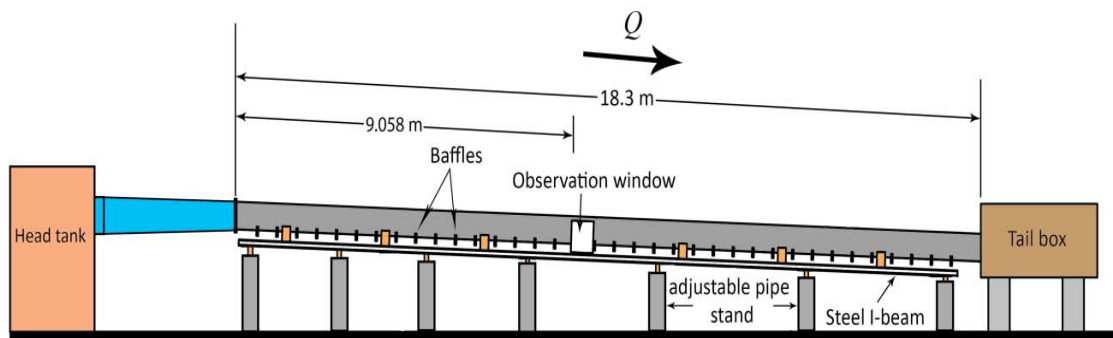
Fig. 4-1. Schematic of baffled-culvert test facility

(a) (b)
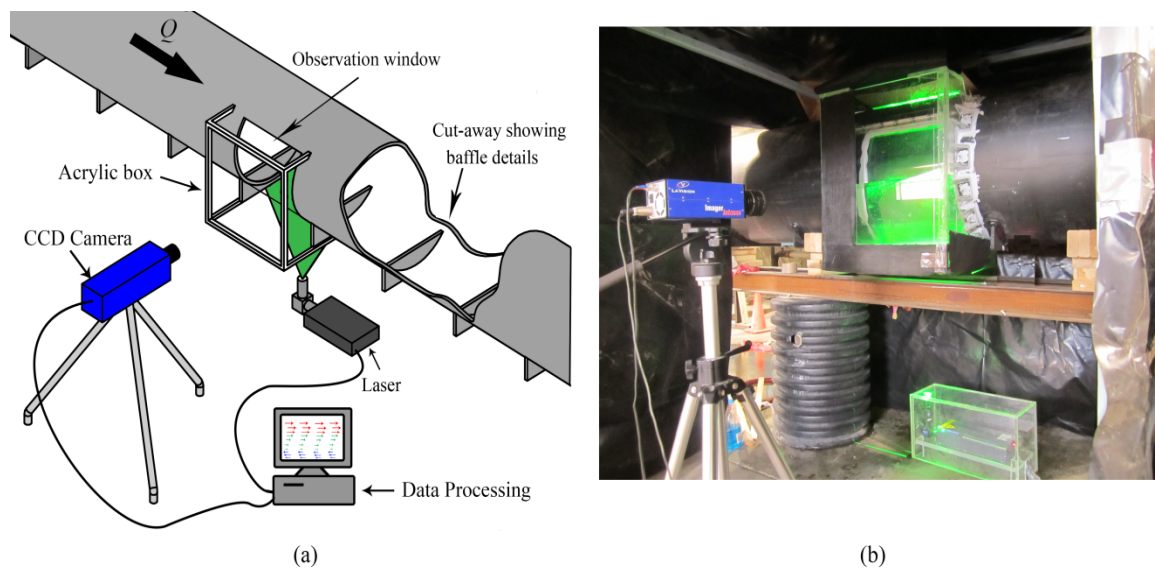
Fig. 4-2. Particle Image Velocimetry (PIV) setup

The PIV system was used to measure the velocity field in the longitudinal, centerline, vertical plane through the culvert. To insure that the PIV data results were independent on the number of images evaluated; large number of images (1000 images) was used to measure the average velocity vector field. A velocity vector field was measured for culvert slopes of 0.5%, 1.5%, 2.5%, 3.0%, 3.5%, 4%, and 6% at flow rates of Q=28.3 L/s, Q=56.5 L/s, and Q=85 L/s. The data obtained by the PIV system were used to validate the numerical simulation results.

Three-Dimensional Simulation

Flow-3D® produced by Flow Science was used to perform numerical flow simulations. This software uses the Volume of Fluid (VOF) method for solving dominant equations on flow at orthogonal mesh gridding. The Fractional Area/Obstacle Representation (FAVOR) was employed to represent the complex geometries for flow field grid generation. In Flow-3D®, three turbulent models are available; k-ϵ model, Renormalized Group k-ϵ model (RNG), and Large Eddy Simulation (LES) model. Fig. 4-3 shows a schematic of the flow domain that was solved using Flow-3D®.
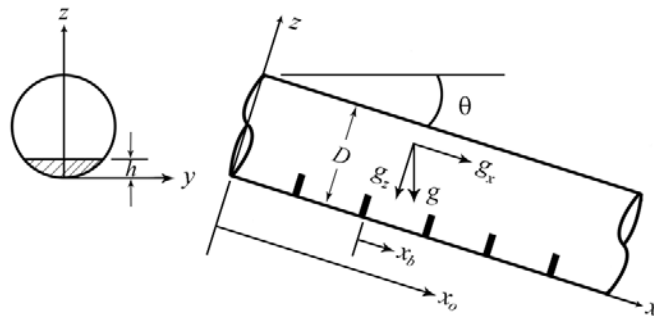
Fig. 4-3. Schematic of the problem

Flow-3D® solves the Reynolds-averaged Navier-Stokes (RANS) equations for conservation of mass and momentum as given per the following equations:

$$\frac{\partial \bar{u}_i}{\partial x_i} = 0 \tag{4-1}$$

$$\frac{\partial \bar{u}_i}{\partial t} + \bar{u}_j \frac{\partial \bar{u}_i}{\partial x_j} = -\frac{1}{\rho}\frac{\partial \bar{p}}{\partial x_i} + \frac{\partial}{\partial x_j}\left[\nu \frac{\partial \bar{u}_i}{\partial x_j} - \overline{u_i' u_j'}\right] + \bar{f}_i \tag{4-2}$$

where ρ is the density of the fluid and x_i represents the coordinate directions (x, y, z), $\bar{u}_i$ is the time-averaged velocity components (u, v, z), t is the time, $\bar{p}$ is the time-averaged pressure, $\bar{f}_i$ is the gravity force, ν is the fluid kinematic viscosity, and $\overline{u_i' u_j'}$ are the turbulent normal and shear stresses which can be expressed in terms of the velocity gradient by

$$-\overline{u_i' u_j'} = \nu_t \left(\frac{\partial \bar{u}_i}{\partial x_j} + \frac{\partial \bar{u}_j}{\partial x_i}\right) - \frac{2}{3}k\delta_{ij} \tag{4-3}$$

$$\nu_t = C_\mu \frac{k^2}{\epsilon} \tag{4-4}$$

In Eqns. (4-3) and (4-4), ν_t is the turbulent eddy viscosity, δ_{ij} is the Kronecker delta, k is the turbulent kinetic energy per unit mass, C_μ is an empirical coefficient, and ϵ is the turbulent energy dissipation rate per unit mass. The turbulent kinetic energy (k) and the turbulent dissipation rate in the k-ϵ model are given by

$$\frac{\partial k}{\partial t} + \bar{u}_i \frac{\partial k}{\partial x_i} = \frac{\partial}{\partial x_i}\left(\frac{\nu_t}{\sigma_k}\frac{\partial k}{\partial x_i}\right) + \nu_t \left(\frac{\partial \bar{u}_i}{\partial x_j} + \frac{\partial \bar{u}_j}{\partial x_i}\right)\frac{\partial \bar{u}_i}{\partial x_j} - \epsilon \tag{4-5}$$

$$\frac{\partial \epsilon}{\partial t} + \bar{u}_i \frac{\partial \epsilon}{\partial x_i} = \frac{\partial}{\partial x_i}\left(\frac{\nu_t}{\sigma_\epsilon}\frac{\partial \epsilon}{\partial x_i}\right) + C_{1\epsilon}\frac{\epsilon}{k}\nu_t \left(\frac{\partial \bar{u}_i}{\partial x_j} + \frac{\partial \bar{u}_j}{\partial x_i}\right)\frac{\partial \bar{u}_i}{\partial x_j} - C_{2\epsilon}\frac{\epsilon^2}{k} \tag{4-6}$$

The standard values of the model constants are

$$\sigma_k = 1.0, \sigma_\epsilon = 1.3, C_{1\epsilon} = 1.44, C_{2\epsilon} = 1.92, C_\mu = 0.09 \tag{4-7}$$

For the RNG model, the k and ϵ are determined from the following equations:

$$\frac{\partial k}{\partial t} + \bar{u}_i \frac{\partial k}{\partial x_i} = \frac{\partial}{\partial x_i}\left(\frac{v_{eff}}{\alpha_k}\frac{\partial k}{\partial x_i}\right) + v_t S_t^2 - \epsilon \tag{4-8}$$

$$\frac{\partial \epsilon}{\partial t} + \bar{u}_i \frac{\partial \epsilon}{\partial x_i} = \frac{\partial}{\partial x_i}\left(\frac{v_{eff}}{\alpha_\epsilon}\frac{\partial \epsilon}{\partial x_i}\right) + C_{1\epsilon}\frac{\epsilon}{k}v_t S_t^2 - C_{2\epsilon}\frac{\epsilon^2}{k} - R \tag{4-9}$$

$$v_{eff} = v_t\left(1 + \sqrt{\frac{v}{v_t}}\right)^2 \tag{4-10}$$

$$R = \frac{C_\mu \eta^3 (1-\eta/\eta_o)}{1+\beta\eta^3}\frac{\epsilon^2}{k} \tag{4-11}$$

$$\eta = \frac{k}{\epsilon}S_t \tag{4-12}$$

$$S_t = \sqrt{2\bar{S}_{ij}\bar{S}_{ij}} \tag{4-13}$$

where α_k and α_ϵ are Prandtl numbers for k and ϵ, respectively, S_t is the mean rate-of-strain tensor, and the standard values of the model constants are

$$C_{1\epsilon} = 1.42, C_{2\epsilon} = 1.68, C_\mu = 0.0845, \eta_o = 4.38, \beta = 0.012 \tag{4-14}$$

The $k\text{-}\epsilon$ model and the RNG model equations are quite similar but there are two main differences between them. The equation constants in the $k\text{-}\epsilon$ model are found empirically whereas the RNG model equation constants are derived explicitly. Furthermore; the equation for ϵ in the RNG model (Eqn. 4-9) has an additional source term (R), which is mainly a function of the mean rate-of-strain (S_t), turbulent kinetic energy (k), and turbulent dissipation (ϵ). According to Flow Science (2006), the changes in the equation constants (and the presence of the source term in the RNG model) makes the RNG model able to more accurately describe the low intensity turbulence flows (i.e., high turbulence flow) and flows having strong shear regions. LES is a time-dependent model that solves for instantaneous velocities in the flow domain. In the LES model, the effects of the

eddies that are too small to be resolved were approximated using an eddy viscosity term, which is proportional to a length scale times a measure of velocity fluctuations (Smagorinsky, 1963). The LES-filtered equations for the continuity and momentum equations are obtained as in equations (4-15) and (4-16), respectively.

$$\frac{\partial \overline{u_i}}{\partial x_i} = 0 \tag{4-15}$$

$$\frac{\partial}{\partial t}(\rho \overline{u}_i) + \frac{\partial}{\partial x_j}(\rho \overline{u}_i \overline{u}_j) = -\frac{\partial \overline{p}}{\partial x_i} + \mu \frac{\partial}{\partial x_j}\left[\frac{\partial \overline{u}_i}{\partial x_j} + \frac{\partial \overline{u}_j}{\partial x_i}\right] - \frac{\partial \tau_{ij}}{\partial x_j} \tag{4-16}$$

The subgrid stress (τ_{ij}) can be written as

$$\tau_{ij} = -2\mu_t \overline{S}_{ij} + \frac{1}{3}\delta_{ij}\tau_{kk} \tag{4-17}$$

$$\overline{S}_{ij} = \frac{1}{2}\left(\frac{\partial \overline{u}_i}{\partial x_j} + \frac{\partial \overline{u}_j}{\partial x_i}\right) \tag{4-18}$$

The eddy viscosity in the Smagorinsky (1963) model is represented as

$$\mu_t = \rho(cL)^2 \sqrt{2\overline{S}_{ij}\overline{S}_{ij}} \tag{4-19}$$

$$L = \left(\delta_x \delta_y \delta_z\right)^{1/3} \tag{4-20}$$

Where c is a constant between 0.1 and 0.2 and L is the length scale. δ_x, δ_y, and δ_z are the grid cell dimension in the x, y, z-direction, respectively.

Results and Discussion

Experimental Flow Field Data (PIV)

Flow field data through the weir-baffled culvert were measured using PIV. Fig. 4-4(a) shows the contours for the flow pattern for the space between two adjacent baffles for one specific flow condition. Based on the velocity data along the longitudinal centerline cross section, Figs. 4-4(a and b) show two distinct flow regions; the upper flow

column region is flowing in the forward direction and there is reverse flow in the lower flow column region between the baffles. The forward flow velocity distribution varies with location; the forward flow velocities are relatively uniform directly above the baffle; the reduced flow velocity values in Fig. 4-4(a) near the free surface are artifacts of an unsteady free surface condition. The water surface location fluctuated temporally in the z direction during data collection. Consequently, the PIV sampled water velocities at those locations when the water surface was above that interrogation point and measured zero-velocity values when air was present (water surface was below the interrogation point). These experimental values are incorrect and will not be included in subsequent data figures. The forward flow region also expands as the flow travels downstream prior to contracting at the next baffle (not shown in the figure).
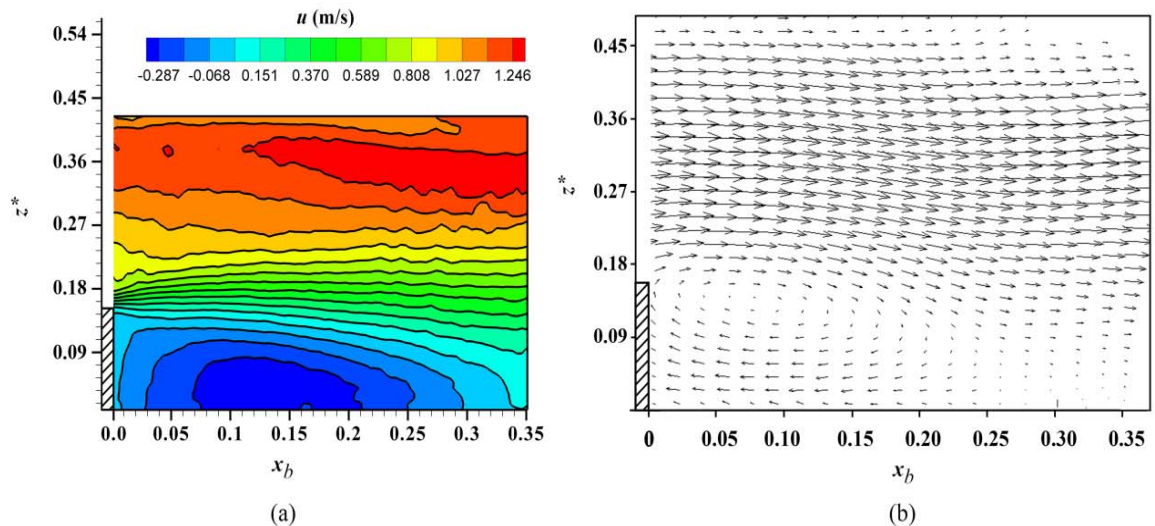
Fig. 4-4. Time-averaged experimental velocity data (PIV) at plane $y^*=0$ for $S=3.5\%$ and $Q=85$ L/s: (a) contours; (b) vectors field. The hatched region at $x_b=0$ represents the baffle location and height

k-ε Model

The *k-ε* model was used to simulate the flow through the weir-baffled culvert in three dimensions. The results of this simulation were compared with the experimental PIV data.

Fig. 4-5 shows a comparison of the *u*-velocity profile for *S*=3.5% and *Q*=85 L/s along the centerline of the culvert at x_b=0.20. As can be seen from Fig. 4-5, the *k-ε* model performed poorly in simulating the experimental velocity profile. The numerical model was limited in its ability to describe the reverse flow (recirculating flow downstream of the baffle) region.

Fig. 4-5. A comparison of *k-ε* and experimental *u*-velocity profiles for *S* =3.5% and *Q* =85 L/s at *y**=0.0 and x_o =9.208 m (x_b=0.20)

With the reverse flow velocity magnitudes under predicted, to maintain continuity, the numerical model under predicted the forward flow velocity magnitudes. The simulated results obtained by the k-ε model were also compared with the experimental results for S=3.5% and Q=85 L/s along the centerline of the culvert at x_b=0.48 (just upstream of the next baffle) and plotted in Fig. 4-6. At this location, the forward flow region has expanded to encompass the entire flow column (no reverse flow near the bottom boundary). Even in the absence of the recirculating flow behavior, the numerical results do not replicate the experimental results.

Fig. 4-6. A comparison of k-ε and Experimental u-velocity profiles for S =3.5% and Q =85 L/s at y^*=0.0 and x_o =9.308 m (x_b=0.48)

Fig. 4-7. A comparison of k-ε and Experimental TKE profiles for S =3.5% and Q =85 L/s at y^*=0.0 and x_o =9.208 m (x_b=0.20)

The turbulent kinetic energy (TKE) data obtained by the k-ε model along the centerline of the culvert at x_b=0.20 was compared with the experimental data for S=3.5% and Q=85 L/s in Fig. 4-7. The data in Fig. 4-7 show that, in general, the k-ε model over predicts the experimental TKE values.

LES Model

Similar numerical simulations were conducted using the LES turbulence model. Fig. 4-8 shows the mesh independent solution for the LES model. The data in Fig. 4-8 show that the minimum cells size required to provide mesh independence was equal to 7.0 mm, which equals half of the baffle wall thickness. To further insure accuracy, a minimum cell size of 3.5 mm was used for all cases. The LES model is a time-dependent
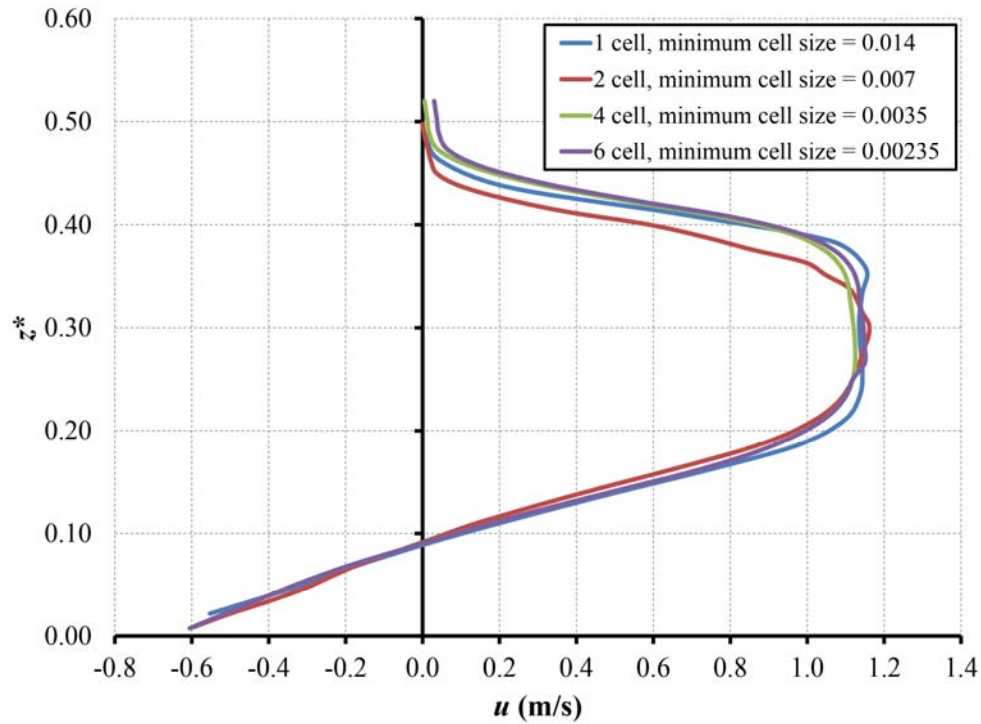
Fig. 4-8. Mesh independent solution for the Large Eddy Simulation (LES) model (S =3.5% and Q =85 L/s at y*=0.0 and x_o =9.208 m)

model that simulates the instantaneous velocities fluctuations. Subsequently, the time-averaged velocity fluctuations obtained by the LES model was compared with the experimental time-average velocity fluctuations measured using the PIV system. Fig. 4-9 shows a comparison of the u-velocity profile between the LES model numerical simulation and the experimental data results for S=0.5% and Q=28.3 L/s along the centerline of the culvert at x_b=0.20. The LES model predicted experimental velocity profile correlated poorly for both the recirculation and forward flow regions.

It should be noted from the experimental data of the PIV of the velocity profiles for all flow conditions discussed previously that there is a maximum velocity under the water surface followed by a decrease in the velocity magnitude near the water surface

represented by the dashed line in Fig. 4-9. This reduction in the velocity is an artificial reduction. The PIV technique is a time-dependent measurement for the instantaneous velocity of the seeds particles. At the fluctuating water surface, the PIV recorded velocity values for the particles at a certain location and certain time. At another time, the PIV recorded a zero velocity for the particles when there is no fluid (fluctuating free surface dropped below the interrogation location). Thus, the time average for the water surface velocity at that location will be artificially less than the actual maximum velocity of the water surface and the average water depth is located somewhere between the maximum and the minimum velocities of the flow near the water surface. The LES model results showed this behavior clearly at water surface because it utilizes a similar method for calculating the time average for the velocity. All the PIV data near the water surface that have a fluctuation between the air and the water were excluded except for Fig. 4-9.

A comparison of the LES and PIV u-velocity profiles for S=3.5% and Q=85 L/s at x_b=0.20 are shown in Fig. 4-10. Fig. 4-11 shows the same u-velocity profile comparison at x_b=0.48. The data in Figs. 4-9 and 4-10 show that the LES model is capable of computing the forward and reverse flows in a single cross section associated with flow separation, however, the LES model over predicts the magnitude of the reverse flow velocities. It can be noted from Figs 4-9 to 4-11 that the LES represents the reverse flow velocities as straight line for all flow conditions. The LES and experimental results, shown in Fig. 4-12, have common trends but the LES model significantly over estimates TKE magnitudes. Note that the deviation in the TKE from the experimental data was maximum at z^*=0.11.

Fig. 4-9. A comparison of LES and Experimental u-velocity profiles for S =0.5% and Q =28.3 L/s at y*=0.0 and x_o =9.208 m (x_b=0.20)
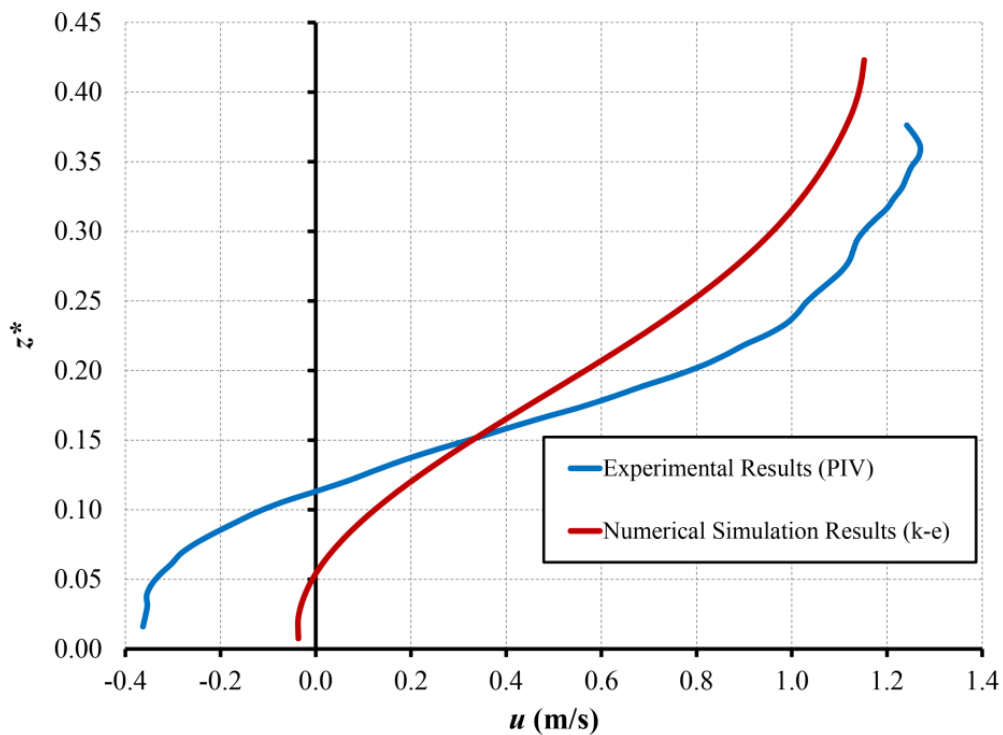

Fig. 4-10. A comparison of LES and Experimental u-velocity profiles for S =3.5% and Q =85 L/s at y*=0.0 and x_o =9.208 m (x_b=0.20)
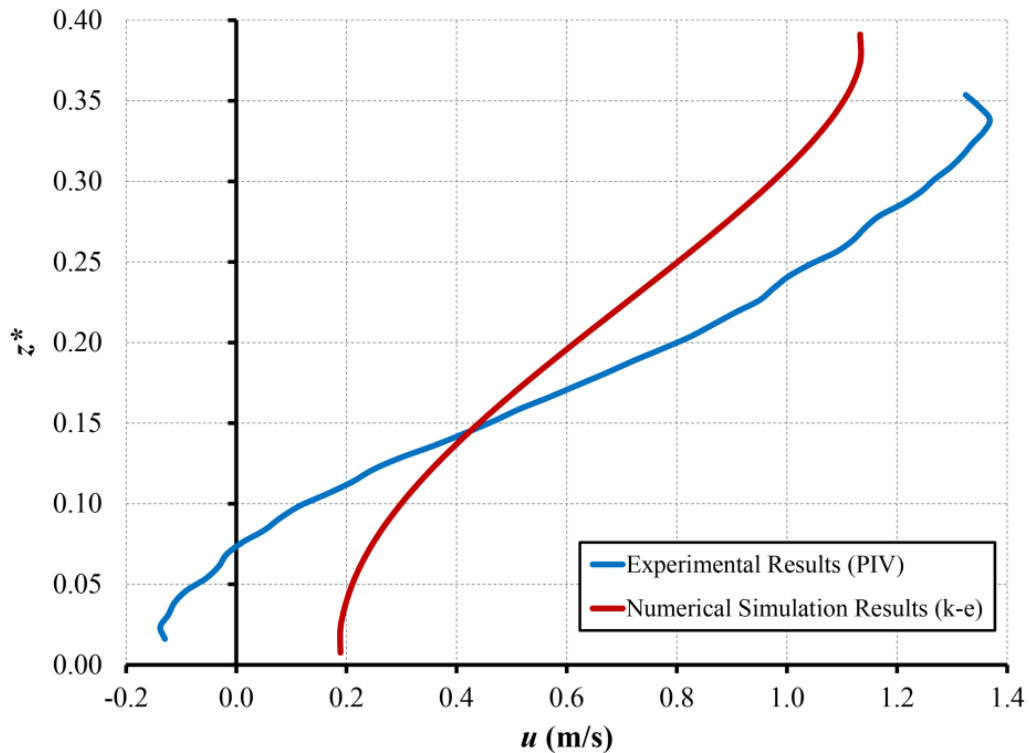
Fig. 4-11. A comparison of LES and Experimental u-velocity profiles for S =3.5% and Q =85 L/s at y^*=0.0 and x_o =9.308 m (x_b=0.48)

Fig. 4-12. A comparison of LES and Experimental TKE profiles for S =3.5% and Q =85 L/s at y^*=0.0 and x_o =9.208 m (x_b=0.20)

RNG Model

Numerical simulations of flow through the baffled culvert were repeated using the RNG model. Fig. 4-13 shows the *u*-velocity profile of the RNG model and PIV results for S=0.5% and Q=56.5 L/s along the centerline of the culvert at x_b=0.20. The comparison shows good agreement between the simulated and experimental results. This good agreement was observed for different flow conditions of S=3.5% and Q=85 L/s at x_b=0.20 and x_b=0.48 as shown in Figs.4-14 and 4-15, respectively. The RNG model simulations also accurately predicted the *u*-velocity profile at steeper culvert slopes like of S=6.0% and Q=85 L/s, as shown in Fig. 4-16. The RNG model predicted the shape and magnitude of the velocity profile far more accurately than the k-ε and LES models for the flow conditions evaluated.
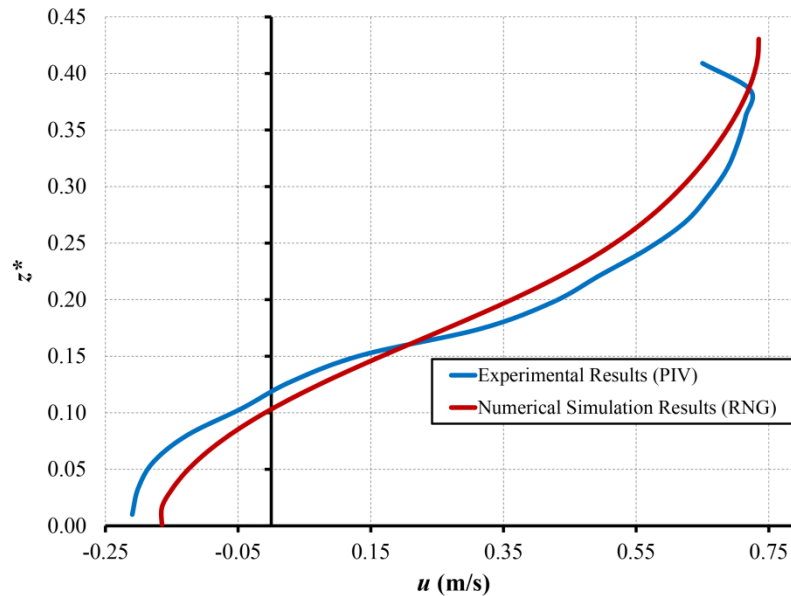
Fig. 4-13. A comparison of RNG and Experimental *u*-velocity profiles for S =0.5% and Q =56.5 L/s at y*=0.0 and x_o =9.208 m (x_b=0.20)
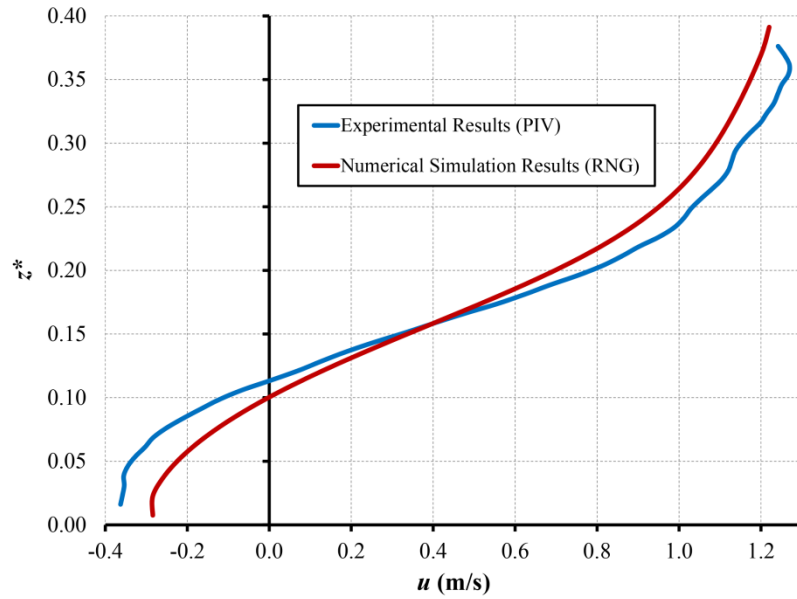
Fig. 4-14. A comparison of RNG and Experimental u-velocity profiles for $S=3.5\%$ and $Q=85$ L/s at $y^*=0.0$ and $x_o=9.208$ m ($x_b=0.20$)
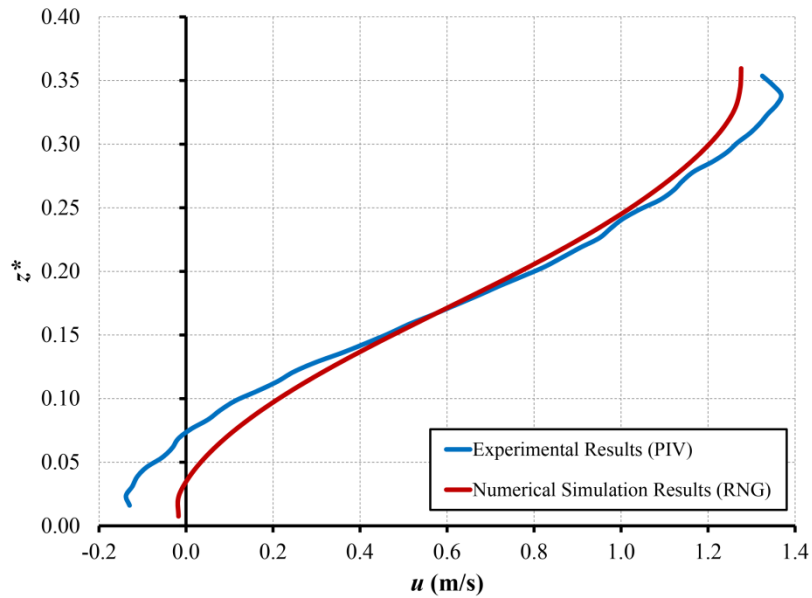
Fig. 4-15. A comparison of RNG and Experimental u-velocity profiles for $S=3.5\%$ and $Q=85$ L/s at $y^*=0.0$ and $x_o=9.308$ m ($x_b=0.48$)
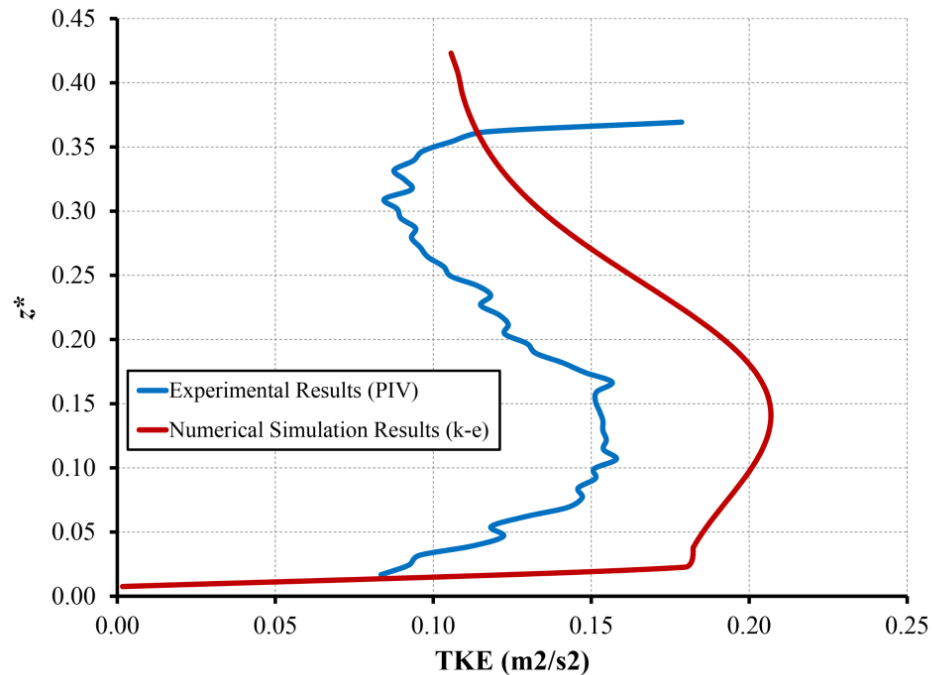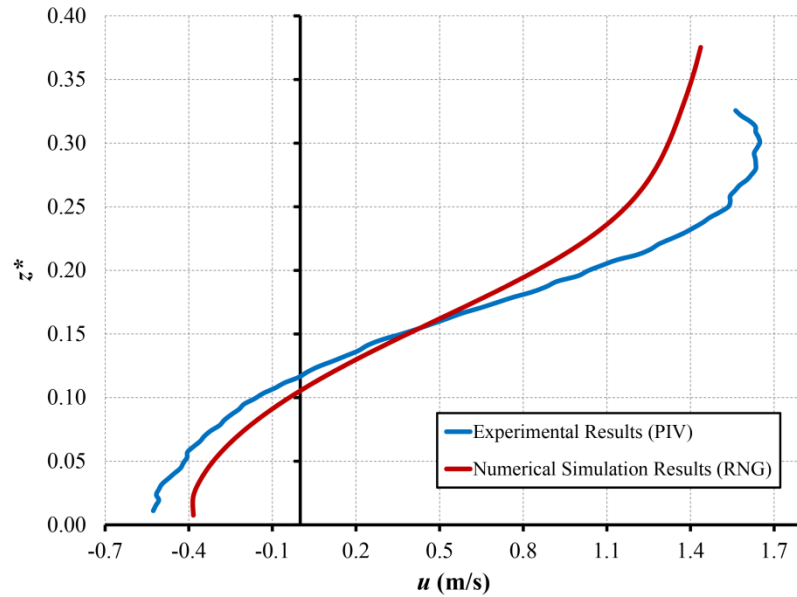
Fig. 4-16. A comparison of RNG and Experimental u-velocity profiles for S =6.0% and Q =85 L/s at y^*=0.0 and x_o =9.208 m (x_b=0.20)

Flow Science (2006) recommended the RNG model for flows having strong shear regions such as recirculation flows. Thus, RNG model is able to predict the reverse velocities better than k-ε and LES models that resulting in accurate results.

Despite the good agreement between the RNG and the experimental PIV data in Figs. 4-14 and 4-16, there are deviations in the u-velocity profile near the wall (culvert invert) and the free surface. The accuracy of the PIV experimental data is limited due to the high degree of curvature near the pipe invert (relative to the camera position) of the clear Lexan™ material used to replace the pipe wall in the viewing section. The refracted laser light, caused by the window curvature near the pipe wall produced a high distortion in the PIV images in addition to the surface reflection of the laser light. Consequently, discrepancies between u-velocity profile data near the pipe wall may be a

result of inaccuracies in the experimental data, numerical data, or both. Near the free surface, the deviation in the results was due to the surface reflection of the laser light from the fluctuation in the turbulent water surface.

In an effort to develop a better understanding of the influence of the window curvature and the fluctuating free water surface on the PIV data quality, PIV velocity data were measured at different several vertical, longitudinal planes offset from the pipe centerline, specifically at y^*=0.18 and y^*=0.36. Fig. 4-17 shows a comparison between the RNG simulated and PIV results for S=6.0% and Q=85 L/s at x_b=0.20 and y^*=0.18. The deviations in the velocity profile between the numerical and experimental results show clearly near the wall and near the water surface regions. For the same flow condition but at a distance of y^*=0.36 (high wall curvature comparing to y^*=0) from the centerline of the culvert, Fig. 4-18 shows larger deviations in the velocity profile of the experimental and the simulated results due to the high curvature of the Lexan wall at that location.

The PIV data in Figs. 4-17 and 4-18 were not smooth especially near the wall and near the free surface although the number of images was sufficient to obtain a smooth curve. Also, the range of the inaccurate PIV data (not shown in the figures) near the wall and near the free surface was expanded. For a more quantitative comparison, predicted data obtained by the RNG model and experimental data of PIV for the TKE for S=3.5% and Q=85 L/s at x_b=0.20 and y^*=0.18 are shown in Fig.4-19. The shape of TKE and the magnitude are accurately predicted. Note that the TKE in the RNG model near the water surface represented as a vertical line (constant fluctuation).
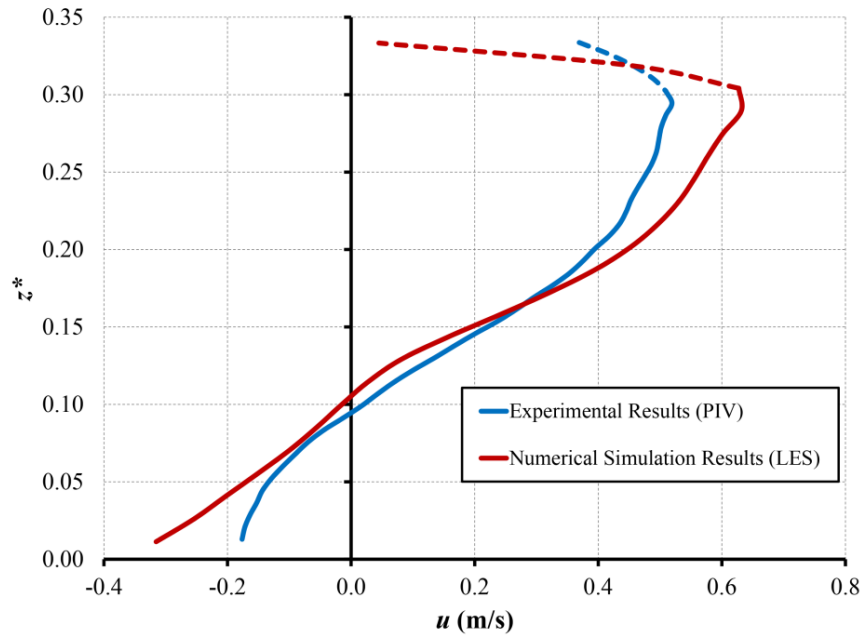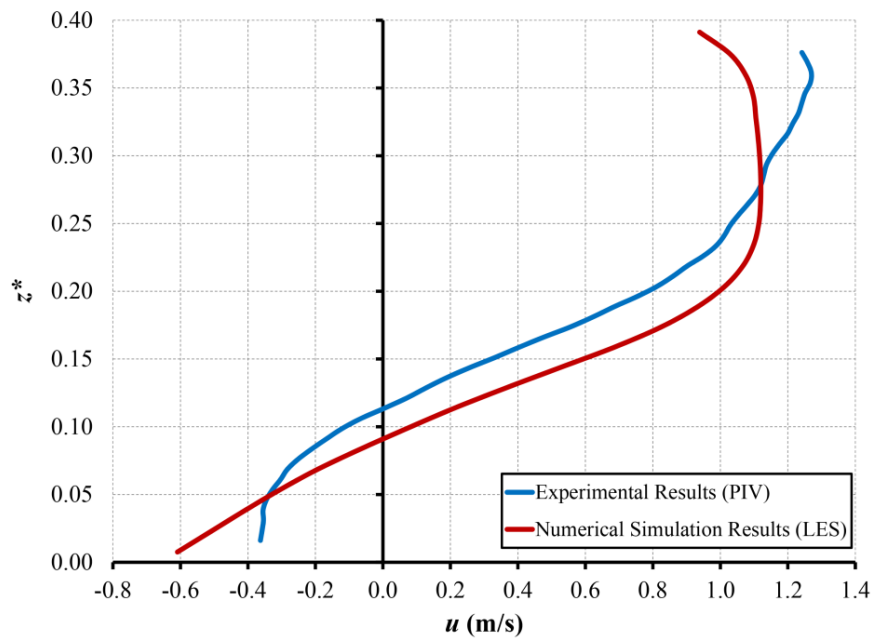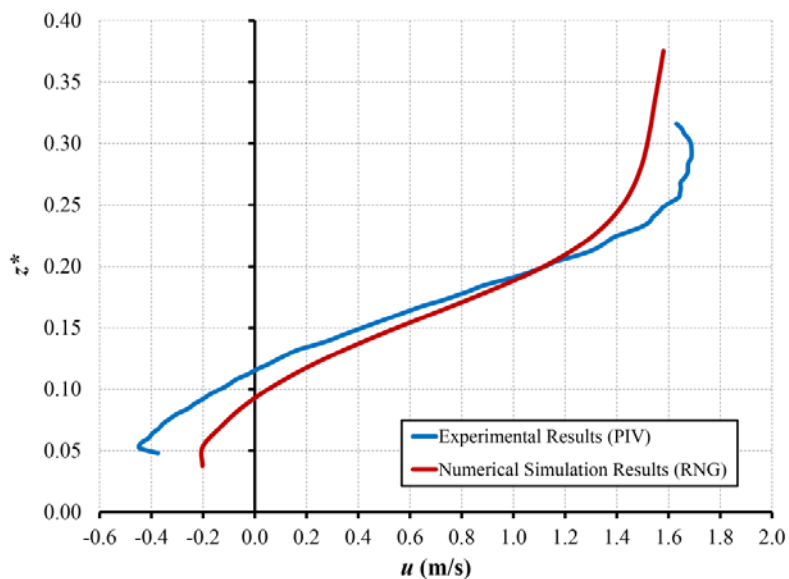
Fig. 4-17. A comparison of RNG and Experimental u-velocity profiles for S =6.0% and Q =85 L/s at y^*=0.18 and x_o =9.208 m (x_b=0.20)
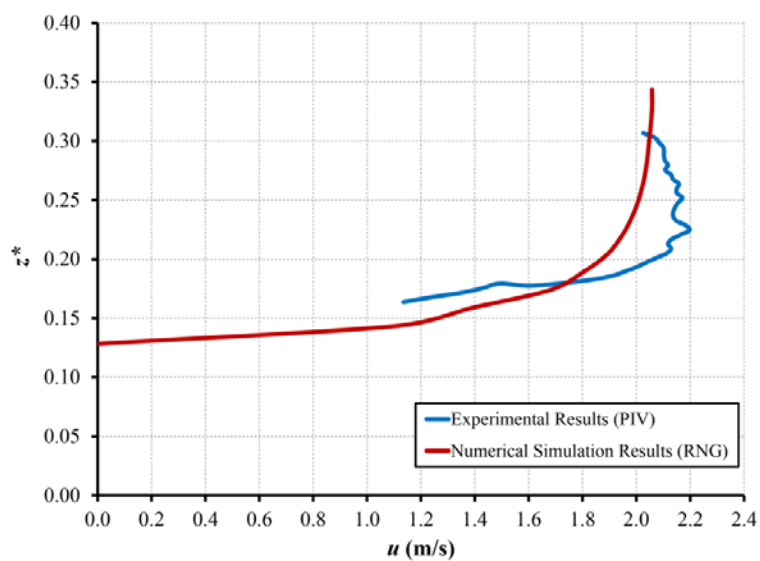
Fig. 4-18. A comparison of RNG and Experimental u-velocity profiles for S =6.0% and Q =85 L/s at y^*=0.36 and x_o =9.208 m (x_b=0.20)
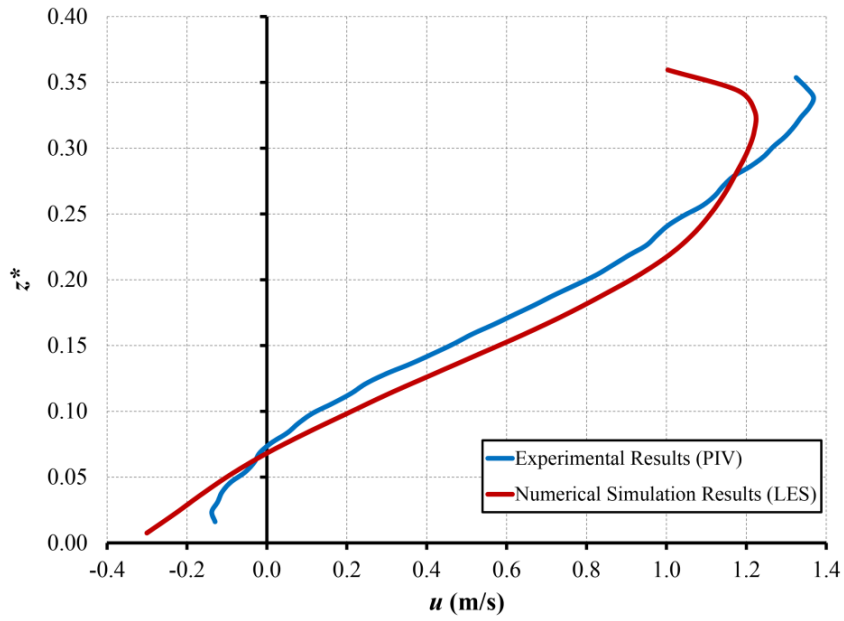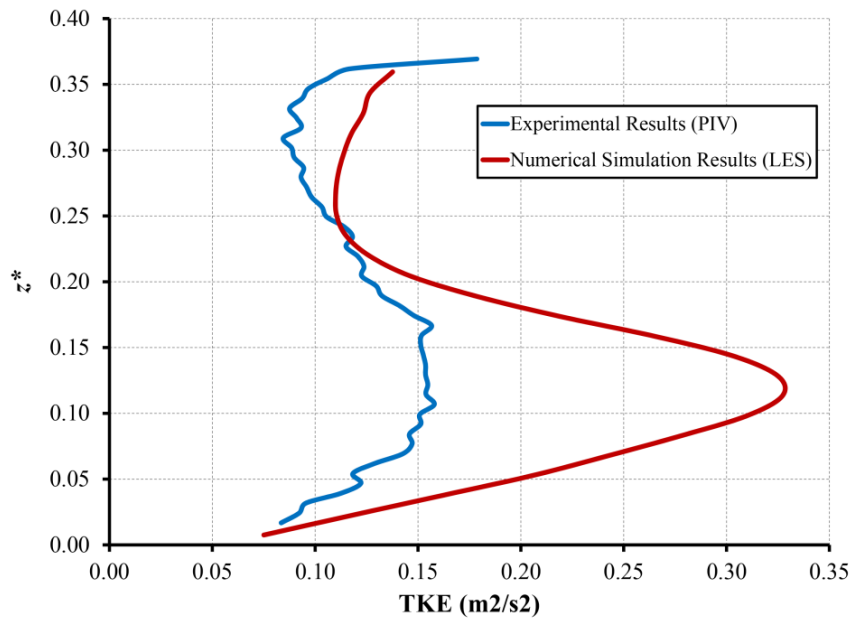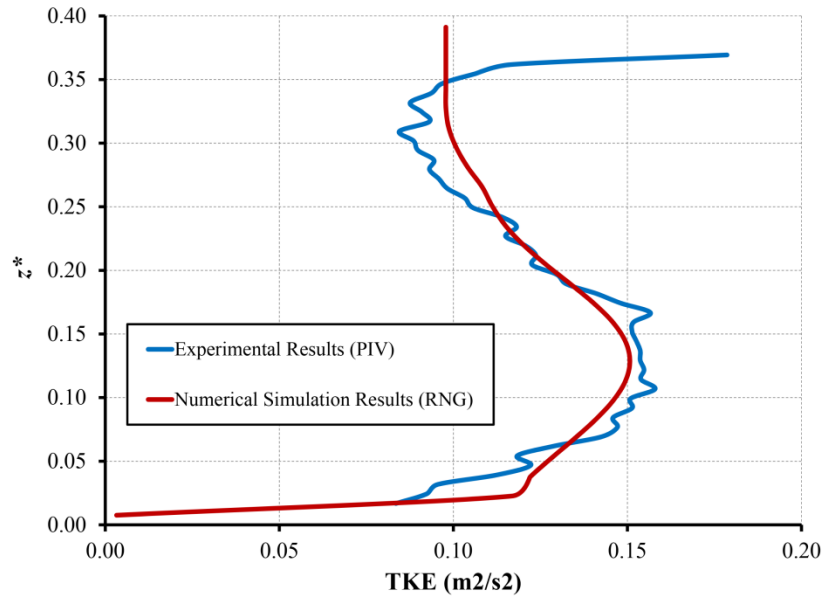
Fig. 4-19. A comparison of RNG and Experimental TKE profiles for S =3.5% and Q =85 L/s at y^*=0.0 and x_o =9.208 m (x_b=0.20)

Conclusions

Particle Image Velocimetry (PIV) data were successfully collected (with limitations near the pipe wall and free surface) for the flow through a large circular culvert featuring weir baffles along the invert. The performance of three turbulent models including (k-ϵ) model, Renormalized Group k-ϵ model (RNG), and Large Eddy Simulation (LES) model was evaluated in predicting the turbulent characteristics of the flow through weir baffled-culvert. The simulated results of the turbulent velocity and turbulent kinetic energy obtained by these models were compared with the measured PIV data. The k-ϵ model was poor in predicting the velocity profile in the recirculation region and forward region. The k-ϵ model results showing a higher velocity magnitude than the measured results in the recirculation region and lower velocity magnitude in the forward

region. The TKE predicted using k-ϵ model was high in magnitude compared with the one obtained with PIV. Furthermore; the LES model was unable to accurately predict the velocity profiles especially in the recirculation region although shape of the velocity profile in the forward region was similar to that obtained using PIV but different in magnitude.

The LES TKE results were higher than the PIV experimental results but featured similar profile shapes. Whereas, RNG predicted relatively accurately the velocity profile and the TKE for all flow conditions at the centerline and at a distance from the centerline of the culvert except in two regions, near the wall and near the free surface. Difficulty of obtaining a high quality PIV data near these two regions due to high wall curvature and high fluctuating in the free surface resulting in a poor agreement between the experimental data and the simulated results of the Renormalized Group k-ϵ model RNG. The agreement between the RNG and experimental PIV data decreased with increasing lateral distance (of the interrogation plane) from the pipe centerline due to limitations of the PIV data. Numerical modeling using Flow-3D® with the RNG turbulence model can likely be used to evaluate baffled culvert hydraulics and for continued research in culvert fish passage.

CHAPTER 5

THREE-DIMENSIONAL NUMERICAL SIMULATION[3]

Abstract

Three-dimensional numerical simulation was conducted on weir baffled-culvert of 18.3-m long and 0.60-m in diameter with 0.15D baffle heights spaced at 0.9D, where D is the culvert inside diameter. The influence of flow rates and culvert slopes on the forward velocities and reverse velocities were evaluated. At smaller slopes (e.g., 1.5%), vertical velocity profiles in the baffled culvert were found to vary little with discharge; at larger slopes (e.g., 6%), the vertical velocity profile varied appreciably with discharge. Turbulent kinetic energy and flow direction effects on flow characteristic were also evaluated. Validation of Manning's equation and Manning's roughness coefficient for the tested culvert were reported.

Introduction

Hydraulic structures that modify stream or river flows often, by the nature of their function, can create barriers for the fish migration. Various studies have evaluated the influence of hydraulic structures on the fish migration (e.g., Bell 1986; Clay 1995; Olsen and Tullis 2013). Installing baffles in the culvert invert represents a potential mitigation for the negative impact of culvert road crossings. Pearson et al. (2006) studied the influence of culvert flow rates and slope on fish passage through baffled and non-baffled culverts. Rajaratnam et al. (1988), Rajaratnam et al. (1989), Rajaratnam and Katopodis (1990), and Rajaratnam et al. (1991) studied the flow characteristic of a variety of baffles

---

[3] Coauthored by Blake P. Tullis

design sets, including offset baffle, slotted-weir baffle, weir baffle, and spoiler baffle. In their studies, they developed a flow equation between the dimensionless flow rate and the relative depth of flow. Numerical investigation was conducted by Feurich et al. (2011) on "spoiler-baffle" geometry. They concluded that spoiler baffles can improve the fish passage by reducing the flow velocity through the culvert. Morrison et al. (2009) studied the relationship between the flow turbulence characteristics and culvert fish passage; they were unable to find significant correlation between the turbulence characteristics and fish passage.

The effect of turbulent eddy diameter and vorticity on the fish swimming speed and stability was investigated by Tritico and Cotel (2010). They found that the turbulent eddies have effects on fish behavior such as migration and station holding. Pearson et al. (2005) performed field testing on juvenile coho salmon (Oncorhynchus kisutch) passage through corrugated nonbaffled culverts with slopes of 1.14% and 4.33%. They correlated the relationship between passage success and mean culvert flow velocity. Smith et al. (2005) observed that juvenile rainbow trout selected the focal positions (the place where there are a large number of fish) with low turbulence and high velocities over high turbulence and low velocities. Khodier and Tullis (see Chapter 3) noted two preferable zones for the fish while swimming upstream in baffled culvert. The first zone was located on the downstream side the baffles and the second zone was near the culvert sidewall. Several studied have evaluated the influence of the physical characteristics of the individual fish (e.g., fish length and weight) on the fish passage (e,g., Watts 1974, Belford and Gould 1989, Behlke et al. 1991, Tillinger and Stein 1996, and Chapter 3).

In this study, a numerical investigation was conducted on weir baffled-culvert culvert slopes of 0.5%, 1.5%, 2.5%, 3.0%, 3.5%, 4%, and 6% at flow rates of 28.3 L/s, 56.5 L/s, and 85 L/s. The maximum forward velocities, reverse velocities, flow vectors field, and turbulent kinetic energy were evaluated at each flow conditions.

Three-Dimensional Simulation

The objective of this numerical simulation was to evaluate the hydrodynamic conditions in a weir baffled-culvert [18.3-m long, 570 mm inside diameter (D)] previously evaluated in the laboratory. The baffle height was 0.15D (85.75 mm); the baffle spacing was 0.9D (514 mm) (see Fig. 5-1). The baffle spacing to baffle height ratio was 6.0. Flow-3D® produced by Flow Science was used to solve the problem. This software used the Volume of Fluid (VOF) method for solving dominant equations on flow at orthogonal mesh gridding.

The Fractional Area/Obstacle Representation (FAVOR) was employed to represent the complex geometries. As discussed in Chapter 4, Renormalized Group (RNG) model was the best model to simulate the baffled-culvert and based on comparisons with experimental Particle Image Velocimetry (PIV) data. Thus, the RNG was utilized to simulate the weir baffled-culvert in three dimensions.

Boundary Conditions and Extent of Flow Domain

Fig. 5-1 shows a schematic for the small, prototype-scale culvert evaluated in the numerical simulation using Flow-3D®. The flow domain axes were aligned relative to the predominant flow direction as shown in Fig. 5-1.
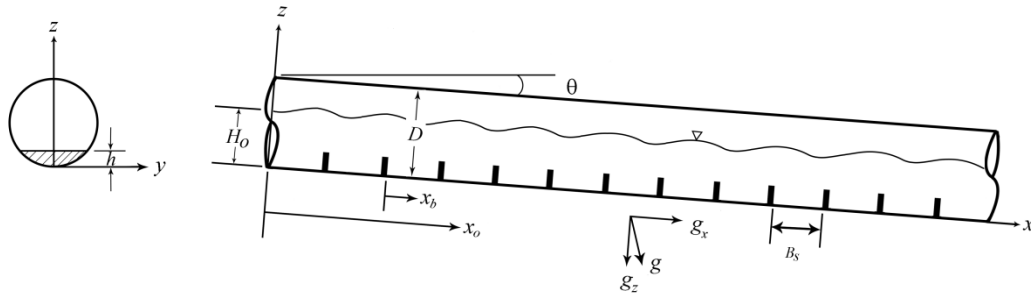
Fig. 5-1. Schematic of the problem

Note that to simulate flow through a sloping culvert, the gravitational field orientation is adjusted relative to the culvert axis rather than adjusting the culvert slope, as shown in Fig. 5-1. Consequently, the gravitational acceleration in the x-direction (g_x) and in the z-direction (g_z) are giving by the following equations:

$$g_x = gsin(\theta) \tag{5-1}$$

$$g_z = gcos(\theta) \tag{5-2}$$

$$\theta = tan^{-1}(S) \tag{5-3}$$

where g is the gravity acceleration and θ is the culvert inclination angle and S represents the culvert slope. A specified volumetric flow rate and flow depth were used as the upstream boundary condition; the outlet flow boundary condition was located at the culvert exit. Extensive simulations were conducted to confirm that the outflow boundary location was sufficiently far enough downstream from the interrogation location to have no influence on the local head-discharge conditions at the interrogation location near the culvert midpoint essentially had no influence on the upstream computational interrogation grid. The appropriate outlet boundary location was at x=14.9 m (the exit of the culvert). In order to reduce the computational time, the culvert was divided in half

with a vertical plane through the culvert centerline (y=0), and only half of the culvert was simulated.

Turbulent Model Parameters

To provide more accuracy for the solution, estimations for the turbulent kinetic energy (k), turbulent dissipation (ε), turbulent intensity (I), and maximum turbulent mixing length (L) were evaluated using the following equations, respectively:

$$k = 1.5(\bar{u}I)^2 \tag{5-4}$$

$$\varepsilon = \frac{0.164(k)^{3/2}}{L} \tag{5-5}$$

$$I = 0.16R^{-1/8} \tag{5-6}$$

$$L = 0.07D_h \tag{5-7}$$

(R) is the Reynolds number defined as:

$$R = \frac{\rho \bar{u} D_h}{\mu} \tag{5-8}$$

and,
$$D_h = \frac{4A}{P} \tag{5-9}$$

$\bar{u}$ is the average velocity in the x-direction at the inlet.

Mesh Size Independence

To insure that the numerical simulations are independent on the computational grid size, an extensive number of simulations were performed using different grid sizes. Non-uniform mesh was used for each grid size. Fig. 5-2 shows the mesh independent solution for the u-velocity profile for (Q=0.085 L/s) and (S=3.5%) at x_o=9.208 (x_b=0.30).
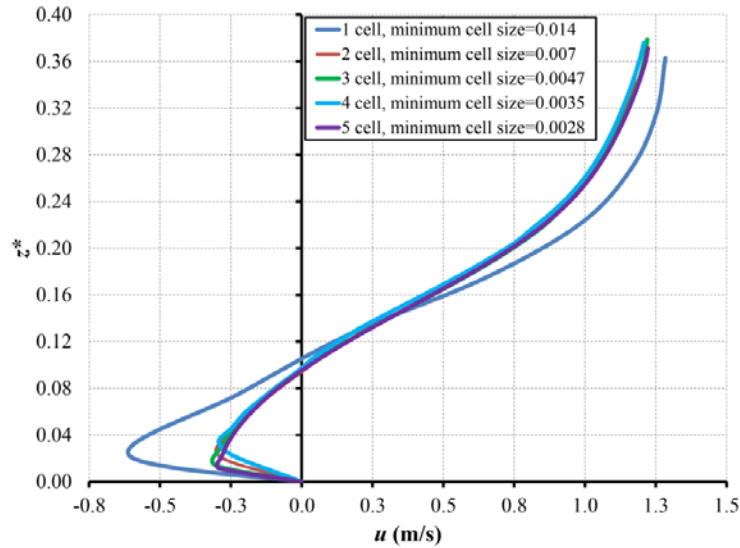
Fig. 5-2. Mesh independence solution for (Q=0.085 L/s) and (S=3.5%) at y^*=0.0 and x_o=9.208 m (x_b=0.30)

The data in Fig. 5-2 show that the minimum cells size required to provide mesh independence was equal to 7.0 mm, which equals half of the baffle wall thickness. To further insure accuracy, a minimum cell size of 3.5 mm was used, which corresponds to 25% of the baffle wall thickness.

Results and Discussion

The flow characteristics through a baffled culvert of 570 mm diameter was simulated numerically for S values equal 0.5%, 1.5%, 2.5%, 3.0%, 3.5%, 4%, and 6% at flow rates (Q) equal to 28.3, 56.5, and 85 L/s. Fig. 5-3 shows the contours for u-velocity for non-baffled and baffled culverts for S=0.5% and Q=85 L/s at x_o=9.208 m (x_b=0.30). In the non-baffled culvert of the same diameter, the maximum velocity occurs at the core of the flow as shown in [Fig. 5-3 (a)]. With baffles installed [Fig. 5-3 (b)], the maximum velocity region in the vertical plane directly above the baffle split into two symmetry

regions near the sidewall and the magnitude of the maximum velocity reduces, relative to the non-baffled culvert. [Fig. 5-3 (c)] shows the forward and reverse flow regions in the vertical plane located mid-distance between two adjacent baffles. The reduction in velocity is due to the increased depth of the forward-flow region and the additional flow shear stress associated with the presence of the reverse flow domain that occurs between baffles. The baffles and corresponding flow separation, reverse flow, and increased shear stress act as an energy dissipation device for the main flow through the culvert. Fig.5-4 shows the reverse flow in the u-velocity at different locations along the y-direction. It can be noted from Fig.5-4 that the maximum reversed velocity occurred at the center of the culvert ($y^*=0$) and decreased as y increased until it diminished at $y^*=0.36$. The lateral variation in the local reverse flow velocity magnitudes downstream of a baffle is proportional to the local baffle height (vertical distance from the top of baffle to the pipe wall).
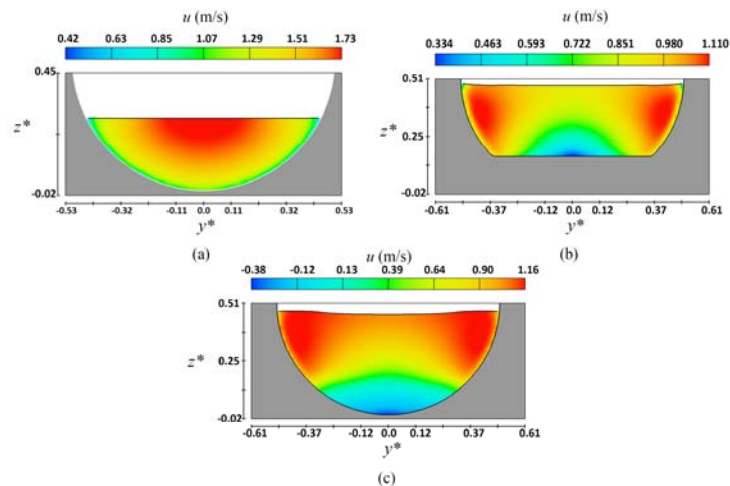
Fig. 5-3. Contours for u-velocity for $S=0.5\%$ and $Q=85$ L/s: (a) non-baffled culvert; (b) baffled-culvert at $x_o=9.058$ m (over the baffle); (c) baffled-culvert at $x_o=9.208$ m ($x_b=0.30$)

The fact that the maximum local velocities, as shown in Fig. 3(b), occur near the distal lateral extents of the flow cross section is likely associated with the reduction in flow separation and reverse flow magnitudes as the distance from the longitudinal centerline increases. To provide a better understanding of the flow feature through baffled culverts, two significant flow domain regions were evaluated in this study. The first region was located at the center of the culvert (y^*=0) where the maximum depth of reversed flow domain occurs. The second region was located where the maximum forward-flow velocity occurred, specifically at y=20.4 mm ($0.358D$ from the centerline). These regions have a significant influence on the fish passage, the maximum velocity region influences the swimming fish toward the upstream and the reverse flow region corresponds to one location where fish rest.
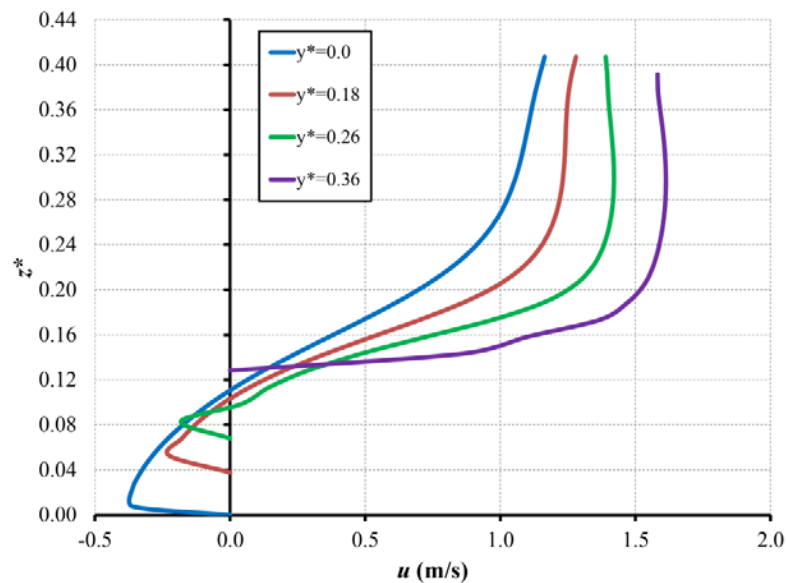
Fig. 5-4. u-velocity profiles for S =3.5% and Q =85 L/s at x_o =9.158 m (x_b=0.20) at different locations along the y^*-direction

Culvert Slope Effects

Figs. 5-5 and 5-6 show the effects of the culvert slope for Q=28.3 L/s on the *u*-velocity profile over the baffle (at y^*=0.36) and at the midpoint between the baffles at y^*=0, respectively. For a common discharge, the data in Figs. 5-5 and 5-6 show the change in shape of the *u*-velocity profile and the local *u*-velocity magnitudes increase with increasing S. The flow depth decreases with increasing flow. Also, the data in Figs. 5-7 to 5-10 show the effects of the culvert slope on the *u*-velocity profile for Q=56.5 L/s and Q=85 L/s at different locations. As can be seen from the data in Figs. 5-6 and 5-8, the magnitude of the reverse flow velocity downstream of the baffle decreases with increasing S for Q=28.3 L/s and Q=56.5 L/s, whereas the reversed flow velocity has an opposite trend for Q=85 L/s (Fig. 5-10).
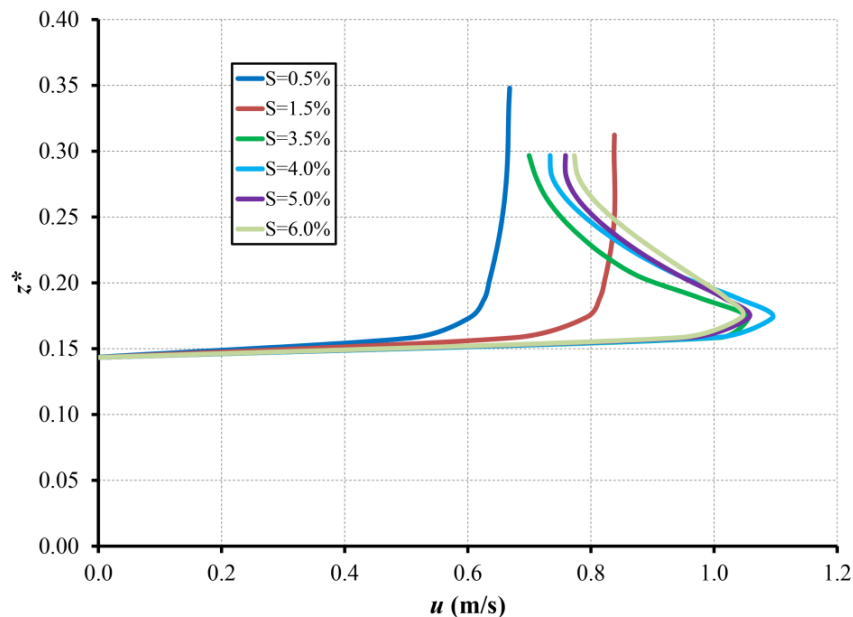
Fig. 5-5. *u*-velocity profiles for Q =28.3 L/s at x_o =9.058 m (over the baffle, x_b=0) and y^*=0.36 for different culvert slope
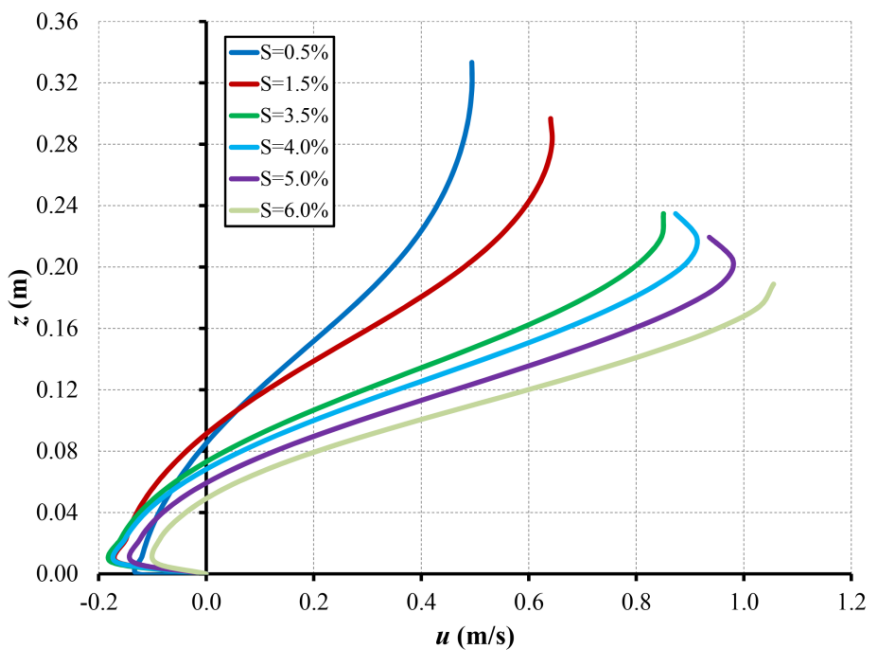
Fig. 5-6. u-velocity profiles for Q =28.3 L/s at x_o =9.208 m (x_b=0.30) and y^*=0 for different culvert slope
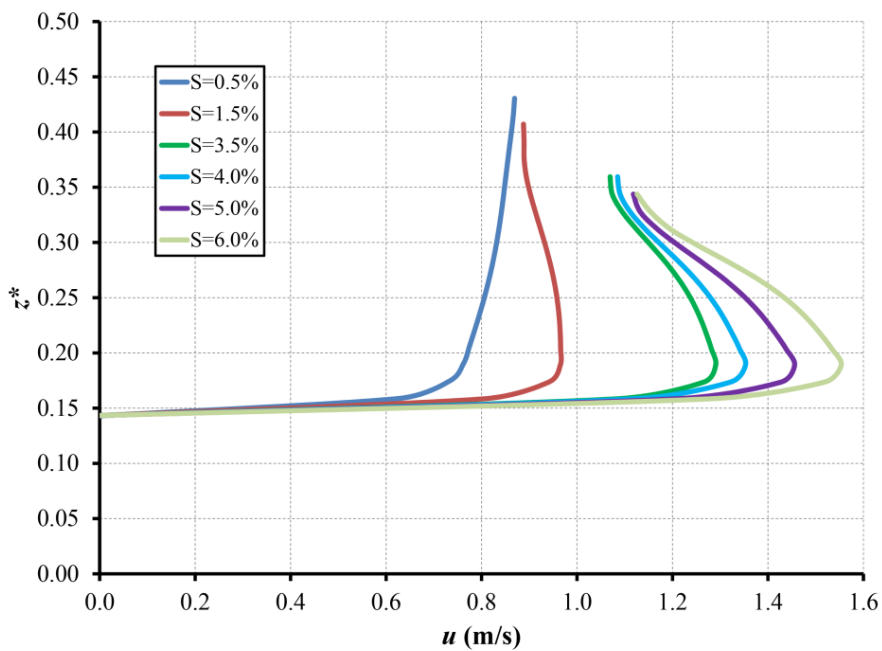
Fig. 5-7. u-velocity profiles for Q =56.5 L/s at x_o =9.058 m (over the baffle) and y^*=0.36 for different culvert slope
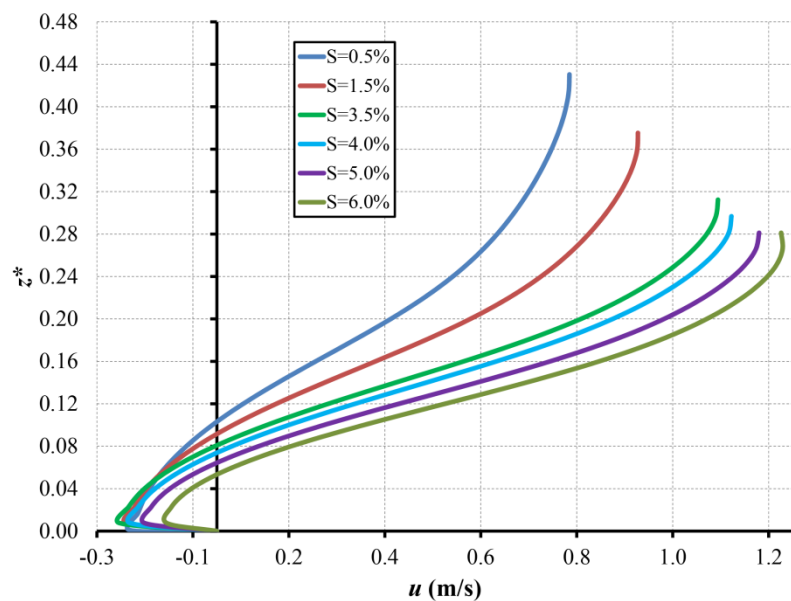
Fig. 5-8. u-velocity profiles for Q =56.5 L/s at x_o =9.208 m (x_b=0.30) and y^*=0 for different culvert slope
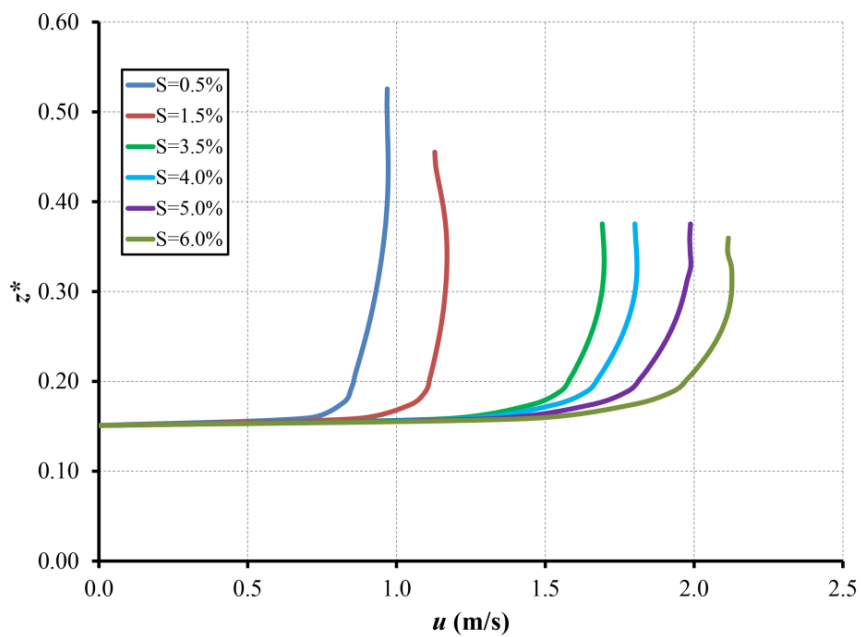
Fig. 5-9. u-velocity profiles for Q =85 L/s at x_o =9.058 m (over the baffle) and y^*=0.36 for different culvert slope
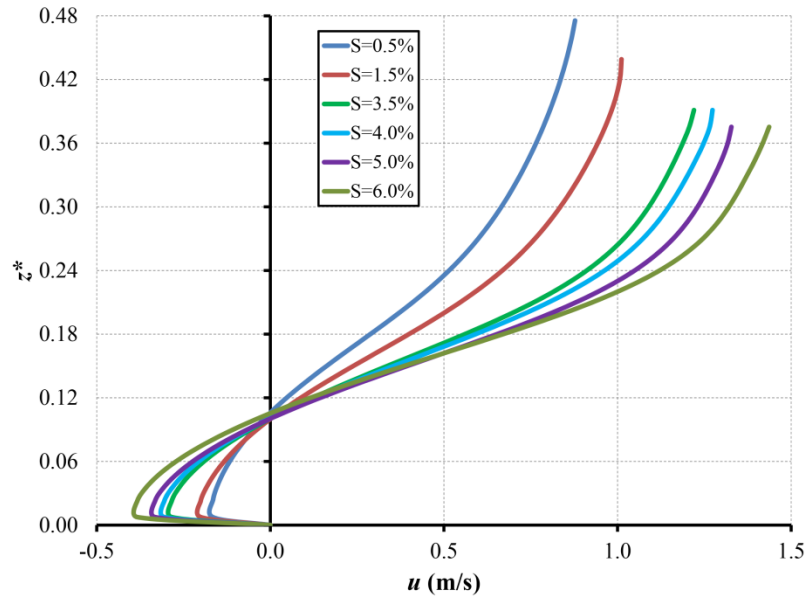
Fig. 5-10. *u*-velocity profiles for Q =85 L/s at x_o =9.208 m (x_b=0.30) and y^*=0 for different culvert slope

Flow Rate Effects

The influence of changing Q on the *u*-velocity profile is slightly different from the influence of changing S. Figs. 5-11 and 5-12 show the *u*-velocity profile for different Q values at x_b =0 ant x_b=0.30 for S=1.5%, respectively. Note in Fig. 5-11 that the forward-flow velocity and the water depth increase as the Q increases. The data in Fig. 5-12 show that the flow depth increases at x_b=0.3 with increasing Q, but the forward flow *u*-velocity profile is essentially independent of Q (for the range of Q values tested) except near the free surface. Fig.5-12 shows that the reverse flow *u*-velocity magnitudes increasing slightly with increasing the Q. One can note that the increasing in the forward velocities is insignificant below a relative depth (z^*) of ~0.20 for the three flow rates and up to z^*=0.27 for 56.5 L/s and 85 L/s. Because of the *u*-velocity profile uniformity (except near the free surface) for forward flow at S=1.5%, and the fact that fish passage

observations in previous studies (see Chapter 3) observed that fish passage typically occurs in the water column just above the weir (not near the free surface), the fish passage behavior should also be relatively uniform for the range of discharges evaluated. The data in Figs. 5-13 and 5-14 show the influence of flow rates at a relatively steep culvert slope (S=6%). The forward velocity over the baffle has similar behavior as in Fig. 5-11, whereas the Fig. 5-14 data differs from that in Fig. 5-12. At the steeper slope, the forward flow u-velocity profile values decrease with increasing Q (Fig. 5-14); the reverse flow u-velocity profile values trend is opposite the of the forward flow (i.e., the reverse flow velocity magnitude increases with increasing Q). Increasing of reverse flow magnitude behind the baffles may produce an unsuitable environment for the fish that use this region for the resting.
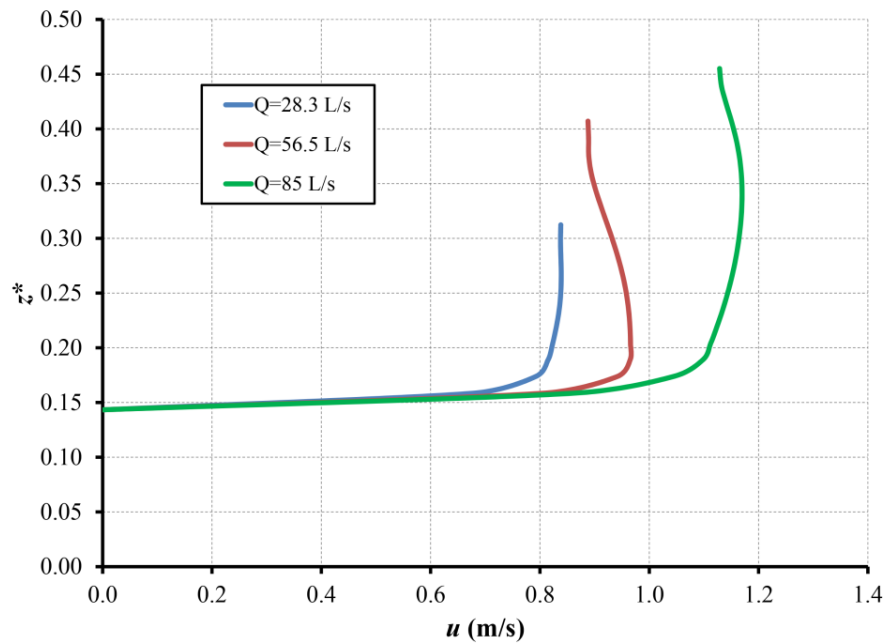
Fig. 5-11. u-velocity profiles for S=1.5% at x_o=9.058 m (over the baffle) and y^*=0.36 for different flow rates
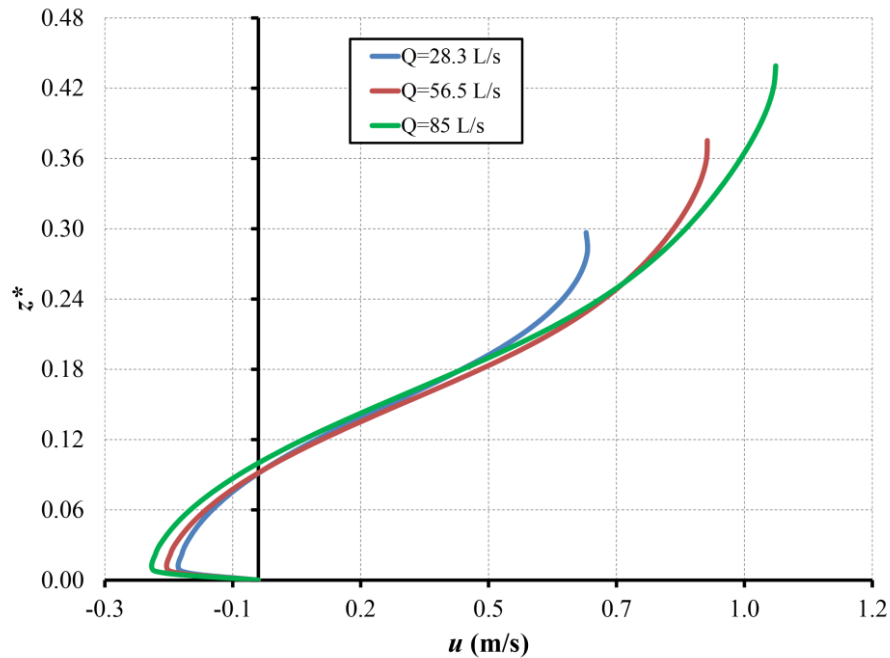
Fig. 5-12. *u*-velocity profiles for $S=1.5\%$ at $x_o=9.208$ m ($x_b=0.30$) and $y^*=0$ for different flow rates

In summary, increased the culvert slope always decreased the water depth and increased the forward velocities for common discharges, while increasing the discharge increased the water depth at a common slope; the corresponding *u*-velocity response is dependent upon the culvert slope. If the culvert slope is relatively small, increasing Q produces no change in the forward flow *u*-velocity profile except near the free surface. At large culvert slopes, the forward *u*-velocity actually decreases with increasing Q.

Turbulent Kinetic Energy (TKE)

The time-averaged turbulent kinetic energy (TKE) is given per the following equation:

$$TKE = \frac{1}{2}\left(\overline{(u')^2} + \overline{(v')^2} + \overline{(w')^2}\right) \qquad (5\text{-}10)$$
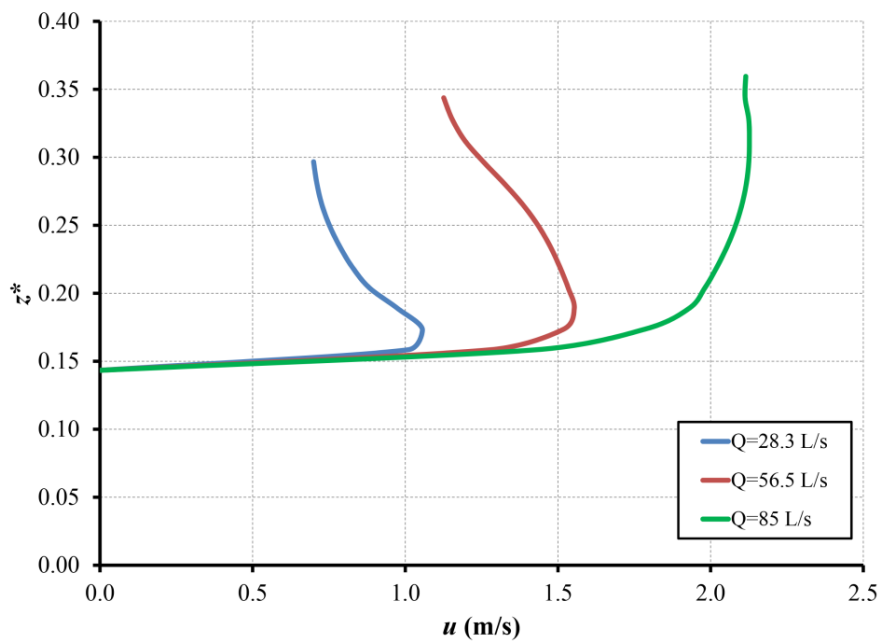
Fig. 5-13. *u*-velocity profiles for *S* =6% at *x_o* =9.058 m (over the baffle) and *y** =0.36 for different flow rates
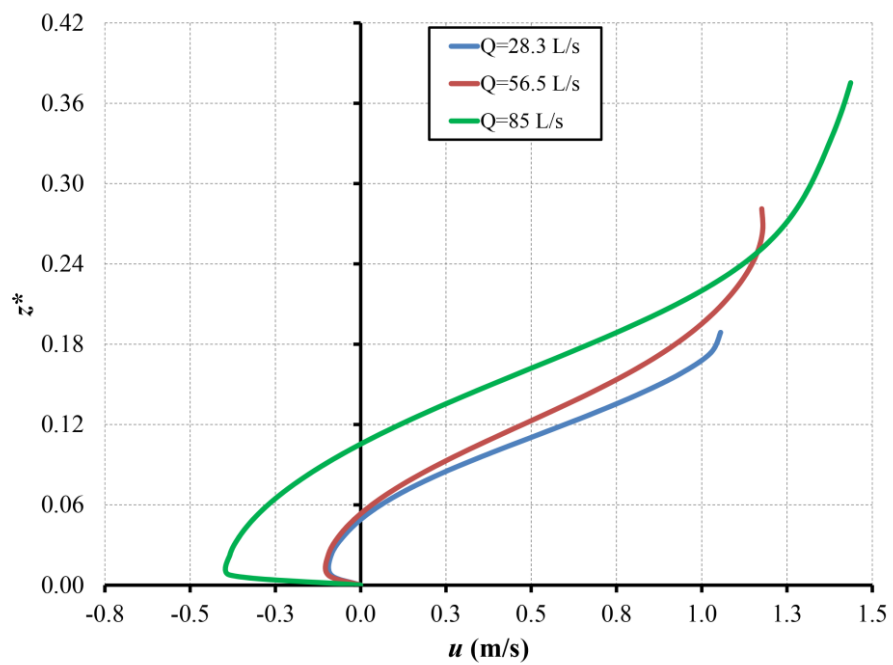
Fig. 5-14. *u*-velocity profiles for *S* =6% at *x_o* =9.208 m (*x_b*=0.30) and *y** =0 for different culvert slope

where *u'*, *v'*, and *w'* are the fluctuating velocities in the *x*, *y*, and *z* directions, respectively, at a single point. TKE is a measurement for the velocities fluctuation or in other word, the turbulence intensity. Fig. 5-15 shows contour comparisons of the time-averaged turbulent kinetic energy between the non-baffled and baffled culvert (*S*=0.5%, *Q*=85 L/s). As shown in Fig. 5-15 (a), the TKE is minimum at the core of the flow and maximum near the culvert wall. The TKE in the baffled culvert, however, has an opposite trend with the maximum near the core of the flow and minimum occurring near the culvert wall [Fig. 15 (b, c)]. The relative magnitudes of TKE in Fig. 15 show that the presence of the baffle causes the TKE to increase, as expected, relative to the non-baffled culvert.

One can note that the maximum TKE corresponds to the location of minimum velocity (i.e., near the wall for non-baffled culvert and at the core of the flow for the baffled culvert). Likewise, the minimum TKE corresponds to the location of maximum velocity (i.e., at the core of the flow for the non-baffled culvert and near the wall for the baffled culvert). This can be explained by the high velocity gradient at the boundary of the maximum velocity region that creates high shear stresses at the boundary. Since the shear stresses are proportional to TKE, TKE increases with increasing shear stress. Fig. 5-16 shows the proportional relationship between the culvert slope and the TKE for *Q*=85 L/s. The effect of discharge on TKE is shown in Fig. 5-17. The TKE increases as *S* increases (larger velocity gradients and shear stress) for a common discharge and increases with increasing discharge (common slope). Khodier and Tullis (see Chapter 3) noted two resting zones utilized by fish in baffled culverts.
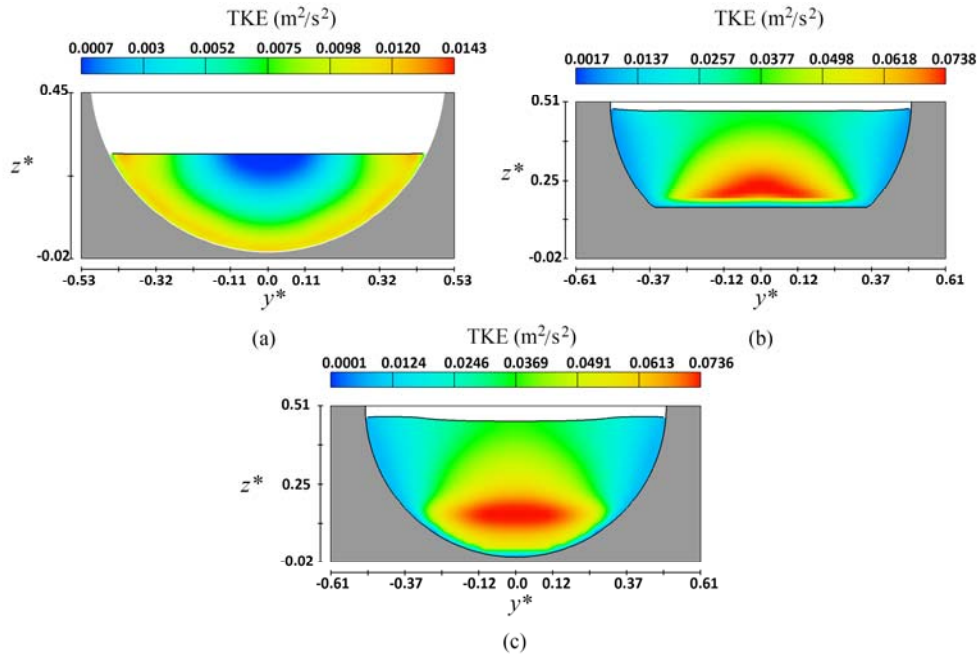
Fig. 5-15. Contours for turbulent kinetic energy (TKE) for S =0.5% and Q =85 L/s: (a) non-baffled culvert; (b) baffled-culvert at x_o =9.058 m (over the baffle); (c) baffled-culvert at x_o =9.208 m (x_b=0.30)
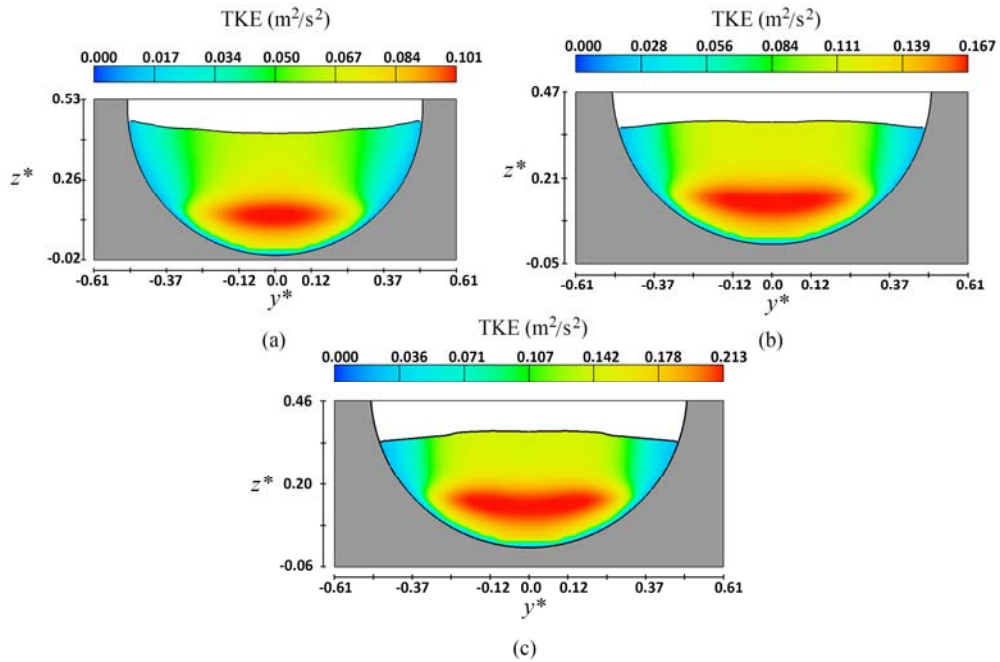
Fig. 5-16. Contours for turbulent kinetic energy (TKE) for Q =85 L/s at x_o =9.208 m (x_b=0.30) : (a) S=1.5%; (b) S=4%; (c) S=6%
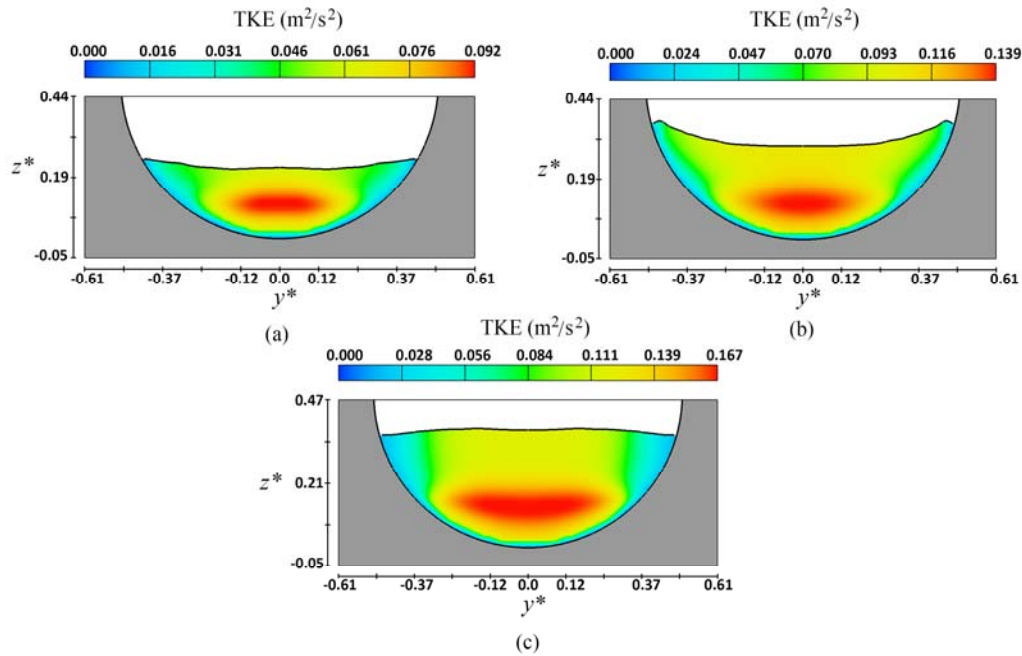
Fig. 5-17. Contours for turbulent kinetic energy (TKE) for S =4% at x_o =9.208 m (x_b=0.30): (a) Q =28.3 L/s; (b) Q =56.5 L/s (c) Q =85 L/s

The first zone was located downstream of the baffle and the second zone was located near the culvert sidewall. In an effort to explain the behavior of the fish based on data from the current study; fish prefer to stay in the first zone (just downstream of the baffles) because it has a minimum reverse velocity that produces a resting zone for fish while passing upstream especially the exhausted and weak ones. As shown in Figs. 5-15 and 5-17, the turbulent kinetic energy in the second zone (near the sidewall) was minimum; this means that the fluctuation in the velocity is low. Fig. 5-18 shows the vector plot for u-w velocities for S=0.5% and Q=85 L/s. At the center of the culvert Fig.5-18 (a) show a series of u-w velocity profiles in a vertical plane (y*=0) at various x_b locations encompassing the region between two baffles. The water surface profile in the y*=0 plane undulates between baffles, reaching a maximum near the baffle station and a

minimum near the midpoint between baffles. The vector angles and magnitudes vary with the water surface variations. By comparison, the *u-w* velocity profiles at y=204 mm are relatively uniform (direction and magnitude); the water surface is nearly horizontal. The uniformity of the flow profile near the sidewall [Fig. 18(b)] would suggest minimal TKE in that region, which may help explain the utilization of zone near the sidewall where fish tended to rest in the Khodier and Tullis (Chapter 3) study.

Manning's Roughness Coefficient (n)

Head-discharge relationships for culverts are commonly quantified using Manning's equation, which features a hydraulic roughness coefficient specific to culvert material, geometry, and size. Manning's roughness coefficient is defined as follows:

$$n = \frac{AR_h^{2/3}\sqrt{S}}{Q} \tag{5-11}$$

In Eq. 5-11, R_h is the hydraulic radius and A is the cross sectional flow area. There are two methods to evaluate Manning's roughness coefficient. Manning's equation is generally applied to uniform flow conditions (spatially constant flow depth and velocity profile).
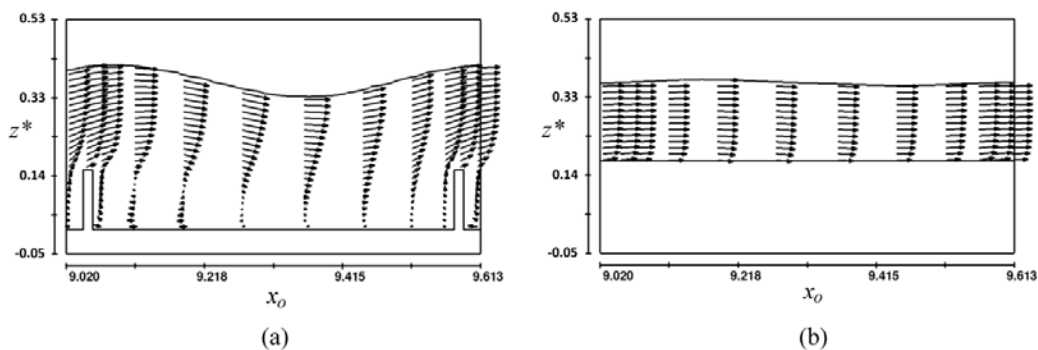
Fig. 5-18. Velocity *u-w* vector plots for *S* =0.5% and *Q* =85 L/s: (a) *y** =0; (b) *y** =0.36

As can be seen in Fig. 5-18, the flow depth and velocity profile varies spatially, which will increase the level of uncertainty or approximation of the Manning's equation solution. Though not uniform, the baffled-culvert flow characteristics might be classified as quasi-uniform or periodic flow (i.e., velocity and flow depth varies spatially but in a repeating pattern, which lends itself to averaging flow parameters). To apply Manning's equation to this quasi-uniform flow problem, "representative" values of A and R_h are needed. In this case, two separate methods for identifying A and R_h were used. Method-1 used the flow cross section above the weir. Method-2 averaged the water surface elevation variations between the baffles and calculated the corresponding A and R_h.

Using the numerical simulation data, Manning's n values were calculated using Method-1 and Method-2. The Method-1 and Method-2 Manning's n values, n_1 and n_2 respectively, are summarized in Table 5-1. As it can be seen from Table 5-1, the average values of n_1 and n_2 were 0.0356 and 0.0637, respectively.

Rajaratnam and Katopodis (1990) developed a flow equation for weir baffled culvert of the following form:

$$Q^* = \frac{Q}{\sqrt{gSD^5}} = C \left(\frac{\overline{H_w}}{D} \right)^E \tag{5-12}$$

where Q^* is the dimensionless discharge and C and E are empirical coefficients. $\left(\frac{\overline{H_w}}{D} \right)$ is the dimensionless water depth. In an effort to investigate the validity of this equation with the present study, the variation of (Q^*) with $\left(\frac{\overline{H_w}}{D} \right)$ was plotted in Fig. 5-19. It can be noted from Fig. 5-19 that data can be fitted with a function of $C \left(\frac{\overline{H_w}}{D} \right)^E$ format. The constants for this function was $C=7.077$ and $E=2.8107$.

Table 5-1. Summary of hydraulic conditions and Manning's roughness coefficient values for the weir-baffled culvert

Case	S (%)	Q (L/s)	Re	Based on the average water H_w (m)	n_1	n_2	Flow Establishment Length
1	0.5	28.3	1.62×10^5	0.2010	0.0267	0.0464	1.610
2	0.5	56.5	2.63×10^5	0.2561	0.0250	0.0362	2.142
3	0.5	85.0	3.67×10^5	0.3033	0.0241	0.0321	2.674
4	1.5	28.3	1.71×10^5	0.1728	0.0292	0.0602	1.610
5	1.5	56.5	2.92×10^5	0.2183	0.0291	0.0470	2.142
6	1.5	85.0	4.00×10^5	0.2803	0.0353	0.0487	2.674
7	3.5	28.3	1.91×10^5	0.1504	0.0273	0.0702	1.610
8	3.5	56.5	3.32×10^5	0.2128	0.0414	0.0684	2.674
9	3.5	85.0	4.63×10^5	0.2489	0.0411	0.0605	3.206
10	4.0	28.3	1.89×10^5	0.1495	0.0285	0.0741	1.610
11	4.0	56.5	3.36×10^5	0.2102	0.0428	0.0715	2.674
12	4.0	85.0	4.72×10^5	0.2446	0.0421	0.0627	2.674
13	5.0	28.3	1.86×10^5	0.1538	0.0355	0.0876	1.610
14	5.0	56.5	3.38×10^5	0.2051	0.0447	0.0763	3.206
15	5.0	85.0	4.78×10^5	0.2346	0.0424	0.0650	3.206
16	6.0	28.3	1.91×10^5	0.1507	0.0361	0.0922	2.142
17	6.0	56.5	3.42×10^5	0.2018	0.0469	0.0811	3.206
18	6.0	85.0	5.01×10^5	0.2269	0.0427	0.0670	3.738
Average					0.0356	0.0637	

Equation (12) will be:

$$Q^* = \frac{Q}{\sqrt{gSD^5}} = 7.077\left(\frac{H_w}{D}\right)^{2.8107} \tag{5-13}$$

In general, the data Fig. 5-19 show that the present experimental data scatter from the flow equation developed by Rajaratnam and Katopodis (1990) especially at higher dimensionless water depth $\left(\frac{H_w}{D}\right)$ and are not well described by Eq. 5-13.

Periodic Flow

Two flow features were noted from the numerical simulation; the first was the entrance region where the *u*-velocity and water depth changed along the culvert. The second was the periodic flow where the flow repeated itself between baffles pairs. Fig. 5-20 shows the *u*-velocity profiles for *S*=3.5% and *Q*=85 L/s at *y**=0 at different *x* locations along the culvert just downstream of the culvert entrance. It can be noted from Fig. 5-20 that the velocity profiles become similar after a distance of 3.356 m from the entrance. Velocity profile at a specific location between baffle spacings is similar to the one of the corresponding location in the adjacent baffle spacing. Also, it can be noted that the reverse velocities region become periodic faster that the forward velocities region. Table 5-1 summarizes the periodic flow establishment length (measured relative to the culvert inlet) for the different flow conditions in the last column. As it can be seen from Table 5-1 that the periodic flow establishment length increasing with increasing Reynolds number at a common culvert slope.

Threshold velocity

The fish passage results (Fig. 3-4 of Chapter 4) show that fish percentage passing was minimum for culvert slope greater than 4%. In an effort to find the flow velocity limit (threshold) for the brown trout fish passage, a procedure is presented to calculate the flow velocity limit. Fig. 5-21 shows the contours for *u*-velocity for *S* =4% at and *Q*=85 L/s x_o =9.058 m (over the baffle). As it shown from Fig. 5-21, there are two symmetrical regions near the culvert walls with a maximum velocities and one region at the center of the culvert with lower velocities.
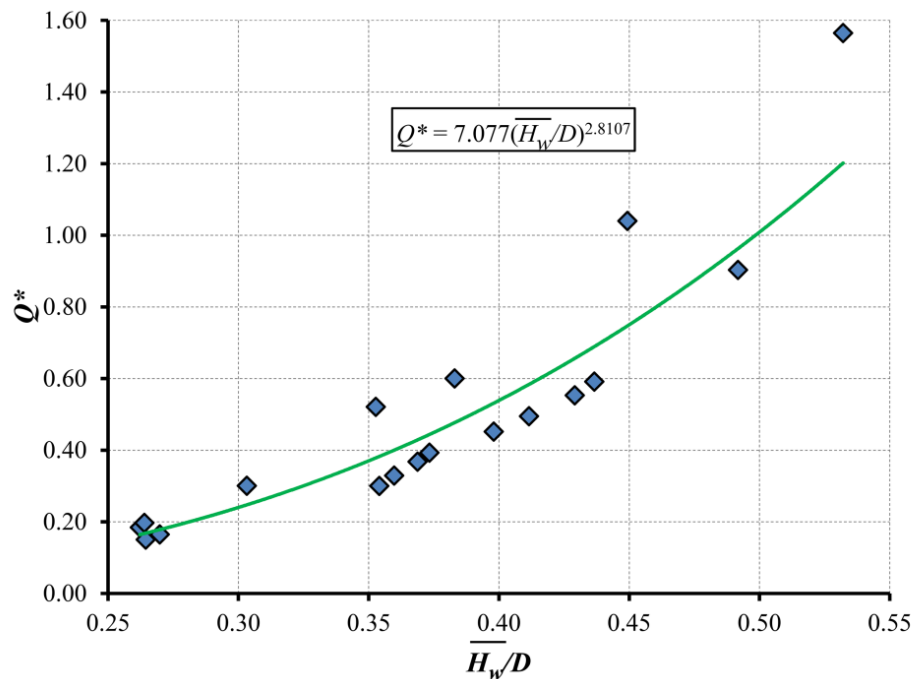
Fig. 5-19. Variation of Q* with $\overline{H}_W/D$
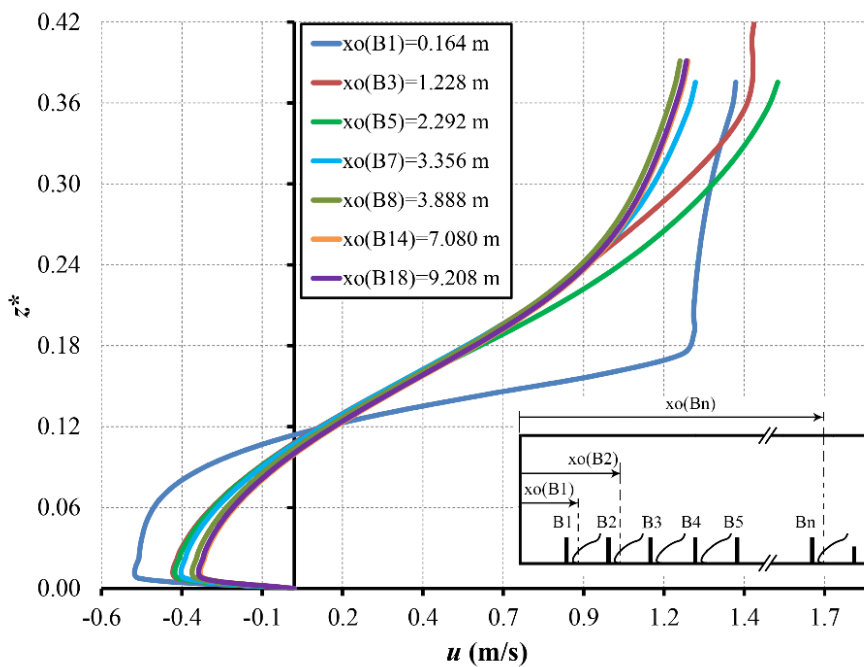
Fig. 5-20. Establishment of fully-developed periodic flow as a function of distance from culvert inlet for S =3.5% and Q =85 L/s at y^*=0 and x_b=0.30

What is important for the fish is to find regions of minimum velocities while passing the culvert. If the average velocity were calculated over the whole region of the flow cross-section (including the regions of maximum velocities), the result will be higher than the actual value that is important for the fish and would not represent the actual threshold velocity.

It was noted from the fish passage observations, especially at steeper culvert slopes and higher flow rates, that the fish while passing upstream across a baffle used a common region near the center of the culvert baffle of 0.0635 m (2.5 inch) in length at the center of the culvert over the baffles. Assume that the wide of this region is 0.08 m (0.0635 m+0.165 m). The additional width (0.165 m) represents the tolerance for the fish wavy movements while swimming and the individual fish length differences. In the non-dimensional form (normalized by the culvert inside diameter), the height is 0.11 and the width is 0.14. Fig. 5-21 shows this region (window). The average velocities for this region were calculated and represented in Table 5-2 for some flow conditions. One can note the average velocity limit is between 0.898 and 0.987 m/s with an average of 0.943 m/s. The cruising speed, sustained speed, and bursting speed for brown trout fish are 0.674 m/s, 1.884 m/s, and 3.875 m/s respectively (Bell, 1986). In order to correlate the velocity limit to the different swimming speeds of the brown trout fish, the ratios were calculated as follows:

$$R_{C\_fs} = \frac{\text{Cruising Speed}}{\text{Region Average Velocity}} = 0.715 \tag{5-14}$$

$$R_{S\_fs} = \frac{\text{Sustained Speed}}{\text{Region Average Velocity}} = 1.998 \tag{5-15}$$

$$R_{B\_fs} = \frac{\text{Bursting Speed}}{\text{Region Average Velocity}} = 4.109 \tag{5-16}$$

where R_{C_fs} is the cruising speed to the region average flow velocity ratio, R_{S_fs} is the sustained speed to the region average flow velocity ratio, and R_{B_fs} is the bursting speed to the region average flow velocity ratio. No fish passed for any swimming speed to the region average velocity ratio higher than the values in Eqns. (5-14), (5-15), or (5-16). In general, it can be concluded that the culvert design should have a region area larger than the cross-sectional area of the fish and have average velocity lower than the velocity limit which depends on the fish type. Also, including all cross-sectional area of the flow across the culvert in the velocity averaging will lead to inaccurate threshold velocity. An investigation is required to validate the applicability of these non-dimensional values with different fish species and different flow conditions.
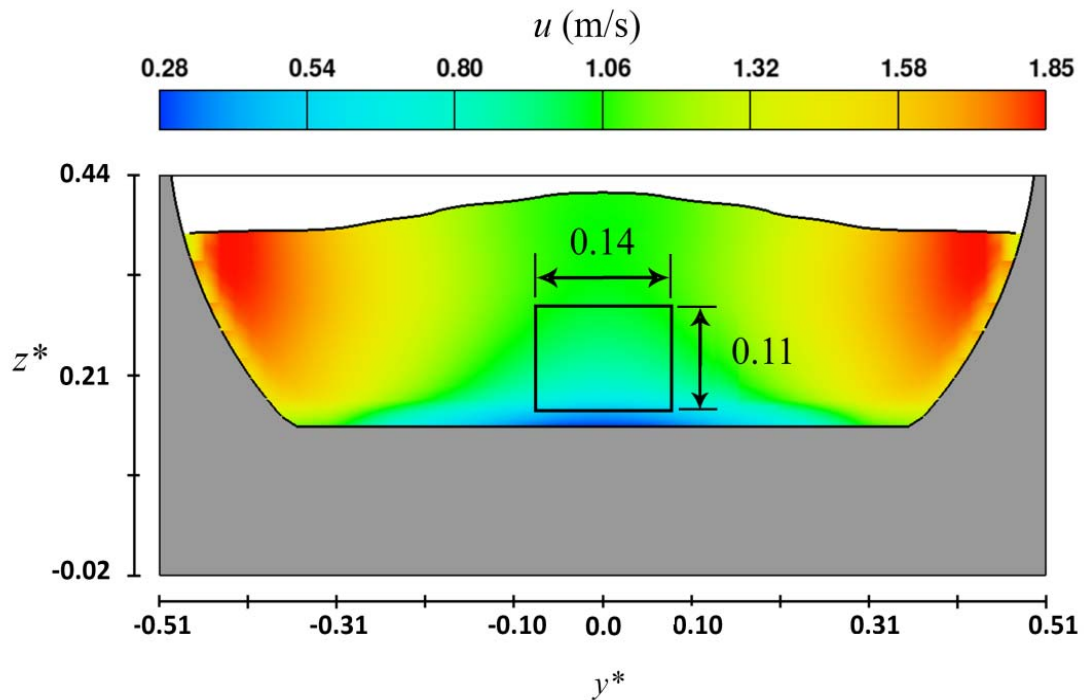
Fig. 5-21. Contours for *u*-velocity for *S* =4% at and *Q*=85 L/s at x_o =9.058 m (over the baffle)

Table 5-2. Fish passage threshold velocity

S (%)	Q (L/s)	U_{w_avg} (m/s)	% Passing
3.5	28.3	0.590	76
4.0	28.3	0.605	85
5.0	28.3	0.608	24
6.0	28.3	0.614	12
3.5	56.5	0.707	64
4.0	56.5	0.734	60
5.0	56.5	0.769	12
6.0	56.5	0.813	4
3.5	85.0	0.842	44
4.0	85.0	0.898	4
5.0	85.0	0.987	0
6.0	85.0	0.998	0

Conclusion

Numerical investigations in flow characteristic in weir baffled-culvert were conducted under variety of steep-culvert slopes and discharge conditions. Tests were conducted at culvert at discharges (Q) of 28.3, 56.5, and 85 L/s at a wide range of culvert slopes (S) of 0.5, 1.5, 3.5, 4, 5 and 6%. Increasing the culvert slope at the same flow rates will increase the forward-flow velocities and the maximum velocities. Whereas, the effects of increasing the flow rates on the forward- and reverse-flow velocities are culvert slope dependent. The influence of increasing the flow rates on the forward velocities was insignificant at small culvert slope ($S \leq 1.5\%$) and significant at large culvert slope (e.g., $S = 6.0\%$). Installation of baffles in culverts will decrease the flow velocity by dissipating the energy of the flow by producing a reverse flow downstream of the baffles. Reduction of velocity results in increasing the water depth and reducing the culvert capacity. Maximum turbulent kinetic energy occurs wherever the velocity is low and vice versa.

CHAPTER 6

SUMMARY AND CONCLUSIONS

Fish passage for brown trout through a prototype-scale weir-baffled culvert (18.3 m long and 0.60 m in diameter, with 0.9D weir baffle spacing and 0.15D baffle height) was conducted under a variety of steep-culvert slopes and discharge conditions. The influence of the sample fish population and the length of the individual fish on passage rates were investigated. Particle Image Velocimetry (PIV) data were collected for different culvert slopes and flow rates. Also, the flow thought this baffled culvert was simulated numerically using three different turbulence models including k-ϵ model, RNG model, and Large Eddy Simulation (LES) model. Based on the fish passage results, PIV data, and the numerical simulation results, the following conclusions are made:

- An inverse relationship between the fish passage and both increasing flow rate and increasing culvert slope was observed.

- The statistical analysis for the fish sample size (9, 17, and 25 fish) effect on fish passage shows that fish passing percentage results are independent on the fish sample size and mainly depends on the culvert slope and flow rates combination.

- In general, the rate of fish passage success through weir baffled-culvert increased with increasing the individual fish length except for fish length of 269 and 272 mm.

- It was noted that the fish using Zone 1, which was located just downstream of the baffles, for resting and Zone 2, which was located along the sidewalls, as a staging area before passing over the next baffle. The PIV data and the numerical

simulation results show that Zone 1 has reverse flow with lower velocities comparing to the forward velocities. Zone 2 has lower turbulent kinetic energy and flow velocities comparing to the core of the flow. It can be concluded that the fish prefer a region of lower velocity for resting and a region of lower turbulent kinetic energy for long term swimming ever if the former region has higher velocity.

- It was observed that fish used a rectangular cross-section region located over a baffle at the center of the culvert approximately while passing a baffle. This rectangular region was estimated (based on the experimental observation) as 0.0635 m height and 0.08 m wide (0.14 height and 0.11 wide in the non-dimensional form). This region was used to calculate the threshold velocity for passing which was 0.943 m/s. The ratios of the different swimming speeds of brown trout to the threshold velocity were calculated as 0.715 m/s for the cruising speed/threshold velocity, 1.998 m/s for the sustained speed/threshold velocity, and 4.109 m/s for the bursting speed/threshold velocity.

- Increasing the flow rates and/or culvert slope will increase the flow velocity and turbulent kinetic energy. The locations for the flow velocity and turbulent kinetic energy are different. Lower turbulent energy associates with higher flow velocity and vice versa.

- Increasing the flow rates at small culvert slopes (e.g., $S = 1.5\%$) will only increase the forward velocities in the additional flow depth (due to increasing in the flow rate) with slightly changes in the rest of the flow velocities.

- The extent of the high-quality PIV data set for the flow through a circular culvert was limited due to the refracted laser light near the wall and near the free surface resulting in a poor agreement between the experimental data and the simulated results of the Renormalized Group k-ϵ model (RNG).

- The k-ϵ model and the Large Eddy Simulation (LES) model were unable to accurately predict the velocity profiles especially in the recirculation region.

- The RNG model was able to more accurately predict the velocity profiles and turbulent kinetic energy for the flow through baffled-culvert except in two regions; near the wall and near the free surface.

- An appropriate culvert design should include a resting region characterized by lower velocity and a small region for swimming fish (rectangular region parallel to the cross-sectional flow) and the designed culvert slope and flow rates should not exceed the fish swimming ability.

- The flow velocities influence the fish passage success whereas the turbulent kinetic energy affects the fish behavior.

REFERENCES

Baker, C. O., and F. E. Votapka. (1990). Fish passage through culverts. FHWA-FL-09-006, USDA Forest Service – Technology and Development Center. San Dimas, CA.

Belford, D. A., and Gould, W. (1989). "An evaluation of trout passage through six highway culverts in Montana." *North. Am. J. Fish. Manage.*, 9(4), 437–445.

Behlke, C. E., Kane, D. L., McLeen, R. F., and Travis, M. D. (1991). *Fundamentals of culvert design for passage of weak-swimming fish*, Alaska Dept. of Transportation and Public Facilities, Fairbanks, AK.

Bell, M. C. (1986). *Fisheries handbook of engineering requirements and biological criteria*, U.S. Army Corps of Engineers, Fish Passage Development and Evaluation Program, North Pacific Division, Portland, OR.

Clay, C. H. (1995). *Design of fishways and other fish facilities*, 2nd Ed., CRC Press, Inc., FL.

Feurich, R., Boubée, J., and Olsen, N. (2011). "Spoiler baffles in circular culverts." *J. Environ. Eng.*, 137(9), 854-857.

Flow Science, Inc. (2006). *Flow-3D® User's Manual*, Version 9.1, Flow Science, Inc.

LaVision (2012). *DaVis*, Version 8.1, LaVision GmbH, Göttingen, Germany.

Liao, J., Beal, D. N. Lauder, G. V. and Triantafyllou, M. S. (2003). "Fish exploiting vortices decrease muscle activity." *Science*, 302(5650), 1556-1569.

Maine DOT. (2007). *Fish passage policy and design guide*, Augusta, ME.

Morrison, R., Hotchkiss, R., Stone, M., Thurman, D., and Horner-Devine, A. (2009). "Turbulence characteristics of flow in a spiral corrugated culvert fitted with baffles and implications for fish passage." *Ecol. Eng.*, 35(3), 381-392.

Olsen, A. H., and Tullis, B. P., (2013). "Laboratory study of fish passage and discharge capacity in slip-lined, baffled culverts." *J. Hydraul. Eng.*, 139(4), 424-432.

Pearson, W., Richmond, M., Johnson, G., Sargeant, S., Mueller, R., Cullinan, V., Deng, Z., Dibrani, B., Guensch, G., May, C., O'Rourke, L. Sobocinski, K., and Tritico, H. (2005). "Protocals for evaluation of upstream passage of juvenile salmonids in an experimental culvert test bed." *Final Rep.*, Washington State Dept. of Transportation, Olympia, WA.

Pearson, W.H., Southard, S.L., May C.W., Skalski, J.R., Townsend, R.L., Horner-Devine, A.R., Thurman, D.R., Hotchkiss, R.H., Morrison, R.R., Richmond, M.C., Deng, D. (2006). "Research on the upstream passage of juvenile salmon through culverts: Retrofit baffles." *Final Rep.*, Washington State Dept. of Transportation, Olympia, WA.

Powers, P. D., and Orsborn, J. F. (1985). *An investigation of the physical and biological conditions affection fish passage success at culverts and waterfalls*, Albrook Hydraulics Laboratory, Dept. of Civil and Environmental Engineering, Pullman, WA.

Rajaratnam, N., and Katopodis, C. (1990). "Hydraulics of culvert fishways III: weir baffle culvert fishways." *Can. J. Civ. Eng.*, 17(4), 558-568.

Rajaratnam, N., Katopodis, C., and Lodewyk, S. (1991). "Hydraulics of culvert fishways IV: Spoiler baffle culvert fishways." *Can. J. Civ. Eng.*, 18(1), 76-82.

Rajaratnam, N., Katopodis, C., and Lodewyk, S. (1988). "Hydraulics of offset baffle culvert fish ways." *Can. J. Civ. Eng.*, 15(6), 1043-1051.

Rajaratnam, N., Katopodis, C., and McQuitty, N. (1989). "Hydraulics of culvert fishways II: Slotted-weir culvert fishways." *Can. J. Civ. Eng.*, 16(3), 375-383.

Smith, D., Brannon, E., and Odeh, M. (2005). "Response of juvenile rainbow trout to turbulence produced by prismatoidal shapes." *Trans. Am. Fish. Soc.*, 134, 741-753.

Tillinger, T. N., and Stein, O. R. (1996). *Fish passage through culverts in Montana: A preliminary investigation*, Dept. of Civil Engineering, Montana State Univ., Bozeman, MT.

Tritico, H., and Cotel, A. (2010). "The effects of turbulent eddies on the stability and critical swimming speed of creek chub (Semotilus atromaculatus)." *J. Exp. Biol.*, 213(13), 2284-2293.

Watts, F. J. (1974). *Design of culvert fishways*, Water Resources Research Institute, Univ. of Idaho, Moscow, ID.

APPENDICES

APPENDIX A: FISH PASSAGE DATA

Table A-1. Brown trout fish physical length

No.	Fish Tag Number	Fish Length (mm)
1	1072-O	225
2	219-Y	227
3	134-P	227
4	216-Y	236
5	222-Y	246
6	223-Y	247
7	215-Y	254
8	224-Y	255
9	133-P	260
10	294-R	260
11	292-R	264
12	136-P	268
13	295-R	268
14	300-R	272
15	135-P	276
16	296-R	279
17	293-R	279
18	298-R	284
19	218-Y	285
20	130-P	285
21	297-R	289
22	221-Y	291
23	129-P	296
24	132-P	314
25	126-P	316
26	131-P	330
27	299-R	346

Table A-2. Statistical analysis for the (fish sample size-flow rates) influence on the fish percentage passing

Fish Sample Size	Q (L/s)		Fish Sample Size	Q (L/s)	Diff.	Lower	Upper	Pr
17	28.3		9	28.3	0.0750	-81.2725	81.4225	1.000
25	28.3		9	28.3	3.9250	-77.4225	85.2725	1.000
9	56.5		9	28.3	-11.1000	-92.4475	70.2725	0.999
17	56.5		9	28.3	-11.9375	-93.2850	69.4100	0.999
25	56.5		9	28.3	-12.2300	-93.5775	69.1175	0.999
9	85.0		9	28.3	-33.3300	-114.6775	48.0175	0.896
17	85.0		9	28.3	-33.9950	-115.3425	47.1175	0.885
25	85.0		9	28.3	-33.2300	-114.5775	85.1975	0.897
25	28.3		17	28.3	3.8500	-77.4975	70.1725	1.000
9	56.5		17	28.3	-11.1750	-92.5225	69.3350	0.999
17	56.5		17	28.3	-12.0125	-93.3600	69.0425	0.999
25	56.5		17	28.3	-12.3050	-93.6525	47.9425	0.999
9	85.0		17	28.3	-33.4050	-114.7525	47.2775	0.895
17	85.0		17	28.3	-34.0700	-115.4179	48.0425	0.884
25	85.0		17	28.3	-33.3050	-96.3725	66.3225	0.896
9	56.5	VS.	25	28.3	-15.0250	-97.2100	65.4849	0.999
17	56.5		25	28.3	-15.8625	-97.5025	65.1925	0.998
25	56.5		25	28.3	-16.1550	-118.6025	44.0925	0.998
9	85.0		25	28.3	-37.2550	-119.2675	43.4275	0.826
17	85.0		25	28.3	-37.9200	-118.5025	44.1925	0.812
25	85.0		25	28.3	-37.1550	-82.1850	80.5100	0.828
17	56.5		9	56.5	-0.8375	-82.4775	80.2175	1.000
25	56.5		9	56.5	-1.1300	-103.5775	59.1175	1.000
9	85.0		9	56.5	-22.2300	-104.2425	58.4525	0.989
17	85.0		9	56.5	-22.8950	-103.4775	59.2175	0.987
25	85.0		9	56.5	-22.1300	-81.6400	81.0550	0.990
25	56.5		17	56.5	-0.2925	-102.7400	59.9550	1.000
9	85.0		17	56.5	-21.3925	-103.4050	59.2900	0.992
17	85.0		17	56.5	-22.0575	-102.6400	60.0550	0.992
25	85.0		17	56.5	-21.2950	-102.4475	59.1175	0.992
9	85.0		25	56.5	-21.1000	-103.1125	60.2475	0.992
17	85.0		25	56.5	-21.7650	-114.2454	59.5825	0.991
25	85.0		25	56.5	-21.0000	-102.3475	60.3475	0.992
17	85.0		9	85.0	-0.6650	-82.0124	80.6825	1.000
25	85.0		9	85.0	0.1000	-81.2475	81.4475	1.000

Table A-3. Statistical analysis for the (fish sample size-culvert slope) influence on the fish percentage passing

Fish Sample Size	S (%)		Fish Sample Size	S (%)	Diff.	Lower	Upper	Pr
17	3.0		9	3.0	0.1900	-67.9798	68.35	1.0000
25	3.0		9	3.0	-3.7333	-71.9032	64.43	1.0000
9	4.0		9	3.0	-25.9333	-94.1032	42.23	0.9584
17	4.0		9	3.0	-23.0167	91.1865	45.15	0.9201
25	4.0		9	3.0	-20.8600	-89.0298	47.30	0.9915
9	5.0		9	3.0	-59.2900	-127.4598	8.879	0.1308
17	5.0		9	3.0	-60.5967	-128.7665	7.573	0.1144
25	5.0		9	3.0	-58.4000	-126.5698	9.769	0.1431
9	6.0		9	3.0	-66.6967	-134.8665	1.473	0.0591
17	6.0		9	3.0	-70.4000	-138.5698	-	0.0387
25	6.0		9	3.0	-65.0667	-133.2365	3.103	0.0708
25	3.0		17	3.0	-3.9233	-72.0932	64.24	1.0000
9	4.0		17	3.0	-26.1233	-94.2932	42.04	0.9563
17	4.0		17	3.0	-23.2067	-91.3765	44.96	0.9809
25	4.0		17	3.0	-21.0500	-89.2195	47.11	0.9909
9	5.0		17	3.0	-59.4800	-127.6498	8.689	0.1283
17	5.0	VS.	17	3.0	-60.7867	-128.9565	7.383	0.1121
25	5.0		17	3.0	-58.5900	-126.7598	9.579	0.1404
9	6.0		17	3.0	-66.8867	-135.0565	1.283	0.0578
17	6.0		17	3.0	-70.5900	-138.7598	-	0.0378
25	6.0		17	3.0	-65.2567	-133.4265	2.913	0.0693
9	4.0		25	3.0	-22.2000	-90.3698	45.96	0.9863
17	4.0		25	3.0	-19.2833	-87.4532	48.88	0.9955
25	4.0		25	3.0	-17.1267	-85.2965	51.04	0.9984
9	5.0		25	3.0	-55.5567	-123.7265	12.61	0.1890
17	5.0		25	3.0	-56.8633	-125.0332	11.30	0.1666
25	5.0		25	3.0	-54.6667	-122.8365	13.50	0.2055
9	6.0		25	3.0	-62.9633	-131.1332	5.206	0.0890
17	6.0		25	3.0	-66.6667	-134.8365	1.503	0.0593
25	6.0		25	3.0	-61.3333	-129.5032	6.836	0.1059
17	4.0		9	4.0	2.9167	-65.2532	71.08	1.0000
25	4.0		9	4.0	5.0733	-63.0965	73.24	1.0000
9	5.0		9	4.0	-33.3567	-101.5265	34.81	0.8211
17	5.0		9	3.0	0.1900	-67.9798	68.35	1.0000
25	5.0		9	3.0	-3.7333	-71.9032	64.43	1.0000

Table A-3 (continued)

Fish Sample Size	S (%)		Fish Sample Size	S (%)	Diff.	Lower	Upper	Pr
17	5.0		9	4.0	-34.6633	-102.8332	33.50	0.7854
25	5.0		9	4.0	-32.4667	-100.6365	35.70	0.8436
9	6.0		9	4.0	-40.7633	-108.6365	27.40	0.5922
17	6.0		9	4.0	-44.4667	-112.6365	23.70	0.4705
25	6.0		9	4.0	-39.1333	-107.3032	29.03	0.6463
25	4.0		17	4.0	2.1567	-66.0132	70.32	1.0000
9	5.0		17	4.0	-36.2733	-104.4432	31.89	0.7377
17	5.0		17	4.0	-37.5800	-105.7498	30.58	0.6968
25	5.0		17	4.0	-35.3833	-103.5532	32.78	0.7645
9	6.0		17	4.0	-43.6800	-11.8498	24.48	0.4958
17	6.0		17	4.0	-47.3833	-115.5532	20.78	0.3815
25	6.0		17	4.0	-42.0500	-110.2918	26.11	0.5493
9	5.0		25	4.0	-38.4300	-106.5998	29.73	0.6693
17	5.0		25	4.0	-39.7367	-107.9065	28.43	0.6263
25	5.0		25	4.0	-37.5400	-105.7984	30.62	0.6981
9	6.0	VS.	25	4.0	-45.8367	-114.0065	22.33	0.4277
17	6.0		25	4.0	-49.5400	-117.7098	18.62	0.3219
25	6.0		25	4.0	-44.2067	-112.3765	23.96	0.4788
17	5.0		9	5.0	-1.3067	-69.4765	66.86	1.0000
25	5.0		9	5.0	0.8900	-67.2798	69.09	1.0000
9	6.0		9	5.0	-7.4067	-75.5765	60.76	1.0000
17	6.0		9	5.0	-11.1100	-79.2798	57.05	1.0000
25	6.0		9	5.0	-5.7767	-73.9465	62.39	1.0000
25	5.0		17	5.0	2.1967	-65.9732	70.36	1.0000
9	6.0		17	5.0	-6.1000	-74.2698	62.06	1.0000
17	6.0		17	5.0	-9.8033	-77.9732	58.36	1.0000
25	6.0		17	5.0	-4.4700	-72.6398	63.69	1.0000
9	6.0		25	5.0	-8.2967	-76.4665	59.87	1.0000
17	6.0		25	5.0	-12.0000	-80.1698	56.16	0.9999
25	6.0		25	5.0	-6.6668	-74.8365	61.50	1.0000
17	6.0		9	6.0	-3.7033	-71.8732	64.46	1.0000
25	6.0		9	6.0	1.6300	-66.5398	69.79	1.0000
25	6.0		17	6.0	5.3333	-62.8365	73.50	1.0000
17	5.0		9	4.0	-34.6633	-102.8332	33.50	0.7854
25	5.0		9	4.0	-32.4667	-100.6365	35.70	0.8436

APPENDEX B: PERMISSION

Copyright Clearance Center

RightsLink®

ASCE
AMERICAN SOCIETY OF CIVIL ENGINEERS

Title: Fish Passage Behavior for Severe Hydraulic Conditions in Baffled Culverts

Author: Khodier, M. and Tullis, B.

Publication: Journal of Hydraulic Engineering

Publisher: American Society of Civil Engineers

Date: 03/01/2014

Copyright © 2014, ASCE. All rights reserved.

User ID

Password

☐ Enable Auto Login

LOGIN

Forgot Password/User ID?

If you're a copyright.com user, you can login to RightsLink using your copyright.com credentials. Already **a RightsLink user** or want to learn more?

Permissions Request

As an ASCE author, you are permitted to reuse you own content for another ASCE or non-ASCE publication.

Please add the full credit line "With permission from ASCE" to your source citation. Please print this page for your records.

Type of use: Dissertation/Thesis

Portion: full article

Format: print and electronic

Use of this content will make up more than 25% of the new work: no

Author of this ASCE work or ASCE will publish the new work: yes

BACK   CLOSE WINDOW

CURRICULUM VITAE

Mohanad Khodier
m.khodier@aggiemail.usu.edu
(June 2014)

Education:

Ph.D. Fluid Mechanics and Hydraulic Engineering , Department of Civil & Environmental Engineering,Utah State University, Logan, Utah. (expected Summer 2014). Advisor Blake P. Tullis.
Dissertation: Weir-Baffled Culvert Hydrodynamics Evaluation for Fish Passage Using Particle Image Velocimetry And Computational Fluid Dynamic Techniques.

M.S. Mechanical Engineering, Department of Mechanical Engineering, Jordan University of Science and Technology, Irbid, Jordan. Spring 2004.
Thesis: Natural Convection in an Inclined Channel-Partially Filled with Porous Media.

B.S. Mechanical Engineering, Department of Mechanical Engineering, Jordan University of Science and Technology, Irbid, Jordan. Spring 2001.

Areas of Research Interest:

Hydraulic Structures, Fluid Mechanics, Free-surface Flows, Open Channel Flow, Applied Computational Fluid Dynamics, Heat Transfer.

Languages:

Arabic (Native), English (Good).

Publications and Conference Presentations:

Khodier, M. A., Tullis, B. P. (2014). "Fish Passage Behavior for Severe Hydraulic Conditions in Baffled Culverts." Journal of hydraulic engineering, 140(3), 322-327.

Khodier, M. A., Tullis, B. P. (2013). "Using Particle Image Velocimetry (PIV) System in Fish Passage through Rehabilitated Culverts." The 4rd International Junior Researcher and Engineer Workshop on Hydraulic Structures, Utah State University, Logan, Utah. June 17-20, 2012.

Harris, J., Nani, D., Jones, K., Khodier, M., Smith, B. L. (2011). "Investigation of the Uncertainty of a Validation Experiment due to Uncertainty in its Boundary Conditions." The 14th International Topical Meeting on Nuclear Reactor Thermalhydraulics, NURETH-14, Toronto, Ontario, Canada. September 25-30, 2011.

Kiwan, S., and Khodier, M. (2008)." Natural Convection Heat Transfer in an Open-Ended Inclined Channel-Partially Filled with Porous Media." *J. Heat Transfer Engineering* , 29(1), 67 – 75.

Experimental and Numerical Modeling

- 2D steady and time-dependent PIV.
- PIV Data processing and post-processing.
- 2D and 3D turbulence modeling using FLUENT, ANSYS, and FLOW3D.

Computer Skills:

- Program with FORTRAN, C++, Visual Basic, MATLAB.
- 2D and 3D drawing with AutoCAD, Mechanical Desktop, and Inventor.

Experiences:

Summer (2000):	University Engineering Training: for three months at Yarmouk University on air conditioning systems.
2002-2003:	Ministry of Work, Department of Building.
2001-2003:	Teacher Assistance in Jordan University of Science and Technology (Mechanical Engineering Department). Teacher Assistant in thermodynamic 1&2, heat transfer 1&2, fluid dynamic, fluid and heat transfer LAB, mechanical drawing (AUTODESK) and strength of material LAB (full assistance).
2004-2008:	Lecturer in Automotive & Engines Technology at College of Technology at Dammam – Saudi Arabia.
2008-2009	Inspector Engineer at Jordan Petroleum Refinery Company, Zarqa, Jordan.